STRUCTURES OF THE KALSILITE-LIKE SILICATES

$MTSiO_4$ (M = Ba, Na/K, Ca/Sr; T = Co, Mg, Zn, Ga, Be)

STRUCTURES OF THE KALSILITE-LIKE SILICATES

$MTSiO_4$ (M = Ba, Na/K, Ca/Sr; T = Co, Mg, Zn, Ga, Be)

by

BO LIU

A Thesis

Submitted to the School of Graduate Studies

in Partial Fulfillment of the Requirements

for the Degree

Master of Science

McMaster University

May 1992

MASTER OF SCIENCE 1992

McMaster University

Hamilton, Ontario

TITLE: Structures of the Kalsilite-like Silicates $MTSiO_4$ (M = Ba, Na/K, Ca/Sr; T = Co, Mg, Zn, Ga, Be)

AUTHOR: Bo Liu, B. Eng. and M. Eng.

SUPERVISOR: Dr. Jacques Barbier

NUMBER OF PAGES: xii, 114

ABSTRACT

A number of silicate compounds $BaTSiO_4$ (T = Co, Mg, Zn), $Na_{0.5}K_{0.5}GaSiO_4$ and $Sr_{1-x}Ca_xBeSiO_4$ (x = 0.0 ~ 0.4) have been characterized by a combination of diffraction techniques. These compounds crystallize with the same ($\sqrt{3}\times$A, C) superstructure of the hexagonal kalsilite ($KAlSiO_4$) structure and belong to the large structural family of stuffed tridymite-derivatives. Their crystal structures have been refined by using powder neutron data ($BaTSiO_4$, T = Mg, Zn), powder X-ray data ($Na_{0.5}K_{0.5}GaSiO_4$) and single crystal X-ray data ($BaCoSiO_4$ and $Sr_{1-x}Ca_xBeSiO_4$, x = 0.0 and 0.27). This study shows that these kalsilite-like structures can accommodate cavity and tetrahedral atoms of variable sizes by relatively minor framework distortions and atomic displacements. The formation of the ($\sqrt{3}\times$A, C) superstructure can be correlated with the relative sizes of the tetrahedral and cavity atoms.

ACKNOWLEDGEMENT

Foremost I would like to sincerely thank my supervisor, Dr. J. Barbier, for his great guidance, patience and support throughout this work. I am grateful to have had the opportunity to work in his group.

A very special thank is due to Dr. J. Britten for the single crystal data collections and his assistance with the structure refinements.

I would also like to thank Mr. J. Garrett and Mr. F. Gibbs for their technical assistance, Mr W. Gong for the powder X-ray data collection and Drs. G. Liu and S.J. Xue for their help and discussions as well as all colleagues in Room ABB-443.

Finally, I would like to thank my parents for their encouragement and support from the other side of the earth, China.

TABLE OF CONTENTS

LIST OF FIGURES

LIST OF TABLES

CHAPTER 1

INTRODUCTION

The stuffed tridymite derivatives form a very large and important structural family whose members are closely related to the high-temperature structure of tridymite (SiO_2) [e.g. Liebau, 1985]. The structure of high tridymite [Dollase, 1967] projected along the c-axis is shown in Fig. 1.1: the silicate tetrahedra form (001) layers of six-membered rings by sharing their corners and pointing up and down alternatively. The successive layers are stacked in the c direction by sharing the apical oxygens to form a three-dimensional framework enclosing cavities or tunnels parallel to the c-axis which are a main feature of this structure-type.

Part of the silicon Si^{4+} ions can be replaced by other cations with lower charge valence (T^{3+} or T^{2+}) and large M^{+} or M^{2+} cations can be stuffed into the framework cavities to maintain the charge balance. The basic natural stuffed-tridymite derivatives are the (Na, K)$AlSiO_4$ compounds which have been extensively studied [e.g. Smith and Tuttle, 1957; Tuttle and Smith, 1958; Henderson and Roux, 1977; Henderson and Thompson, 1980; Abbott, 1984; Merlino, 1985]. The (Na, K)$AlSiO_4$ system is known for its complex polymorphism with numerous structures forming at different temperatures and compositions, the most important of which are kalsilite ($KAlSiO_4$), nepheline ($K_{0.25}Na_{0.75}AlSiO_4$) and beryllonite-type $NaAlSiO_4$.

Fig. 1.2 shows the structure of kalsilite: the unit-cell is hexagonal ($P6_3$ space group) with the dimensions A = 5.16 Å and C = 8.69 Å [Perrotta and Smith, 1965].

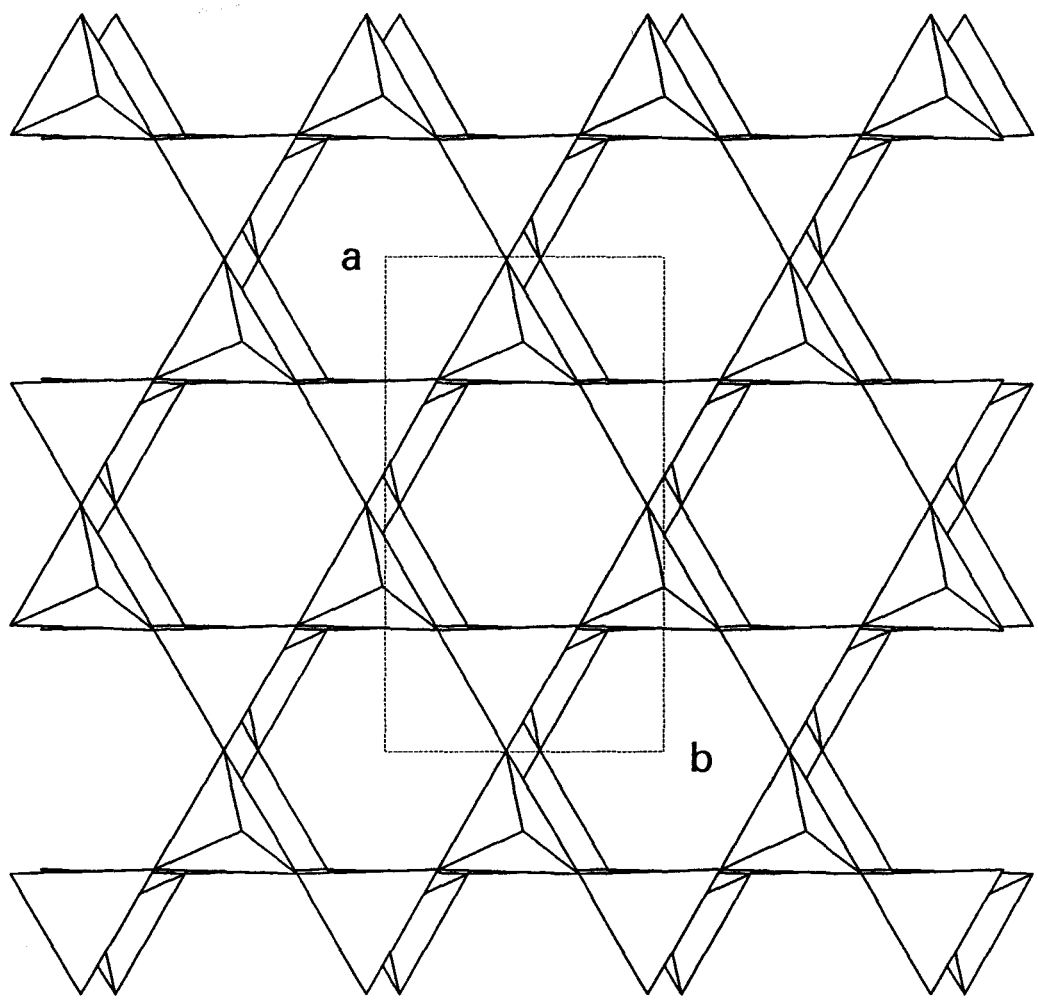

Fig. 1.1 The structure of the high-temperature form of tridymite projected along the c-axis. Successive tetrahedral layers are stacked along the c-direction. The orthorhombic cell dimensions are: a = 8.74, b = 5.04 and c = 8.24 Å.

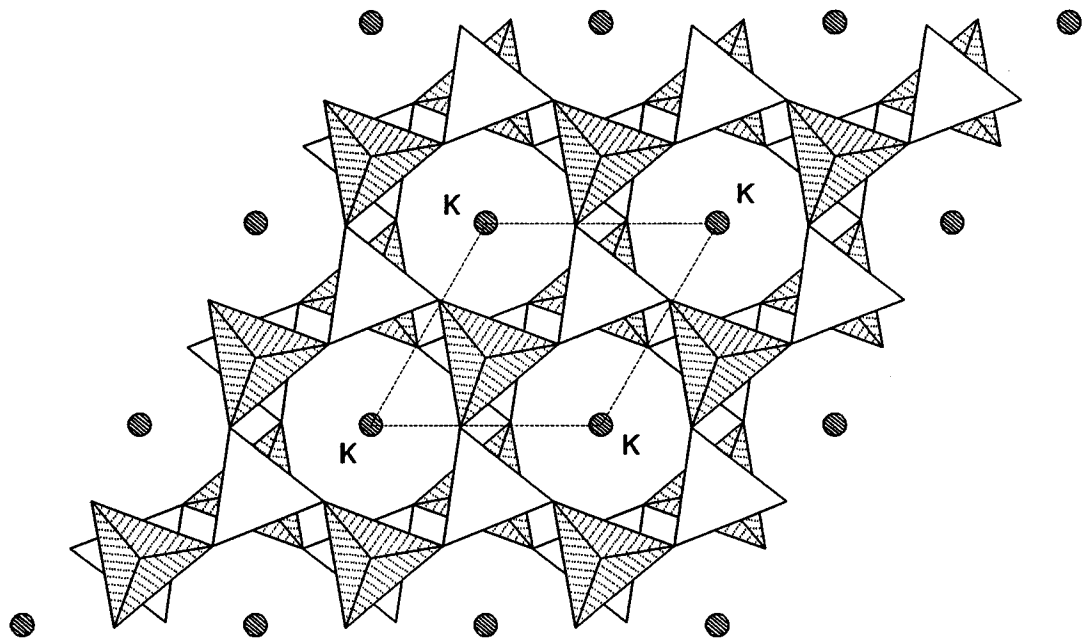

Fig. 1.2 The structure of kalsilite viewed along the c-axis. The Al and Si atoms are fully ordered with AlO_4 tetrahedra pointing up and SiO_4 tetrahedra pointing down. The cavities are filled with large K atoms. The hexagonal cell dimensions are A = 5.16 and C = 8.69 Å.

The corner-shared tetrahedra form a three-dimensional framework of six-membered rings with the UDUDUD topology (where U and D represent tetrahedra pointing up and down, respectively). Unlike the high tridymite structure, all six-membered rings in the kalsilite structure have a ditrigonal shape and the successive (001) tetrahedral layers are stacked along the c-axis according to a "staggered" conformation.

In the nepheline structure (Fig. 1.3), the unit cell is hexagonal ($P6_3$ space group) with the cell dimensions, a $\approx$ 2A and c $\approx$ C [e.g. Simmons and Peacor, 1972]. The corner-shared tetrahedra form a three-dimensional framework of six-membered rings with the same UDUDUD topology as in the kalsilite structure but the successive layers are stacked along the c-axis in an "eclipsed" conformation. Three quarters of the rings are strongly distorted leading to two different kinds of cavities: the larger cavities are filled by nine-coordinated K atoms while the smaller cavities are filled by six-coordinated Na atoms.

Starting from the (Na, K)$AlSiO_4$ compositions, the tetrahedral (Al, Si) and stuffing (Na, K) atoms can be substituted by many other atoms giving rise to a large variety of compounds which form a large structural family. The study of these tridymite derivatives is of interest in view of their complex polymorphism and also in view of the effect of atomic substitution on the topology and distortion of the tetrahedral framework. For instance, investigations of Ga/Al and Ge/Si substitution in the analogous systems (Na, K)$AlGeO_4$, (Na, K)$GaSiO_4$ and (Na, K)$GaGeO_4$ have been recently reported [Barbier and Fleet, 1987, 1988; Lampert and Böhme, 1986; Weber and Barbier, 1990]. These studies showed that all K end-members are isostructural with tetrahedral frameworks containing UDUDUD and UUUDDD rings whereas all Na end-members are isostructural with beryllonite ($NaBePO_4$) with UDUDUD and UUDDUD rings. The

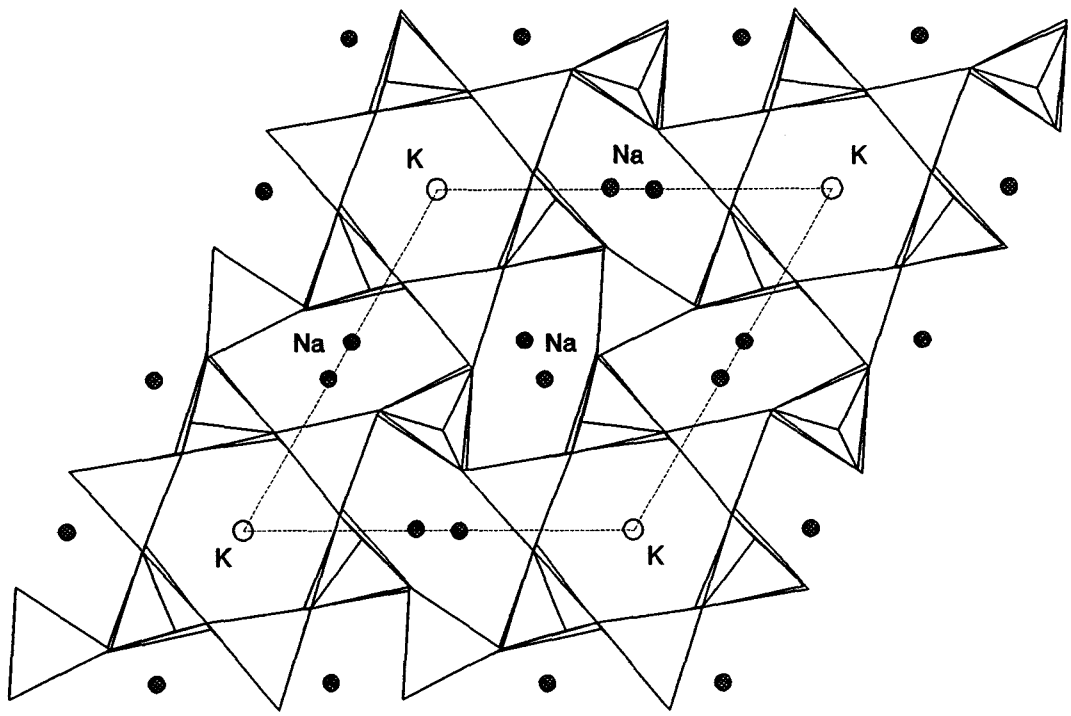

Fig. 1.3 The structure of nepheline viewed along the c-axis. The Na atoms occupy the small oval cavities and the K atoms occupy the large hexagonal cavities. The hexagonal cell dimensions are a $\approx 2\times$A and c $\approx$ C.

framework topologies of the end-members are therefore distinct from the simple UDUDUD tridymite topology occurring in the nepheline and kalsilite structures of the (Na, K)$AlSiO_4$ system. Some compounds with intermediate compositions, such as, $Na_{1-x}K_xAlGeO_4$ (x = 0.5 ~ 0.9) [Barbier and Fleet, 1988] and $Na_{1-x}K_xGaSiO_4$ (x = 0.5 ~ 0.6) [Weber and Barbier, 1990], crystallize with a ($\sqrt{3}\times$A, C) hexagonal cell, suggesting that they are a simple superstructure of the basic (A, C) kalsilite cell.

The aluminate tridymite-derivatives MAl_2O_4 (M = Ca, Sr, Ba) have also been extensively studied. Their structures consist of a three-dimensional framework of corner-connected AlO_4 tetrahedra, the cavities of which are filled with alkaline earth metal atoms (Ca, Sr, Ba). $CaAl_2O_4$ crystallizes with a beryllonite-type structure [Hörkner and Müller-Buschbaum, 1976] while both $SrAl_2O_4$ [Schulze and Müller-Buschbaum, 1981] and $BaAl_2O_4$ [Hörkner and Müller-Buschbaum, 1979] crystallize with kalsilite ($KAlSiO_4$)-type structures. The mixed compounds (Sr,Ba)Al_2O_4 [Henderson and Taylor, 1982; Taylor et al., 1985] and (Ca,Sr)Al_2O_4 [Barbier and Neuhausen, 1990] have been investigated with respect to their structural behaviour at different temperatures and compositions. The original studies of the compounds $SrBeSiO_4$ [JCPDS[1] #26-978] and $BaAl_2O_4$, $BaMgSiO_4$, $BaZnSiO_4$ and $BaZnGeO_4$ [Dinh and Durif, 1964] had reported them to crystallize with small, hexagonal unit-cells (with A = 4.85, C = 8.19 Å for $SrBeSiO_4$ and A $\approx$ 5.25, C $\approx$ 8.75 Å for the Ba-stuffed compounds), suggesting that they were simply isostructural with kalsilite. However, later studies established the existence of a (2$\times$A, C) superstructure for $BaAl_2O_4$ [Hörkner and Müller-Buschbaum, 1979] and a temperature dependent ($\sqrt{3}\times$A, 4$\times$C) superstructure for $BaZnGeO_4$ [Takei et al., 1980; Takei, 1980]. For the latter, only an approximate structure of the room-

[1]JCPDS - International Centre for Diffraction Data

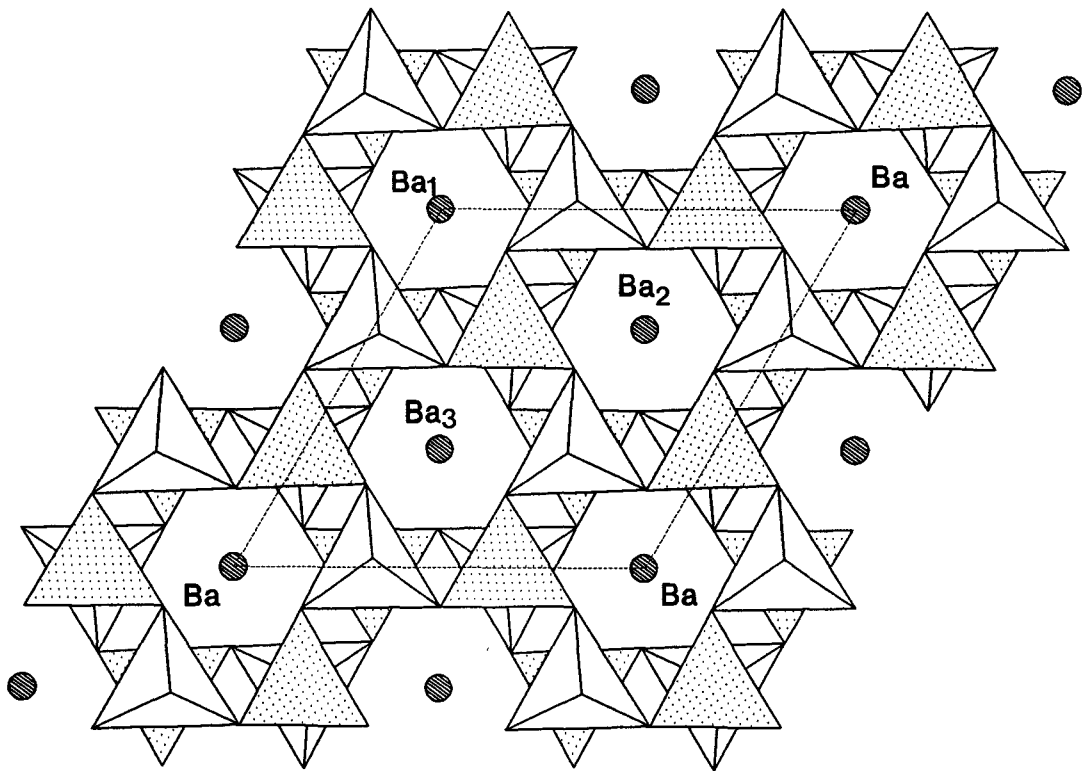

Fig. 1.4 The structure of $BaZnGeO_4$ viewed along the c-axis. The Zn and Ge atoms are fully ordered with ZnO_4 tetrahedra pointing up and GeO_4 tetrahedra pointing down. The cavities are filled by the Ba atoms. The structure is a $\sqrt{3}\times A$ superstructure of kalsilite, with hexagonal cell dimensions a = 9.291 and c = 8.728 Å.

temperature phase could be determined using single crystal X-ray diffraction by neglecting the very weak and incommensurate $4\times C$ superstructure [Iijima et al., 1982]. The structure of $BaZnGeO_4$ is shown in Fig. 1.4: although the framework topology is the same as in kalsilite, the framework is collapsed around the Ba atoms and the apical oxygens atoms are displaced off the three-fold axes resulting in the formation of the $\sqrt{3}\times A$ superstructure. Furthermore, the (001) oxygen atom layers are not planar but puckered.

The purpose of the present study is to investigate the structures of a number of tridymite-derivatives including $BaTSiO_4$ (T = Co, Mg, Zn), (Na, K)$GaSiO_4$ and (Ca, Sr)$BeSiO_4$, all crystallizing with the same ($\sqrt{3}\times A$, C) kalsilite-type superstructure. Their detailed structural refinements using powder neutron and X-ray data or single crystal X-ray data should provide new insight into their crystal chemistry.

CHAPTER 2

DESCRIPTION OF EXPERIMENTS

2.1 Sample Preparation

The sample preparations included the syntheses of both powders and single crystals. The powders were synthesized by solid state reactions involving the sintering of stoichiometric mixtures of starting materials at high temperature. The single crystals were grown by using the melt growth technique and the flux technique. All samples were prepared from mixtures of powders finely ground and thoroughly mixed with a mortar and pestle under ethanol.

Chemicals used in the syntheses:

Barium Acetate ($Ba(CH_3COO)_2$)	J.T. Baker Chemical Co. (99.6%)
Cobalt Carbonate ($CoCO_3$)	Johnson Matthey (Alfa Products)
Magnesium Oxide (MgO)	Aldrich Chemical Company (99.99%)
Zinc Oxide (ZnO)	BDH Chemicals (Analytical reagent)
Silica Gel ($SiO_2.xH_2O$, 80.04 wt% SiO_2 determined by TGA)	
Silica Gel ($SiO_2.nH_2O$ (89.00 wt% SiO_2 determined by TGA)	
	Matheson, Coleman and Bell (Reagent Grade)

Strontium Carbonate ($SrCO_3$)	Cerac Incorporated (99.5%)
Calcium Carbonate ($CaCO_3$)	BDH Chemicals (Analytical reagent)
Beryllium Oxide (BeO)	Johnson Matthey (99% BeO)
Potassium Carbonate (K_2CO_3)	BDH Chemicals (Analytical reagent)
Sodium Carbonate (Na_2CO_3)	BDH Chemicals (Analytical reagent)
Gallium (III) Oxide (Ga_2O_3)	Aldrich Chemical Company (99.99%)
Nickel Oxide (NiO)	Johnson Matthey (99%)
Nickel Carbonate ($NiCO_3$)	Johnson Matthey (99%)

2.1.1 Syntheses of the $BaTSiO_4$ Powders (T = Co, Mg, Zn)

The syntheses of the four compounds, $BaCoSiO_4$, $BaMgSiO_4$, $BaMg_{0.5}Zn_{0.5}SiO_4$ and $BaZnSiO_4$, were started by using $Ba(CH_3COO)_2$, ZnO (first dried at 900°C), MgO, $CoCO_3$ and silica gel (80.04 wt% SiO_2). The stoichiometric powder mixtures of 1 gram for $BaCoSiO_4$ and $BaMg_{0.5}Zn_{0.5}SiO_4$ or 10 grams for $BaMgSiO_4$ and $BaZnSiO_4$ were pressed into pellets and heated up to 700°C and 900°C to dehydrate the silica gel and decompose the acetate and carbonate. Then the powder mixtures were remixed and fired at 1250°C for $BaCoSiO_4$, 1560°C for $BaMgSiO_4$, 1450°C for $BaMg_{0.5}Zn_{0.5}SiO_4$ and 1300°C for $BaZnSiO_4$ for about 48 ~ 72 hours with intermediate remixings. Finally the samples were quenched in air and ground into fine powders for powder X-ray and neutron diffraction experiments.

The $BaMgSiO_4$, $BaMg_{0.5}Zn_{0.5}SiO_4$ and $BaZnSiO_4$ powders were white whereas the $BaCoSiO_4$ was deep blue in colour as expected for a compound containing tetrahedral Co^{+2} ions. The blue colour of the Co compound was observed to turn slightly darker

after annealing at temperatures below 1100°C. By analyzing the powder X-ray diffraction pattern of the annealed sample (see Table 2.1), this colour change was found to be associated with the decomposition of $BaCoSiO_4$ into a mixture of CoO and $Ba_2CoSi_2O_7$.

2.1.2 Synthesis of the $(Na_{0.5}K_{0.5})GaSiO_4$ Powder

Following a previous investigation of the (Na, K)$GaSiO_4$ system [Weber & Barbier, 1990], a 1 gram sample of the $(Na_{0.5}K_{0.5})GaSiO_4$ compound was synthesized by using K_2CO_3, Na_2CO_3, Ga_3O_2 and $SiO_2.nH_2O$ (80.04 wt% SiO_2) as starting materials. The stoichiometric powder mixture was pressed into a small pellet and preheated slowly from 600°C up to 900°C at a rate of 3°C/min to dehydrate the silica gel and decompose the carbonates. Because of the low melting points of K_2CO_3 and Na_2CO_3 (891°C and 851°C respectively), the preheating temperature was slowly increased to avoid the loss of K and Na oxides. After remixing and repressing into a pellet, the mixture was fired at 925°C for 60 hours with two intermediate remixings and quenched from this temperature.

After several trials, it was found that the temperature of 925°C was the lowest possible temperature to synthesize this compound. The sample was observed to melt above 1100°C and decompose at about 875°C. From its powder X-ray diffraction pattern, the decomposed product was found to be a mixture of a Na-rich phase (beryllonite-type) and a K-rich phase ($KAlGeO_4$-type [Lampert, 1986]). The compound $Na_{0.5}K_{0.5}GaSiO_4$ was studied by electron diffraction and powder X-ray diffraction using a Guinier camera and diffractometer.

TABLE 2.1

COMPARISON BETWEEN THE POWDER X-RAY PATTERNS OF $Ba_2CoSi_2O_7$/CoO AND THE DECOMPOSITION PRODUCT OF $BaCoSiO_4$ ANNEALED AT 1100°C

Sample		CoO*		$Ba_2CoSi_2O_7$**	
d(Å)	I/I_o	d(Å)	I/I_o	d(Å)	I/I_o
3.9362	18			3.95	10
3.4885	11			3.51	10
3.1761	100			3.19	100
2.9806	3			2.99	5
2.9255	20			2.92	20
2.8604	7			2.87	10
2.7267	20			2.73	16
2.5496	6			2.55	8
2.4618	5	2.46	75		
2.3874	9			2.39	16
2.1280	12	2.13	100	2.13	6
2.0922	7			2.09	8
2.0502	6			2.05	8
1.9511	32			1.953	30
1.9100	8			1.912	16
1.7833	5			1.783	10
1.7463	9			1.747	10
1.7069	16			1.710	16
1.5068	3	1.5062	50		
1.4584	1			1.458	6
1.4079	3			1.410	8
1.3003	15			1.302	10
1.2290	1	1.2298	16		

* [International Centre for Diffraction Data, #9-402]

** [International Centre for Diffraction Data, #6-859] isostructural with $Ba_2CuSi_2O_7$ [Malinovskii, 1984].

2.1.3 Syntheses of the $(Sr_{1-x}Ca_x)BeSiO_4$ Powders (x = 0.0 ~ 1.0)

A series of powder samples, about 0.4 to 1 gram each, were prepared at 10 mol% intervals along the $SrBeSiO_4$-$CaBeSiO_4$ join. The starting materials were stoichiometric mixtures of $SrCO_3$, $CaCO_3$, BeO and silica gel (80.04 wt% SiO_2). The samples were first fired at 900°C to dehydrate the silica gel and decompose the carbonates, sintered at 1200°C (1400°C for $CaBeSiO_4$) for about 48 hours with one intermediate remixing and finally quenched in air.

All the reaction products were characterized by powder X-ray diffraction using a Guinier camera and a few (x = 0 ~ 0.3) were further examined by electron diffraction and high resolution electron microscopy .

2.1.4 Syntheses of the $(Ba_{1-x}Ca_x)BeSiO_4$ Powders (x = 0.0 ~ 1.0)

The syntheses were performed using stoichiometric mixtures of $Ba(CH_3COO)_2$, $CaCO_3$, BeO and $SiO_2.nH_2O$ (80.04 wt% SiO_2). A series of powder samples were made at 10 mol% intervals along the $BaBeSiO_4$-$CaBeSiO_4$ join. All samples were preheated at 700°C and 900°C to dehydrate the silica gel and decompose the acetate and carbonate, sintered at 1200°C for 48 hours with intermediate mixing and quenched in air. Most samples were nearly melted at 1400°C. The products were characterized by powder X-ray diffraction using a Guinier-Hägg camera ($CuK_{\alpha 1}$ radiation, λ = 1.540598 Å). Apart from a very narrow solid solution range at the Ba-end ($x \leq 0.1$), a new single phase with the composition $Ba_{0.4}Ca_{0.6}BeSiO_4$ was found with the orthorhombic unit-cell: a = 4.7550(2) Å, b = 7.9332(4) Å, c = 8.5718(3) Å and V = 323.35(2) $Å^3$, determined

from the indexing of powder X-ray diffraction data by an automatic indexing program [Visser, 1969] (Table 2.2). The cell dimensions suggest that this compound may also be a stuffed tridymite derivative with c/a $\approx \sqrt{3}$ and c = $C_{kalsilite}$ but no further work was carried out.

2.1.5 Growth of the $BaCoSiO_4$ Single Crystals

Single crystals of $BaCoSiO_4$ were obtained by a melt growth technique. A 10g stoichiometric mixture of $Ba(CH_3COO)_2$, $CoCO_3$ and silica gel (80.04 wt% SiO_2) was finely ground and pressed into a pellet. The pellet was first fired at 700 ~ 900°C to dehydrate the silica gel and decompose the acetate and carbonate, then remixed and heated in a platinum crucible up to 1350°C (the melting point being around 1300°C). The sample was soaked at this temperature for two hours, cooled down to 1150°C at a rate of 2°/hr and finally quenched from this temperature to prevent the decomposition reaction of $BaCoSiO_4$ (c.f. 2.1.1). The sample was carefully crushed and examined with an optical microscope. A few single crystals were chosen according to their size, shape and appearance and further examined with an X-ray precession camera in order to check for twinning and/or superstructure and obtain unit-cell information. After a suitable single crystal was selected, intensity data were collected on a computer-controlled diffractometer.

TABLE 2.2

X-RAY POWDER DIFFRACTION PATTERN FOR $Ba_{0.4}Ca_{0.6}BeSiO_4$ INDEXED ON THE ORTHORHOMBIC CELL a = 4.7550(2) b = 7.9332(4), c = 8.5718(3) Å, V = 323.35(2) Å^3

h	k	l	d_{cal}(Å)	d_{obs}(Å)	I/I_o
0	1	1	5.8223	5.8181	15
0	0	2	4.2859	4.2834	17
1	0	1	4.1581	4.1570	22
1	1	0	4.0785	4.0786	32
1	1	1	3.6829	3.6818	6
1	1	2	2.9545	2.9542	10
0	2	2	2.9111	2.9119	47
1	2	1	2.8701	2.8708	100
0	0	3	2.8573	2.8568	12
0	1	3	2.6882	2.6883	28
0	3	1	2.5269	2.5276	9
1	0	3	2.4491	2.4490	34
2	0	0	2.3775	2.3779	32
1	3	0	2.3110	2.3113	15
2	1	1	2.2011	2.2011	14
0	0	4	2.1429	2.1434	6
1	2	3	2.0839	2.0839	61
2	2	0	2.0392	2.0393	10
1	3	2	2.0342	2.0346	6
2	2	1	1.9839	1.9837	19
0	4	0	1.9833		
0	2	4	1.8854	1.8852	10
2	2	2	1.8414	1.8416	19
0	4	2	1.7999	1.8000	6
1	4	1	1.7901	1.7903	12
2	1	3	1.7809	1.7811	18
2	3	1	1.7315	1.7316	8
2	3	2	1.6344	1.6339	4
1	0	5	1.6127	1.6127	5
2	0	4	1.5918	1.5919	5
1	3	4	1.5714	1.5714	7
3	1	0	1.5543	1.5542	5
1	4	3	1.5413	1.5413	15
2	4	0	1.5230	1.5231	12
1	5	0	1.5051	1.5048	6

1	2	5	1.4940	1.4938	13
2	2	4	1.4773	1.4773	10
0	4	4	1.4556	1.4555	4
3	2	1	1.4506	1.4506	12
2	4	2	1.4351	1.4352	8
0	0	6	1.4286	1.4285	10
0	5	3	1.3871	1.3867	22
3	0	3	1.3860		
3	3	0	1.3595	1.3593	5
1	1	6	1.3483	1.3484	6
3	2	3	1.3084	1.3085	6
3	3	2	1.2959	1.2958	6
1	6	1	1.2600	1.2600	5
1	4	5	1.2513	1.2513	5
2	4	4	1.2414	1.2412	5
2	0	6	1.2246		
0	0	7	1.2245	1.2244	13
2	5	3	1.1981	1.1980	11
3	0	5	1.1638		
1	6	3	1.1635	1.1636	16
0	4	6	1.1592	1.1592	9
4	2	0	1.1387		
2	4	5	1.1386	1.1384	4
1	2	7	1.1362	1.1363	19
3	4	3	1.1361		
3	2	5	1.1167	1.1169	10
2	6	2	1.1157		
3	5	1	1.1119	1.1124	6
0	3	7	1.1112	1.1109	5

2.1.6 Growth of $SrBeSiO_4$ and $Sr_{1-x}Ca_xBeSiO_4$ Single Crystals

Single crystals of $SrBeSiO_4$ and $Sr_{1-x}Ca_xBeSiO_4$ were grown by a flux method, using mixtures of $SrCO_3$, $CaCO_3$, BeO and silica gel and excess silica as a flux. A stoichiometric mixture (10 g) of $SrBeSiO_4$ with an excess of 40 wt% SiO_2 and a stoichiometric mixture (10 g) of $Sr_{0.65}Ca_{0.35}BeSiO_4$ with an excess of 25 wt% SiO_2 were preheated at 900°C for about 10 hours to dehydrate the silica gel and decompose the carbonates. The powders were then melted at 1450°C for $SrBeSiO_4$ and 1625°C for $Sr_{1-x}Ca_xBeSiO_4$, soaked at these temperatures for 4 hours and then slowly cooled at a rate of 3°C/hr down to 1150°C for $SrBeSiO_4$ and 1300°C for $Sr_{1-x}Ca_xBeSiO_4$. After quenching from these temperatures, the samples were then carefully crushed and examined under an optical microscope. The final products were inhomogeneous, consisting of a mixture of thin transparent and translucent lamellae. Powder X-ray diffraction showed that the thin transparent lamellae were well-crystallized $SrBeSiO_4$ or $Sr_{1-x}Ca_xBeSiO_4$ single crystals and the translucent lamellae were a mixture of the same poorly-crystallized compounds and silica glass.

A few single crystals with a colourless plate habit were chosen and further examined with an X-ray precession camera in order to check for twinning and/or superstructure phenomena. The best crystals were selected for data collection on a computer-controlled diffractometer.

2.2 Instrumentation

A combination of diffraction techniques, including powder X-ray and neutron

diffraction, electron diffraction and single crystal X-ray diffraction, was used for the characterization of reaction products and the determination of crystal structures. The principles of these techniques are briefly described below.

2.2.1 Powder X-ray Diffraction

In all syntheses, the nature of the final products was first analyzed by powder X-ray diffraction using a focusing Guinier-Hägg camera (CuKα_1 radiation, λ = 1.540598 Å) and silicon powder as an internal standard. The Guinier camera geometry makes use of an incident-beam monochromator which is simply a large single crystal cut and oriented so as to diffract the α_1 component of the Cu K_α incident radiation according to the Bragg's equation, $\lambda = 2d\sin\theta$. In addition to giving a very narrow wavelength band, the monochromator curvature is designed so that the divergent incident beam is diffracted into a convergent beam focused onto the diffraction circle which holds a strip of photographic film. The scheme graph of the camera is shown in Fig. 2.1a. The monochromatic radiation passes through the sample at X. Radiation which is not diffracted by the sample is focused on a beam stop at A, while diffracted beams are focused on the circle at B, C, etc., where their positions are recorded by the film. A schematic diffraction pattern is as shown in Fig. 2.1b where the line at $2\theta = 0°$ corresponds to the undiffracted beam at A in Fig 2.1(a). In the present work, the positions and intensities of the diffraction lines on the film were read with a computer-controlled LS-20 digital scanner (laser beam, scan step = 40 pm) and the diffraction data were then used to determine and refine the unit-cell parameters by means of a local least-squares refinement program.

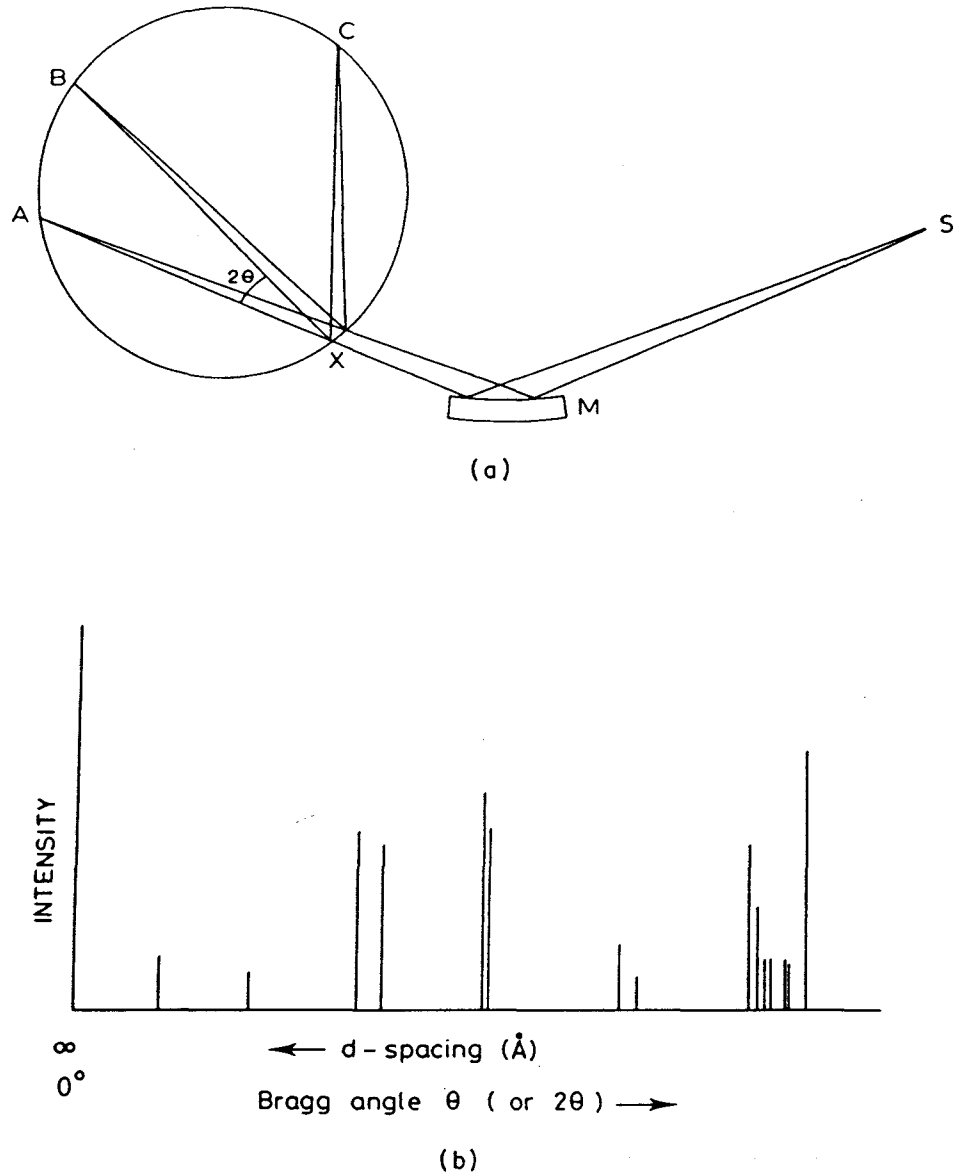

Fig. 2.1 (a)The geometry of the Guinier camera. Crystal monochromator M, Source S and sample X. (b) Schematic Guinier X-ray powder diffraction pattern.

Because of the similarity between the neutron nuclear scattering lengths of Na and K (0.363 and 0.367 $\times 10^{-12}$ cm) and the high resolution of the X-ray diffractometer, the powder diffraction data for $Na_{0.5}K_{0.5}GaSiO_4$ were collected on a Nicolet I2 automated X-ray diffractometer (Cu radiation, Cu $K_{\alpha 1}$ = 1.5406 Å and Cu $K_{\alpha 2}$ = 1.5448 Å). A detector, instead of film, is used to measure the scattered intensity of X-rays as a function of 2θ (Fig. 2.2). Diffraction data were collected over the diffraction angle range of $10° \leq 2\theta \leq 85°$ with a scanning speed of 0.06° 2θ/min (2θ step 0.03°, step time 30 seconds). The data were used to determine the structure of the $Na_{0.5}K_{0.5}GaSiO_4$ compound by a profile refinement carried out with a Rietveld analysis computer program [Young & Wiles, 1982; Howard & Hill, 1985].

2.2.2 Powder Neutron Diffraction

The compounds $BaMgSiO_4$ and $BaZnSiO_4$ contain both heavy Ba and light O atoms. Since X-rays are scattered by electrons, the intensity scattered by the oxygen atoms is very low relative to that scattered by the Ba atoms, therefore making it difficult to locate the oxygen atoms accurately. On the other hand, neutrons are scattered by nuclei and the intensities scattered by heavy atoms and light atoms are similar. For this reason, neutron powder diffraction data for $BaMgSiO_4$ and $BaZnSiO_4$ were collected at the McMaster Nuclear Reactor. The data were collected using a position sensitive detector (PSD) and a monochromatic neutron beam with a wavelength of 1.3913 Å obtained from the (200) reflection of a Cu single crystal monochromator. Four detector settings were used to cover a scattering range from 10° to 100° (2θ). The samples were loaded in a thin walled vanadium can (vanadium having a very small coherent scattering

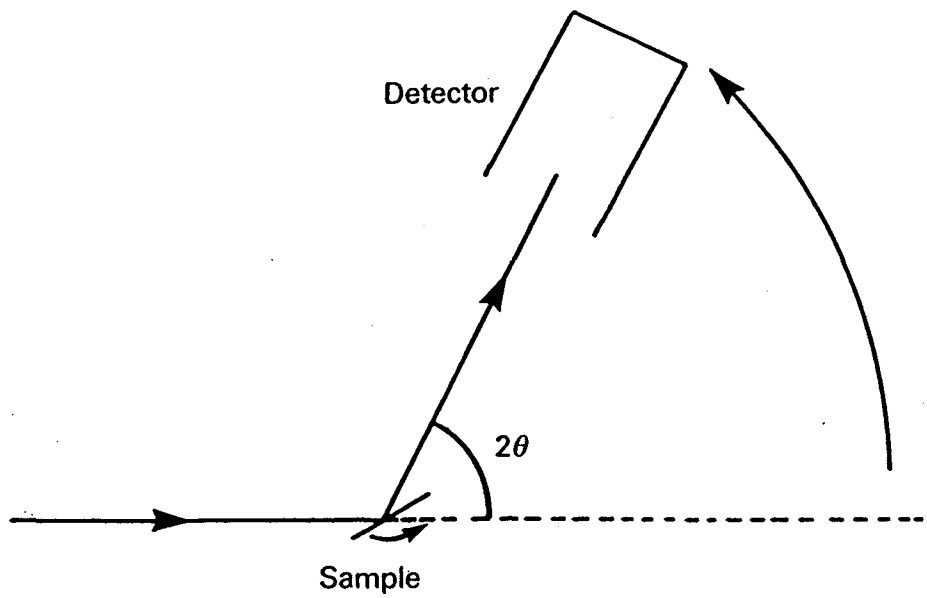

Fig. 2.2 Schematic diagram of a simple X-ray powder diffractometer.

length -0.038×10^{-12} cm). The raw data were corrected for detector geometry according to procedures established previously [Tompson et al., 1984] and the profile refinements were carried out with a local version of the Rietveld Profile Refinement program.

2.2.3 Electron Diffraction

Electrons that are diffracted by a crystal in a transmission electron microscope will form a diffraction pattern which can be projected on to a viewing screen (Fig. 2.3). Single crystal diffraction patterns, similar in appearance to zero-level X-ray precession photographs, can be obtained by selecting appropriately oriented individual crystallites from a powder sample. For this purpose, a finely ground powder is deposited onto a holey carbon film supported by a copper grid and the grid is fitted onto a double-tilt goniometer stage. In this study, a Philips CM-12 transmission electron microscope (TEM) operating at 120 keV was used to examine microscopic single crystals from the powder samples.

The interpretation of electron diffraction patterns is schematically shown in Fig. 2.4 in which the incident electron beam strikes a specimen and is diffracted by a set of lattice planes to form a diffraction spot on the photographic plate at a distance R from the centre of the diffraction pattern. By simple geometry, R is related to the camera length (L) by the equation

$$R/L = \tan 2\theta$$

The diffraction angles, θ, are very small ($1 \sim 2°$ for $\lambda = 0.0317$ Å corresponding to an accelerating potential of 120 kV) and the approximation $\tan 2\theta = 2\sin\theta$ can be made with very little error. Then $R/L = \lambda/d$ or $d = \lambda L/R$. Therefore, by measuring the

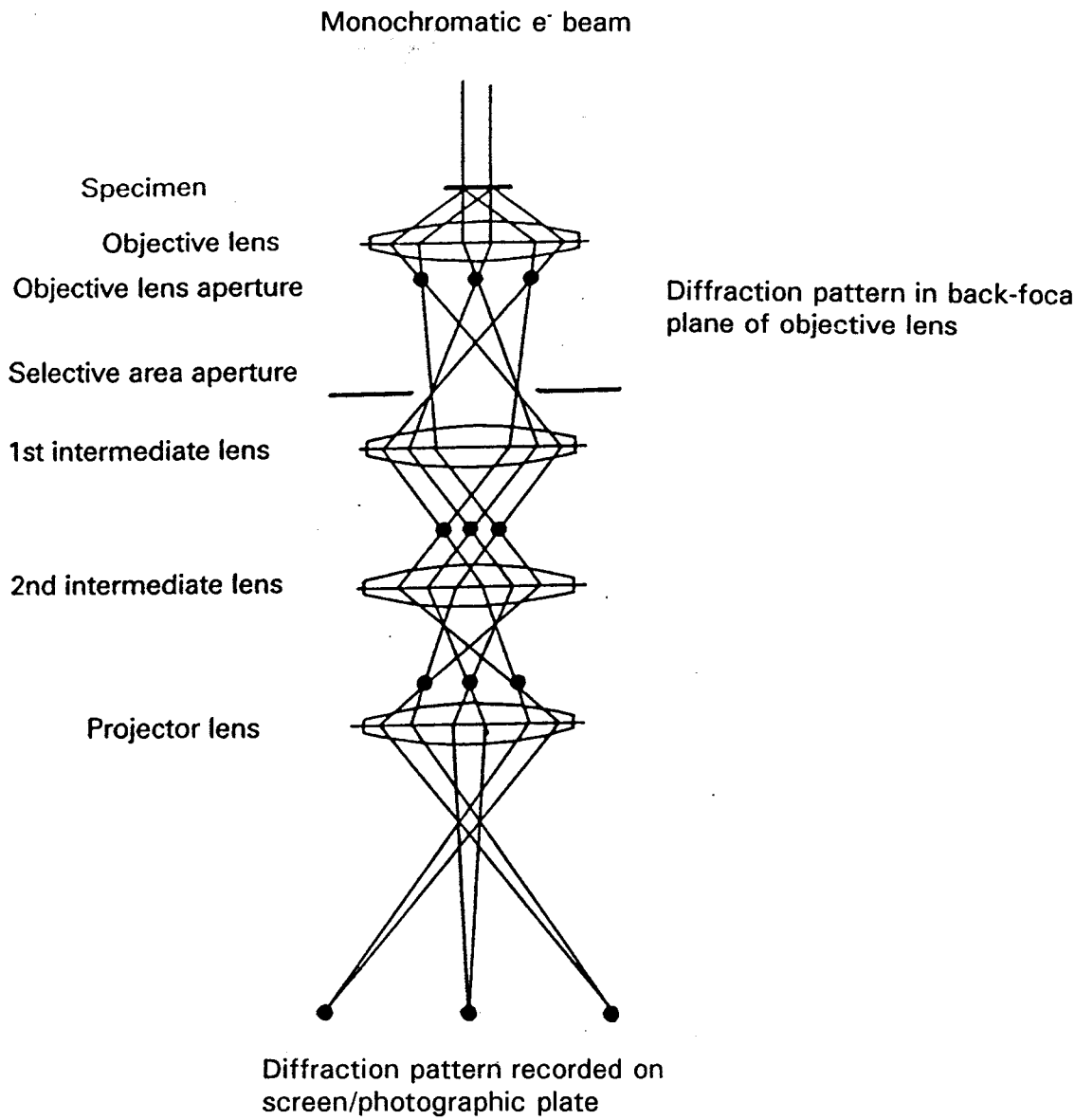

Fig. 2.3 Ray diagrams for the generation of diffraction patterns in a transmission electron microscope.

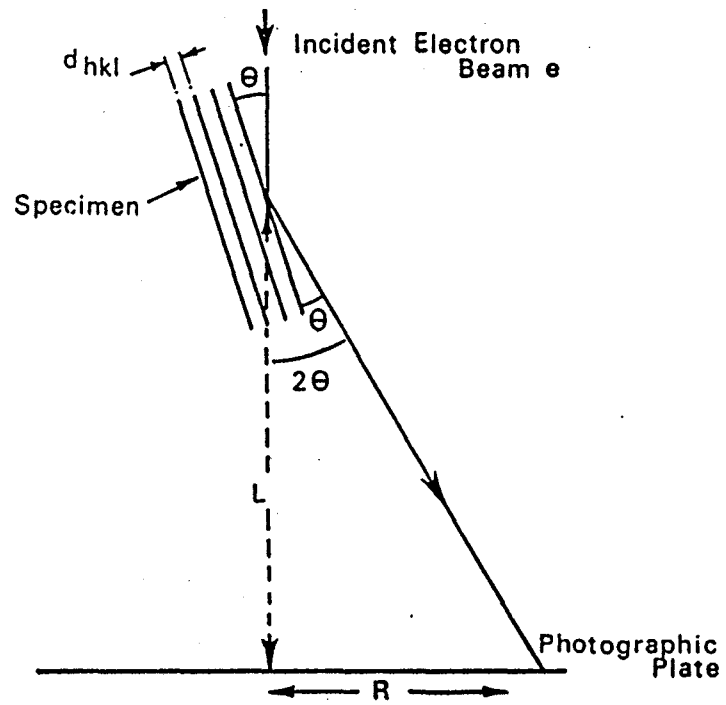

Fig. 2.4 The electron microscope considered as a simple electron diffraction camera.

distance R for individual reflections, the d-spacing of the set of lattice planes giving rise to these reflections can be determined. These d-spacings can then be used to obtain information relative to the size and symmetry of the unit-cell.

2.2.4 Single Crystal X-ray Precession Photographs

Single crystal X-ray precession photographs (λ Mo K_α = 0.7107 Å, with Zr filter; λ Cu K_α = 1.5418 Å, with Ni filter) were taken to examine twinning and superstructure phenomena of single crystals of $BaCoSiO_4$, $SrBeSiO_4$ and $Sr_{1-x}Ca_xBeSiO_4$. Each crystal was glued to the tip of a glass fibre and the fibre was mounted on a goniometer head and aligned on the camera so that one cell-axis was parallel to the X-ray beam. By keeping a piece of film tangential to the sphere of reflection of the moving crystal, the precession camera allows undistorted images of the reciprocal lattice to be obtained. In the present work, all compounds crystallized with hexagonal cells (cf. sections 3.1, 4.1 and 5.1) and, according to the interpretation of the diffraction patterns, photographs of two zero-layers containing the a_1^* and a_2^*-axes and the a^* and c^*-axis were taken for each candidate crystal. Based on these photographs , the best crystals were selected for data collection on a single crystal diffractometer.

2.2.5 Single Crystal X-ray diffractometer

The single crystal X-ray diffractometer data were collected on a Siemens R3m/V diffractometer (Ag K_α λ = 0.56086 Å) using the Siemens P3/V Data Collection System for the $BaCoSiO_4$ and $Sr_{1-x}Ca_xBeSiO_4$ compounds and on a P4 diffractometer (Mo K_α λ

= 0.71073 Å) using XSCANS Data Collection software for $SrBeSiO_4$. In both instruments, the monochromatic X-ray beam is obtained from a highly oriented graphite crystal monochromator. Both diffractometers are four-circle type and a schematic diagram of this type of diffractometer is shown in Fig. 2.5. Each set of planes hkl can be brought into the reflection position using the four ϕ, χ, ω and 2θ rotation. A counter mounted on the 2θ circle can then scan across the reflection to measure the diffracted intensity. Data sets containing 5080 collected reflections for $BaCoSiO_4$, 4128 (1065 used, cf. section 5.2) for $SrBeSiO_4$ and 4528 for $Sr_{1-x}Ca_xBeSiO_4$ were measured. Corrections were made for Lorentz, polarization and absorption effects (cf. 2.4). The resulting lists of observed $|F_{hkl}|$ values provided the basis for the determination of the crystal structures.

2.3 Powder Data Analysis

The Rietveld refinement method can be used for the analysis of both powder X-ray and neutron diffraction patterns. This is a method for crystal structure refinement which does not use integrated diffraction peak intensities, but directly employs the profile intensities obtained from step-scanning measurements of the powder pattern [Rietveld 1976; Rieltveld 1969].

During a Rietveld refinement, the structure parameters (unit-cell parameters, atom positions, temperature and occupancy factors), the scale factor, the background coefficients and the profile parameters describing peak widths and shapes, are varied in a least-squares procedure until the calculated powder pattern, based on the structure model, best matches the observed pattern. The quantity that is minimized by the least-

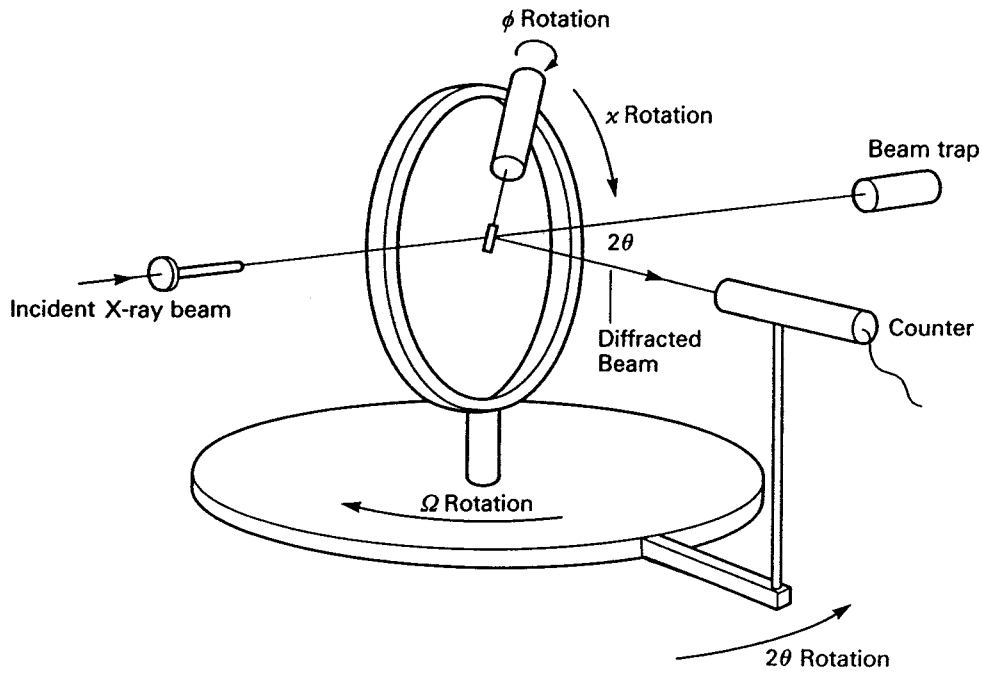

Fig. 2.5 A schematic graph of a four-circle diffractometer.

squares procedure is :

$$R = \sum w_i (Y_{iobs} - \frac{1}{c} Y_{ical})^2 \qquad (2.1)$$

The observed intensity, Y_{iobs}, at each step i in the diffraction pattern consists of a contribution from the Bragg reflections at the step plus the background. The Bragg peaks in a powder diffraction pattern are the integrated intensities and determined by atom positions and other structural parameters, such as scattering factors or lengths and temperature and occupancy factors. The background intensity can arise from several factors, including fluorescence from the sample, detector noise, thermal-diffuse scattering from the sample, disordered or amorphous phases in the samples, incoherent scattering, and scatter of the beam by the air, diffractometer slits and sample holder.

The calculated intensity, Y_{ical}, at point i in the diffraction pattern is determined according to the following equation:

$$Y_{ic} = Y_{ib} + \sum_{k} G_{ik} I_k \qquad (2.2)$$

where Y_{ib} is the background intensity, G_{ik} is a normalized peak profile function, I_k is the Bragg intensity, and k1...k2 are the reflections contributing intensity to point i.

The weighting factor, w_i, is equal to the inverse of the statistical counting error (generally equal to the square root of the observed intensity at step i).

The basic requirements for a Rietveld refinement are: (1) accurate powder diffraction intensity data measured in small intervals of 2θ, (2) a starting model that is reasonably close to the actual crystal structure and (3) a model that accurately describe shapes, widths and any systematic errors in the position of the Bragg peaks in the powder pattern.

The quality of the fit of the calculated model to the observed intensities is indicated by the following agreement indices:

Profile R-factor

$$R = \frac{\Sigma \left| Y_{io} - \frac{1}{c} Y_{ic} \right|}{\Sigma Y_{io}} \tag{2.3}$$

Weighted profile R-factor

$$R_{wp} = \left\{ \frac{\Sigma w_i \left[Y_{io} - \frac{1}{c} Y_{ic} \right]^2}{\Sigma w_i Y_{io}^2} \right\}^{\frac{1}{2}} \tag{2.4}$$

Nuclear (Bragg's) R-factor

$$R_B = \frac{\Sigma \left| I_{ko} - \frac{1}{c} I_{kc} \right|}{I_{ko}} \tag{2.5}$$

Expected R-factor

$$R_{exp} = \left\{ \frac{N-P}{\Sigma w_i Y_{io}^2} \right\}^{\frac{1}{2}} \tag{2.6}$$

Goodness-of-fit

$$GOF = \frac{\Sigma w_i (Y_{io} - Yic)^2}{N-P} = \left\{ \frac{R_{wp}}{R_{exp}} \right\}^2 \tag{2.7}$$

where Y_{io} and Y_{ic} are the observed and calculated intensities at point i, w_i is the weight assigned to each step intensity, I_{ko} and I_{kc} are the observed and calculated intensities for the Bragg peak k. N is the number of data points in the pattern and P is the number of parameters refined.

2.4 Single Crystal Data Analysis

After the collection of single crystal X-ray intensity data, a crystal structure can be solved by different methods among which the Patterson method and the direct methods are the most commonly used nowadays. A basic structure model with approximate coordinates for the heavy atoms or all the atoms in the unit-cell is set up by these methods first and then the positions can be optimized by a least-squares refinement. The coordinates are adjusted to minimize the function:

$$D = \sum_{hkl} w_{hkl}(|F_{hkl}^{obs}| - |F_{hkl}^{cal}|)^2 \qquad (2.8)$$

$|F_{hkl}^{obs}|$ in equation (2.8) is the observed structure factor and is related to the intensity of the reflection according to

$$I_{hkl} = sLPF^2 \qquad (2.9)$$

where s is a scale factor; L is the Lorentz (geometrical) correction ($L = (\sin 2\theta)^{-1}$ for single crystal data), P is the polarization correction ($P = (1 + \cos^2 2\theta)/2$). Psi-scan absorption correction is also made according to the shape of the single crystal. $|F_{hkl}^{cal}|$ in equation (2.8) is the corresponding calculated structure factor and is described by the following equation:

$$F_{hkl}^{cal} = \sum_j f_j\{\exp[2\pi i(hx_j + ky_j + lz_j)]\} \exp[-B_j(\sin^2\theta)/\lambda^2] \qquad (2.10)$$

where f_j is the scattering factor of atom j with the fractional coordinates x_j, y_j and z_j; B_j is the isotropic temperature factor equal to $8\pi^2 u_j^2$ (u: the mean square amplitude of

vibration of atom j). In most refinements, The thermal motion is described anisotropically by an ellipsoid, with six parameters. w_{hkl} in equation (2.8) is the weight given to the observation $|F_{hkl}^{obs}|$, $w_{hkl} = 1/(\sigma^2|F_{hkl}^{obs}|)$.

The quality of the fit for a structure refinement is measured in terms of a "reliability factor" or R-factor:

$$R=\frac{\sum_{hkl} |F_{hkl}^{obs} - F_{hkl}^{cal}|}{\sum_{hkl} |F_{hkl}^{obs}|} \tag{2.11}$$

or , a weighted R-factor

$$wR=\left[\frac{\sum_{hkl} w_{hkl}^2 |F_{hkl}^{obs} - F_{hkl}^{cal}|^2}{\sum_{hkl} w_{hkl} |F_{hkl}^{obs}|^2}\right]^{1/2} \tag{2.12}$$

and the goodness-of-fit

$$GOF=\left[\frac{\sum w_{hkl} \left(|F_{hkl}^{obs}| - |F_{hkl}^{cal}|\right)^2}{n-m}\right]^{\frac{1}{2}} \tag{2.13}$$

where n is the number of observed reflections and m is number of the parameters refined.

CHAPTER 3

THE $BaTSiO_4$ (T = Co, Mg, Zn) COMPOUNDS

The compounds $BaTSiO_4$ (T = Zn, Mg) and $BaZnGeO_4$ had been previously reported to crystallize with small hexagonal unit cells ($A \approx 5.25$ Å and $C \approx 8.75$ Å) [Dinh, 1964], suggesting them to be isostructural with kalsilite ($KAlSiO_4$) [Perrotta, 1965]. However, later studies established the existence of a ($\sqrt{3}\times A, 4\times C$) superstructure in the case of $BaZnGeO_4$ [Takei, 1980] and the average structure was determined by neglecting the weak and incommensurate $4\times C$ superstructure at room temperature [Iijima, 1982]. This chapter deals with the re-investigation of the compounds $BaTSiO_4$ (T = Mg, Zn) and the study of a new compound $BaCoSiO_4$ by means of single-crystal X-ray diffraction (T = Co) and powder neutron diffraction (T = Mg, Zn).

3.1 Powder X-ray and Electron Diffraction

The nature of all four compounds $BaCoSiO_4$, $BaMgSiO_4$, $BaMg_{0.5}Zn_{0.5}SiO_4$ and $BaZnSiO_4$ was characterized by powder X-ray diffraction using a Guinier-Hägg camera ($CuK_{\alpha 1}$ radiation, $\lambda = 1.540598$ Å). Their diffraction patterns were indexed by means of the computer program LSUDF on a similar ($\sqrt{3}\times A$, C) hexagonal unit cell, corresponding to a superstructure of the basic (A, C) kalsilite cell required by the presence of a few weak {hkl, $h-k \neq 3n$} reflections (cf. Tables 3.1 and 3.2). The unit

cell parameters of the four compounds are shown in Table 3.3. Interestingly, the variation in cell parameters and cell volume do not correlate with the practically identical Mg-O, Zn-O and Co-O bond lengths predicted from ionic radii (1.95, 1.96 and 1.98 Å for tetrahedrally-coordinated atoms) [Shannon, 1976] (but cf. Section 3.4).

All four compounds were also examined by electron diffraction /microscopy using a Philips CM-12 transmission electron microscope operating at 120 kV and equipped with a double-tilt goniometer stage. The electron diffraction patterns confirmed the presence of a $\sqrt{3}\times A$ superstructure in the basal plane of the hexagonal cell (Fig.3.1a) and also showed the absence of a superstructure along the c axis (Fig.3.1b).

These results therefore indicate that the compounds $BaCoSiO_4$ $BaMgSiO_4$, $BaMg_{0.5}Zn_{0.5}SiO_4$ and $BaZnSiO_4$ adopt a structure more complex than the simple kalsilite structure and that they are structurally closely related to the room-temperature form of $BaZnGeO_4$ [Iijima, 1982]. No extra reflections were found for the $BaMg_{0.5}Zn_{0.5}SiO_4$ compound, which indicates that the tetrahedral Mg and Zn atoms are randomly distributed in the tetrahedral framework. As expected, the cell parameters of $BaMg_{0.5}Zn_{0.5}SiO_4$ are intermediate between those of $BaMgSiO_4$ and $BaZnSiO_4$ (cf. Table 3.3) with values indicating that the system obeys Vegard's law well [West, 1988].

3.2 Powder Neutron Refinement of the $BaMgSiO_4$ and $BaZnSiO_4$ Structures

The powder neutron diffraction data were recorded at room temperature over the angular range $10° < 2\theta < 92°$ at four different settings of the position-sensitive detector. After correction of the raw data for detector geometry [Tompson, 1984], the

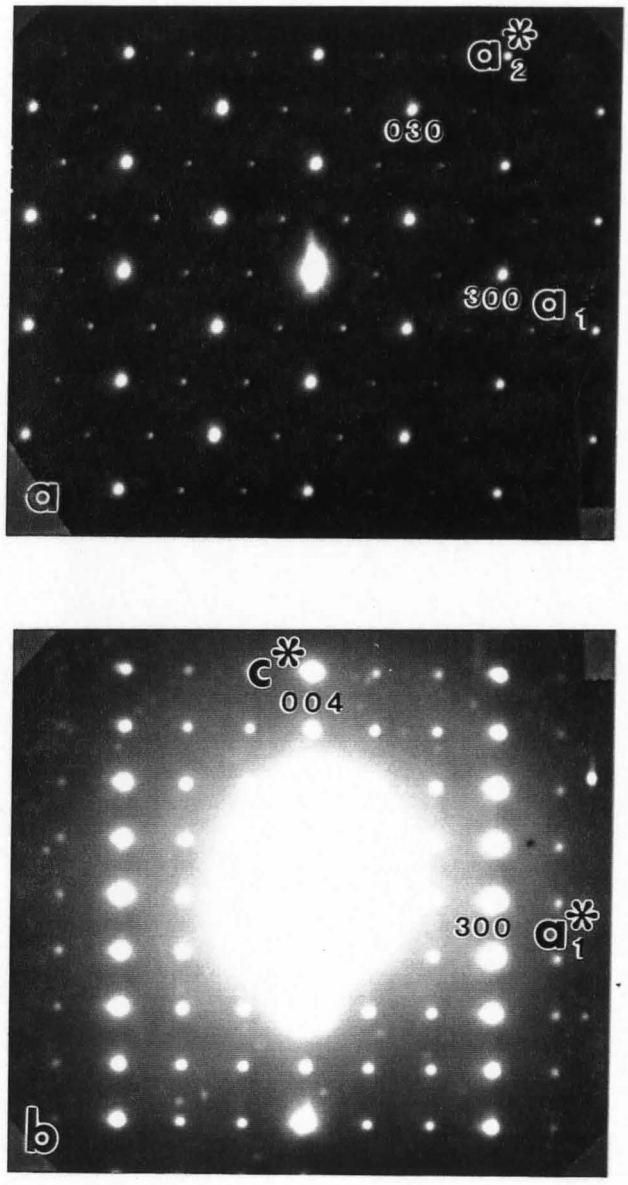

Fig. 3.1 [001] (a) and [010] (b) zone-axis electron diffraction patterns of $BaTSiO_4$ (T = Co, Mg, Zn). Note the $\sqrt{3}\times A$ superstructure in the basal plane of the hexagonal unit-cell and the absence of superstructure along the c axis. The $\{00l,\ l = 2n+1\}$ reflections (forbidden in the $P6_3$ space group) appear by double diffraction.

profile refinement was carried out with a local version of the Rietveld program. The following scattering lengths (10^{-12} cm) were used: Ba (0.525), Mg (0.5357), Zn (0.568), Si (0.4149) and O (0.5805) [Sears, 1984].

The refinements of the $BaMgSiO_4$ and $BaZnSiO_4$ structures were performed in a similar way, starting with the cell parameters determined by powder X-ray diffraction (cf. Table 3.3) and the atomic positions determined in the $P6_3$ space group for the isostructural sub-cell of the $BaZnGeO_4$ compound [Takei, 1980]. The Ba atoms were positioned on the 2a and 2b sites, and the Si, O and Mg (or Zn) atoms occupied three sets of general 6c sites.

The structural parameters allowed to vary during the refinements included the cell parameters, the atomic coordinates and the isotropic temperature factors. A complete ordering of the Si/Mg and Si/Zn atoms was assumed initially and later confirmed by the final refinements and bond length data. Due to strong correlations between variables, it was found necessary to apply constraints on the temperature factors of similar atoms: the temperature factors of the three Ba atoms were constrained to be equal as well as those of the tetrahedral atoms Si and Mg (or Zn); the temperature factors of the first three oxygen atoms were also set to be equal but that of O(4) was left unconstrained. The refinements then converged smoothly to the following agreement indices: weighted profile index R_{wp} = 0.042/0.054, nuclear index R_n = 0.026/0.046, and expected index Re = 0.026/0.027 for $BaMgSiO_4$/$BaZnSiO_4$ respectively. The final positional and thermal parameters are listed in Tables 3.4 and 3.5. The calculated, observed and difference profiles are shown in Fig. 3.2 and Fig. 3.3 for $BaMgSiO_4$ and $BaZnSiO_4$. The intensities of the $\sqrt{3}\times A$ superstructure reflections are similar for both compounds and much stronger than those observed by X-ray diffraction (cf. Table 3.1). Selected bond lengths,

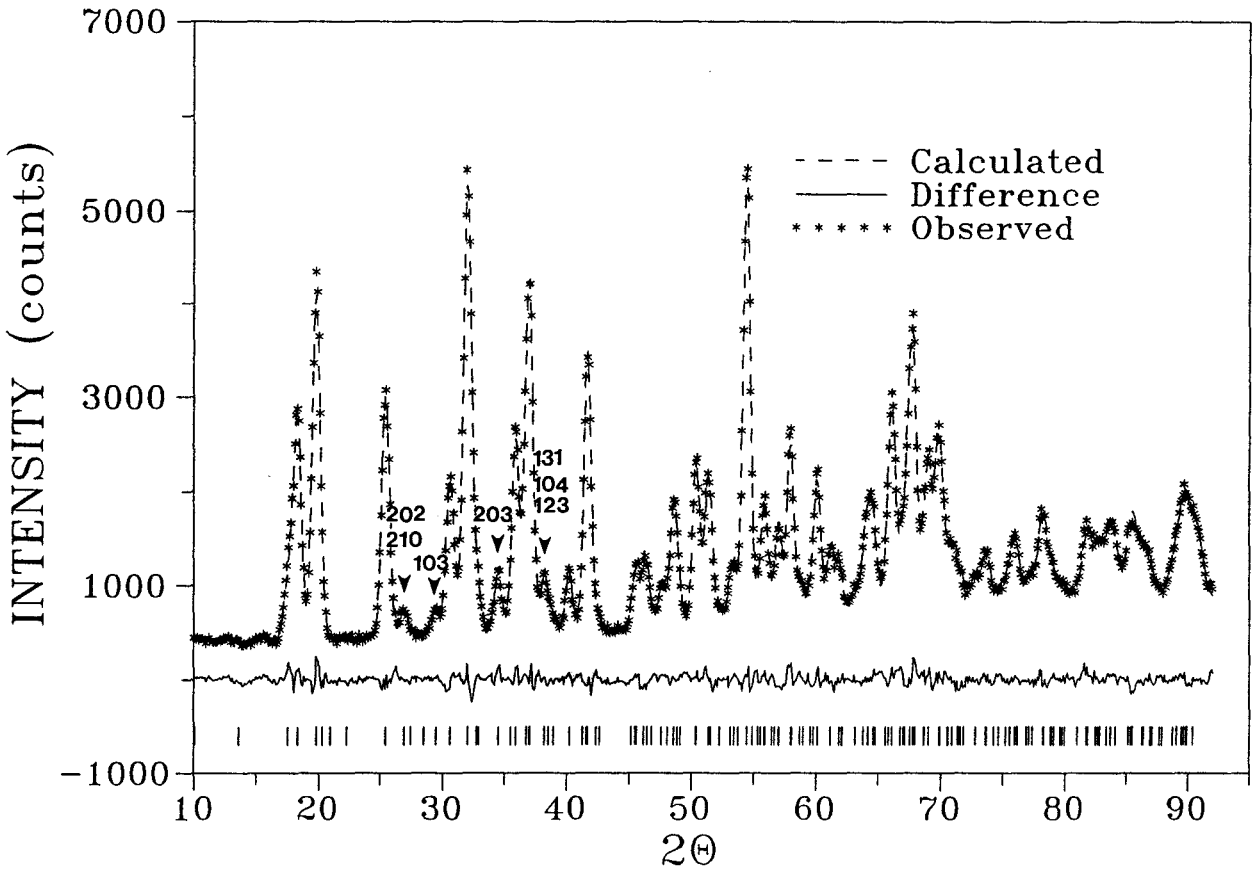

Fig. 3.2 Observed, calculated, and difference powder neutron diffraction profiles for $BaMgSiO_4$. The (|) signs indicate the Bragg peak positions. The (↓) signs indicate the ($\sqrt{3}\times A$) superstructure reflections.

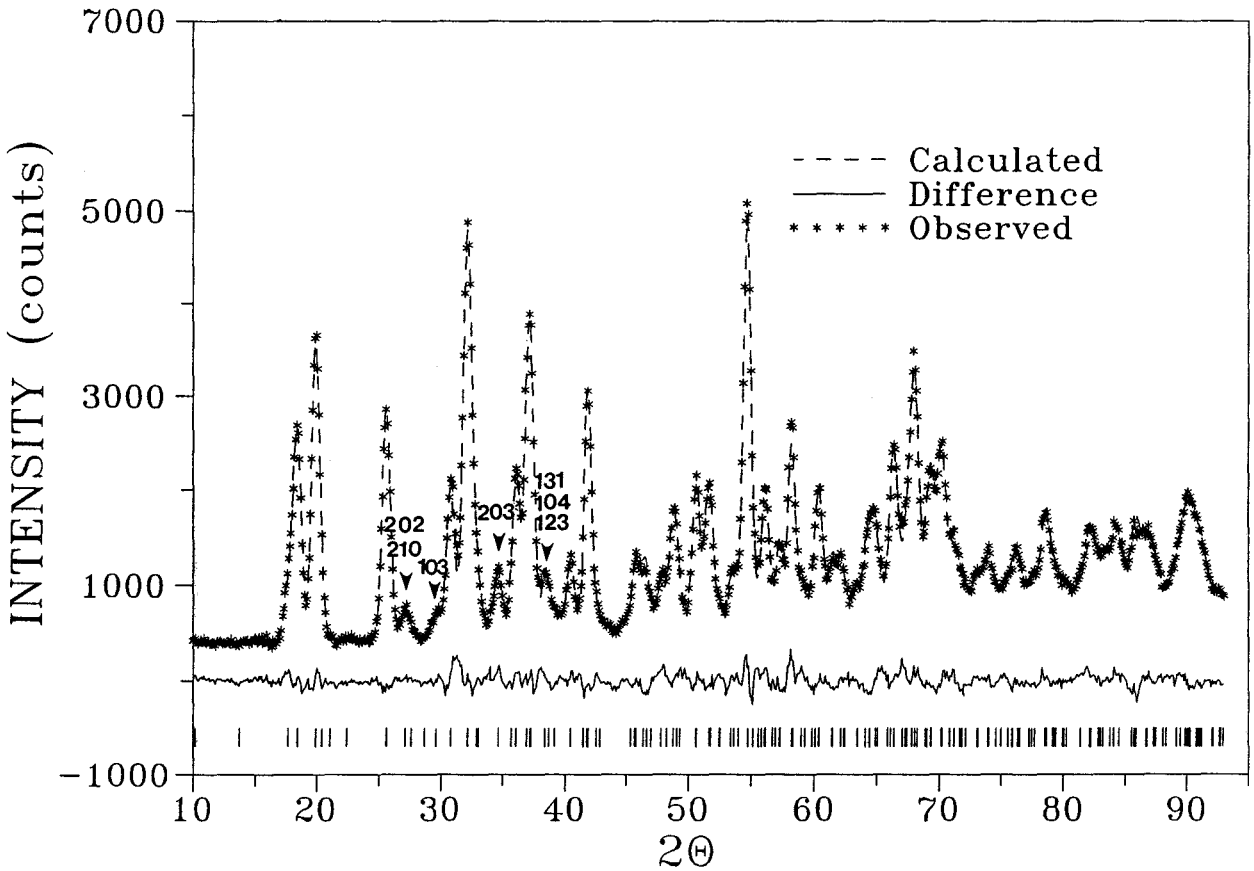

Fig. 3.3 Observed, calculated, and difference powder neutron diffraction profiles for $BaZnSiO_4$. The (|) signs indicate the Bragg peak positions. The (↓) signs indicate the ($\sqrt{3}\times A$) superstructure reflections.

bond angles and bond valences (s calculated from the empirical parameters of Altermatt and Brown [1985]) are listed in Tables 3.6 and 3.7. It should be noted that the larger esd's for the z-coordinates in Tables 3.4 and 3.5 are a result of the strong correlations noted earlier and that the larger unconstrained temperature factors of the O(4) atoms suggest positional disorder similar to that observed in , for instance, $KAlSiO_4$ [Perrotta, 1965] and $BaZnGeO_4$ [Iijima, 1982].

3.3 Single Crystal X-ray Refinement of the $BaCoSiO_4$ Structure

The X-ray intensity data for $BaCoSiO_4$ were collected from a single crystal with dimensions of 0.30 × 0.80 × 0.10 mm^3 on a Siemens R3m/v diffractometer using graphite-monochromatized AgKα radiation. All crystal data, data collection parameters, and results of analysis are listed in Table 3.8. The unit cell constants a (= 9.126(2) Å) and c (= 8.683(4) Å) determined from 25 single reflections are in very close agreement with those refined from powder diffraction data (cf. Table 3.3). The structure was solved in the $P6_3$ space group by direct methods and successive Fourier syntheses. In order to be consistent with the $BaMgSiO_4$ and $BaZnSiO_4$ structures, the Ba(1) atom was chosen to fix the origin at (0 0 1/4). An ordered arrangement of the tetrahedral Co and Si atoms was also assumed initially and later confirmed during the refinement. Using 1062 observed reflections ($F > 6\sigma(F)$), a full-matrix least-squares refinement was carried out with anisotropic temperature factors for all atoms, converging to final agreement indices $R = 0.035$ and $R_w = 0.042$. The final atomic positions and equivalent isotropic displacement parameters are listed in Table 3.9 and the anisotropic thermal parameters are shown in Table 3.10. Selected bond lengths, bond angles and associated bond

valences [Altermatt and Brown, 1985] are given in Table 3.11.

The single crystal X-ray refinement of the $BaCoSiO_4$ structure yields a better precision (by about a factor of 10) for the atomic coordinates and bond distances than the neutron powder refinements of the $BaMgSiO_4$ and $BaZnSiO_4$ structures. The three compounds are, nevertheless, clearly isostructural with very similar atomic positions and environments. It should be noted in particular that the temperature factor of the O(4) atom in the Co compound is again larger than those of the other oxygen atoms (especially U_{11} and U_{22}, cf. Table 3.10), suggesting positional disorder of O(4) around the pseudo 3-fold axis.

3.4 Description of the Structures and Discussion

Except for minor shifts in atomic positions (cf. Tables 3.4, 3.5 and 3.9), the structures of the three compounds $BaTSiO_4$ (T = Co, Mg, Zn) are identical and only the more accurately determined structure of $BaCoSiO_4$ is shown in Fig.3.4, viewed along the c-axis of the hexagonal unit-cell. Like in the structure of kalsilite, $KAlSiO_4$ [Perrotta, 1965], the tetrahedral framework of the $BaCoSiO_4$ structure consists of six-membered rings of corner-shared tetrahedra pointing alternatively up and down. All rings are identical with an almost triangular shape and are stacked along the c-direction, joined via the O(4) oxygen atoms in a staggered configuration, again similar to that found in kalsilite.

As indicated by the structural refinements and the bond length data (cf. Tables 3.6, 3.7 and 3.11), the tetrahedral T (= Co, Mg, Zn) and Si atoms are completely ordered and, in the $BaCoSiO_4$ structure shown in Fig.3.3, all the large CoO_4 tetrahedra

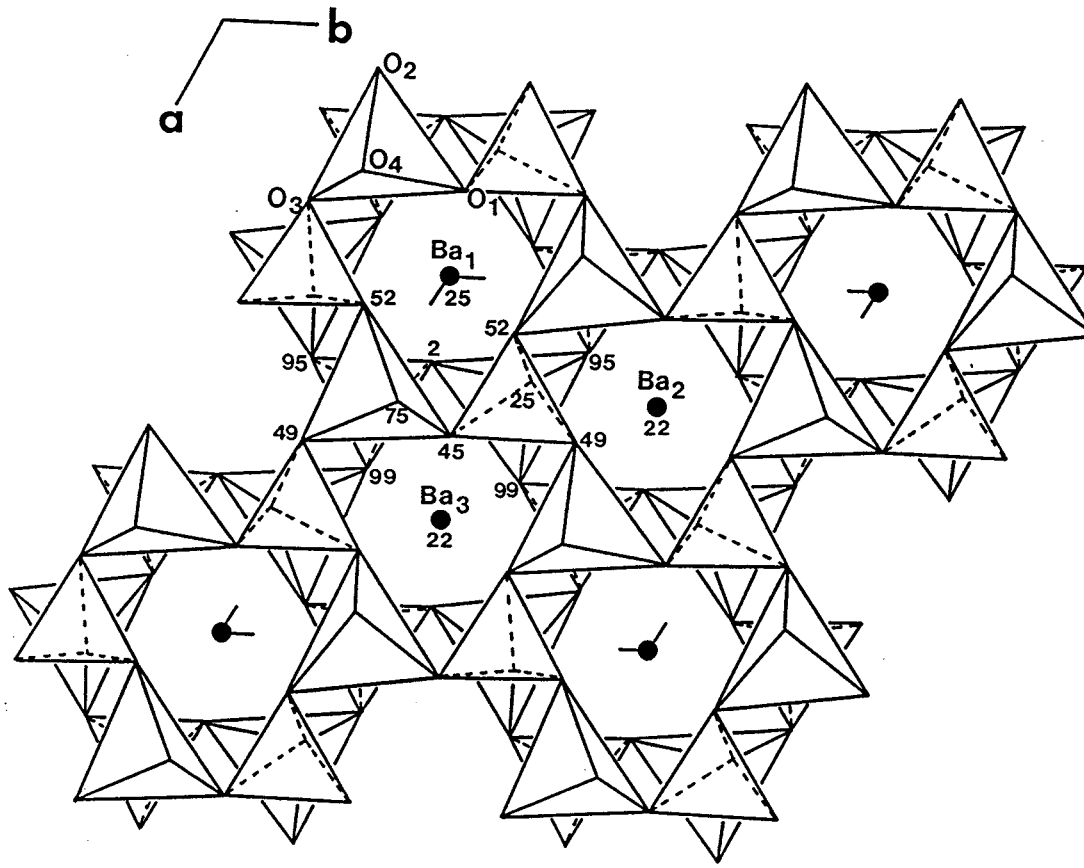

Fig. 3.4 The structure of $BaCoSiO_4$ viewed along the c-axis. It consists of a Ba-stuffed tetrahedral framework derived from that of SiO_2 tridymite and similar to that of $KAlSiO_4$ kalsilite. The Co and Si atoms are fully ordered with large CoO_4 tetrahedra pointing up and small SiO_4 tetrahedra pointing down. Atom heights are given in units of c/100. The structures of $BaMgSiO_4$ and $BaZnSiO_4$ are essentially identical.

point up while all the small SiO_4 tetrahedra point down. Such a fully ordered arrangement could be expected in spite of the high temperatures used for the powder syntheses and the single crystal growth (1150 ~ 1560°C) because of the large differences in formal ionic valences (T^{2+} vs Si^{4+}) and in bond lengths (1.92 ~ 1.96 Å for T-O vs 1.63 Å for Si-O). A similar tetrahedral ordering has also been reported for the isostructural room-temperature phase of $BaZnGeO_4$ [Iijima, 1982].

All three crystallographically independent Ba atoms of the $BaTSiO_4$ structure are located on the three-fold axes of the unit-cell with, however, different coordination environments: in $BaCoSiO_4$ for example, Ba(1) is nine-coordinated (six O(1)'s plus three O(4)'s at an average distance of 2.89 Å), Ba(2) is also nine-coordinated (three O(2)'s, three O(3)'s and three O(4)'s at an average distance of 2.91 Å) but Ba(3) is only six-coordinated (three O(2)'s plus three O(3)'s at a shorter average distance of 2.73 Å) (cf. Table 3.11). It can be seen in Fig. 3.4 that the lower coordination of the Ba(3) atom arises from the displacement of the O(4) atom (at height 25) away from Ba(3) and towards Ba(1) and Ba(2) so that the distance between Ba(3) and O(4) is raised to 3.62 Å. [Note that the Ba(2) and Ba(3) positions alternate at heights 25 and 75 on the three-fold axes so that the O(4) atom at height 75 is also displaced away from Ba(3)]. It is clear also from Fig.3.4 that this shift of the O(4) atom from its ideal position at (1/3,1/3,1/4) or (2/3,2/3,3/4) is the main factor behind the formation of the $\sqrt{3}\times A$ superstructure in the basal plane of the $BaTSiO_4$ unit-cells. This atom shift is similar to that commonly observed in the structures of the kalsilite-nepheline series, $(K,Na)AlSiO_4$, [e.g. Merlino, 1984] and appears necessary in order to i) release the strain in the Co-O(4)-Si bond angle which is reduced to 148.6(5)° and ii) accommodate the bonding requirements of all three Ba atoms which, in spite of different environments,

end up with similar bond valence sums (cf. Table 3.11). [The small variations in bond valence sums observed in the cases of $BaMgSiO_4$ and $BaZnSiO_4$ in Tables 3.6 and 3.7 are probably the result of less accurate refinements using powder data]. It is worth noting, however, that the bond valence sums around the Ba atoms in all three compounds are lower than expected and indicate that the Ba-O bonds are stretched in the room-temperature structures (i.e. the Ba atoms are somewhat too small relative to the size of the framework cavities). This result is consistent with the observation that, at least for $BaCoSiO_4$, the structure is stable at high temperature only.

The displacement of the O(4) atom off the pseudo 3-fold axis also corresponds to the collapse of the tetrahedral framework around the barium atoms, involving the tilting of the CoO_4 and SiO_4 tetrahedra around horizontal axes approximately parallel to the [110] or equivalent directions (cf. Fig.3.4). The degree of framework collapse in the $BaTSiO_4$ structures can be qualitatively estimated from the difference (Δz) between the z-coordinates of the O(1) and O(3) atoms: Δz is equal to 0.060(6), 0.064(6) and 0.075(1) for $BaMgSiO_4$, $BaZnSiO_4$ and $BaCoSiO_4$ respectively (cf. Tables 3.4, 3.5 and 3.9), indicating an increasing degree of tetrahedral tilting. The same effect is also apparent from a comparison of the T-O(4)-Si bond angles which are equal to 157.9(13), 156.1(16) and 148.6(5) for T = Mg, Zn and Co respectively. Interestingly, these Δz values and bond angles correlate very well with the trend observed for the c-parameters of the hexagonal unit-cells (cf. Table 3.3) showing that the shorter c-axis of the $BaCoSiO_4$ structure results from a more pronounced collapse of its tetrahedral framework, the origin of which probably resides in the slightly larger size of the CoO_4 tetrahedron.

TABLE 3.1

X-RAY POWDER DIFFRACTION PATTERNS FOR $BaTSiO_4$ (T = Zn, Mg, Co)

			$BaZnSiO_4$			$BaMgSiO_4$			$BaCoSiO_4$**		
h	k	l	d_{cal}(Å)	d_{obs}(Å)	I/I_o	d_{cal}(Å)	d_{obs}(Å)	I/I_o	d_{cal}(Å)	d_{obs}(Å)	I/I_o
1	1	0	4.5478	4.5440	28	4.5613	4.5632	40	4.5616	4.5663	13
0	0	2	4.3626	4.3567	5	4.3748	4.3753	5	4.3404	4.3392	5
1	1	1	4.0328	4.0316	17	4.0447	4.0483	8	4.0381	4.0415	6
1	1	2	3.1482	3.1498	100	3.1573	3.1592	100	3.1446	3.1473	100
3	0	0	2.6257	2.6246	70	2.6335	2.6363	44	2.6336	2.6344	31
3	0	1	2.5143	2.5143	6	2.5217	2.5225	4	2.5202	2.5201	3
2	1	2#	2.4591	2.4571	3	2.4663	2.4671	-*	2.4603	2.4595	2
1	1	3	2.4502	2.4486	9	2.4572	2.4559	-*	2.4436	2.4429	2
2	2	0	2.2739	2.2740	8	2.2806	2.2820	10	2.2808	2.2815	4
3	0	2	2.2496	2.2499	16	2.2562	2.2565	28	2.2516	2.2515	8
2	2	1	2.2004	2.1999	7	2.2069	2.2070	-*	2.2059	2.2051	2
0	0	4	2.1813	2.1812	14	2.1874	2.1879	11	2.1704	2.1709	5
3	1	1#	2.1193	2.1212	-*						
1	0	4#	2.1022	2.1023	-*	2.1081	2.1103	-*	2.0929	2.0928	-*
2	2	2	2.0164	2.0161	38	2.0223	2.0233	28	2.0191	2.0196	16
1	1	4	1.9668	1.9667	19	1.9723	1.9725	15	1.9599	1.9601	6
3	0	3	1.9546	1.9555	-*						
2	2	3	1.7914	1.7912	6	1.7966	1.7969	-*	1.7913	1.7919	1
2	1	4#	1.7596	1.7604	-*						
4	1	0	1.7189	1.7187	7	1.7240	1.7244	8	1.7241	1.7238	3
4	1	1	1.6865	1.6867	4	1.6911	1.6898	-*			
3	0	4	1.6778	1.6776	22	1.6827	1.6830	13	1.6749	1.6743	6
1	1	5	1.6292	1.6289	9	1.6228	1.6225	2			
4	1	2	1.5992	1.5988	40	1.6040	1.6042	29	1.6023	1.6025	17
2	2	4	1.5741	1.5741	10	1.5787	1.5787	8	1.5723	1.5716	4
3	1	4	1.5481	1.5474	-*	1.5421	1.5417	2			
3	3	0	1.5159	1.5156	22	1.5204	1.5204	14	1.5205	1.5204	10
4	1	3	1.4798	1.4801	7	1.4841	1.4844	1	1.4812	1.4816	2
0	0	6	1.4542	1.4543	2	1.4583	1.4580	1			
3	0	5				1.4575					
3	3	2	1.4319	1.4324	-*	1.4362	1.4361	2			
3	2	4#	1.3916	1.3914	-*						
1	1	6	1.3851	1.3849	10	1.3890					
2	2	5	1.3844			1.3883	1.3884	5	1.3816	1.3808	2
1	1	6							1.3792		
4	1	4	1.3501	1.3503	12	1.3540	1.3536	10	1.3500	1.3503	-*
6	0	0	1.3128	1.3127	9	1.3167	1.3161	5	1.3168	1.3167	3
2	1	6#	1.3067	1.3069	2	1.3104			1.3022		
4	0	5	1.3061			1.3098	1.3096	-*			
6	0	1							1.3019	1.3015	1

5	1	3	1.2722			1.2760					
3	0	6	1.2721	1.2721	12	1.2757	1.2755	8	1.2682	1.2682	4
5	2	0	1.2613	1.2614	3	1.2651	1.2649	3			
6	0	2	1.2571	1.2571	3	1.2609	1.2600	3	1.2601	1.2602	2
3	2	5				1.2589					
3	3	4	1.2448	1.2448	-*	1.2485	1.2486	9			
2	2	6	1.2251	1.2251	8	1.2286					
4	1	5	1.2246			1.2281	1.2277	6			
5	2	2	1.2117	1.2116	20	1.2153	1.2147	15	1.2146	1.2143	9
5	2	3	1.1572	1.1575	3						
5	3	0	1.1253								
6	0	4	1.1248	1.1249	6	1.1281	1.1280	5	1.1258	1.1261	2
6	1	3				1.1135					
4	1	6	1.1102	1.1105	21	1.1134	1.1133	5			
4	4	2							1.1030	1.1029	-*

* The positions of these very weak lines could only be measured by eye.

** Fewer lines could be measured because of the higher background resulting from cobalt fluorescence with Cu $K\alpha_1$ radiation.

Superstructure reflections of the type { hkl, h-k $\neq$ 3n } requiring a $\sqrt{3} \times$A axis.

TABLE 3.2

X-RAY POWDER DIFFRACTION PATTERN FOR $BaMg_{0.5}Zn_{0.5}SiO_4$

h	k	l	d_{cal}(Å)	d_{obs}(Å)	I/I_o
1	1	0	4.5537	4.5505	26
0	0	2	4.3667	4.3624	25
1	1	1	4.0378	4.0355	10
1	1	2	3.1518	3.1517	100
3	0	0	2.6291	2.6288	58
3	0	1	2.5175	2.5172	6
1	1	3	2.4528	2.4524	4
2	2	0	2.2768	2.2767	12
3	0	2	2.2523	2.2525	24
2	2	1	2.2032	2.2032	4
0	0	4	2.1834	2.1832	12
2	2	2	2.0189	2.0190	38
1	1	4	1.9688	1.9687	20
2	2	3	1.7935	1.7935	3
4	1	0	1.7211	1.7212	10
3	0	4	1.6797	1.6797	20
1	1	5	1.6308	1.6309	6
4	1	2	1.6012	1.6013	43
2	2	4	1.5759	1.5760	12
3	3	0	1.5179	1.5180	23
4	1	3	1.4816	1.4819	4
0	0	6	1.4556	1.4558	3
3	0	5	1.4549		
5	0	3#	1.3869		
1	1	6	1.3865	1.3864	9
4	1	4	1.3517	1.3518	16
6	0	0	1.3145	1.3146	8
2	1	6#	1.3080	1.3078	3
4	0	5#	1.3075		
5	1	3#	1.2738		
3	0	6	1.2734	1.2734	12
5	2	0	1.2630	1.2628	3
6	0	2	1.2587	1.2587	3
2	2	6	1.2264	1.2262	9
4	1	5	1.2260		
5	2	2	1.2132	1.2133	23
5	3	0#	1.1267		
6	0	4	1.1262	1.1264	6
6	1	3#	1.1116	1.1116	9
4	1	6	1.1114		

Superstructure reflections of the type { hkl, h-k ≠ 3n } requiring a $\sqrt{3}\times$A axis.

TABLE 3.3

UNIT-CELL PARAMETERS (Å) AND VOLUMES (Å^3) FOR THE $BaTSiO_4$ (T=Co,Mg,Zn) AND $BaMg_{0.5}Zn_{0.5}SiO_4$ COMPOUNDS REFINED FROM POWDER X-RAY DIFFRACTION DATA

	a	c	V
$BaCoSiO_4$	9.1231(6)	8.6818(10)	625.79(9)
$BaZnSiO_4$	9.0955(5)	8.7251(9)	625.11(7)
$BaMg_{0.5}Zn_{0.5}SiO_4$	9.1073(3)	8.7335(6)	627.34(5)
$BaMgSiO_4$	9.1226(7)	8.7496(15)	630.6(1)

TABLE 3.4

THE FINAL ATOMIC POSITIONS AND ISOTROPIC TEMPERATURE FACTORS FOR THE NEUTRON POWDER REFINEMENT OF $BaMgSiO_4$. The estimated standard deviations on the last digits are given in brackets.

Atom	Site	x	y	z	B(Å^2)*
Ba(1)	2a	0	0	1/4#	0.91(8)
Ba(2)	2b	0.333	0.667	0.236(3)	0.91(8)
Ba(3)	2b	0.667	0.333	0.231(3)	0.91(8)
Si	6c	0.653(2)	-0.017(2)	0.435(3)	0.50(7)
Mg	6c	0.674(1)	0.668(2)	0.539(3)	0.50(7)
O(1)	6c	0.762(1)	0.903(1)	0.516(3)	1.17(6)
O(2)	6c	0.468(1)	0.898(1)	0.498(3)	1.17(6)
O(3)	6c	0.767(1)	0.192(1)	0.456(3)	1.17(6)
O(4)	6c	0.7090(9)	0.658(1)	0.751(3)	2.2(2)

Weighted profile index:	R_{wp}=4.23%
Nuclear index:	R_n=2.61%
Expected index:	R_e=2.57%
Goodness-of-fit:	2.71
Number of data points:	785
Number of reflections:	133
Number of variables:	39

* The temperature factors of the Ba atoms, tetrahedral atoms and O(1-3) atoms were constrained to be equal during the refinement.
# Used to fix the origin in the $P6_3$ space group.

TABLE 3.5

THE FINAL ATOMIC POSITIONS AND ISOTROPIC TEMPERATURE FACTORS FOR THE NEUTRON POWDER REFINEMENT OF $BaZnSiO_4$. The estimated standard deviations on the last digits are given in brackets.

Atom	Site	x	y	z	B(Å^2)*
Ba(1)	2a	0	0	0.250#	1.1(1)
Ba(2)	2b	0.333	0.6667	0.232(4)	1.1(1)
Ba(3)	2b	0.667	0.333	0.233(3)	1.1(1)
Si	6c	0.649(2)	-0.021(2)	0.434(4)	0.31(8)
Zn	6c	0.670(2)	0.664(2)	0.538(3)	0.31(8)
O(1)	6c	0.762(2)	0.902(2)	0.519(4)	1.32(8)
O(2)	6c	0.468(2)	0.897(2)	0.499(4)	1.32(8)
O(3)	6c	0.764(2)	0.193(2)	0.455(3)	1.32(8)
O(4)	6c	0.710(2)	0.660(2)	0.751(4)	4.1(3)

Weighted profile index:	R_{wp} =5.35%
Nuclear index:	R_n=4.61%
Expected index:	R_e= 2.67%
Goodness-of-fit:	4.01
Number of data points:	795
Number of reflections:	135
Number of variables:	39

* The temperature factors of the Ba atoms, tetrahedral atoms and O(1-3) atoms were constrained to be equal during the refinement.
# Used to fix the origin in the $P6_3$ space group.

TABLE 3.6#

SELECTED BOND LENGTHS (Å), BOND VALENCES (s) AND BOND ANGLES (°) IN THE $BaMgSiO_4$ STRUCTURE. The estimated standard deviations on the last digits are given in brackets.

	l	s
Ba(1)-O(1)×3	2.78(2)	0.262(×3)
Ba(1)-O(1)×3	2.99(2)	0.175(×3)
Ba(1)-O(4)×3	2.91(1)	0.185(×3)
	mean 2.89	Σ 1.87
Ba(2)-O(2)×3	2.93(2)	0.175(×3)
Ba(2)-O(3)×3	3.11(2)	0.108(×3)
Ba(2)-O(4)×3	2.789(9)	0.256(×3)
	mean 2.94	Σ 1.62
Ba(3)-O(2)×3	2.74(2)	0.292(×3)
Ba(3)-O(3)×3	2.74(2)	0.292(×3)
{Ba(3)-O(4)×3	3.47(1)}*	
	mean 2.74	Σ 1.75
Si-O(1)	1.62(2)	1.011
Si-O(2)	1.60(2)	1.067
Si-O(3)	1.66(1)	0.907
Si-O(4)	1.64(1)	0.958
	mean 1.63	Σ 3.94
O-Si-O	105.4 ~ 113.5°	
Mg-O(1)	1.88(2)	0.603
Mg-O(2)	1.96(1)	0.486
Mg-O(3)	1.95(1)	0.499
Mg-O(4)	1.87(1)	0.620
	mean 1.92	Σ 2.21
O-Mg-O	100.0 ~ 117.2°	

* The mean bond lengths and bond valence sums of Ba(3) were calculated by excluding the long bonds.

The bond lengths/angles were calculated based on the cell parameters (a = 9.1118(6), c = 8.7371(8) Å) obtained from powder neutron data.

TABLE 3.7#

SELECTED BOND LENGTHS (Å), BOND VALENCES (s) AND BOND ANGLES (°) IN THE $BaZnSiO_4$ STRUCTURE. The estimated standard deviations on the last digits are given in brackets.

		l		s
Ba(1)-O(1)×3		2.98(3)		0.175×3
Ba(1)-O(1)×3		2.78(3)		0.262×3
Ba(1)-O(4)×3		2.88(2)		0.290×3
	mean	2.88	Σ	1.91
Ba(2)-O(2)×3		2.96(4)		0.161×3
Ba(2)-O(3)×3		3.06(4)		0.123×3
Ba(2)-O(4)×3		2.79(1)		0.255×3
	mean	2.94	Σ	1.62
Ba(3)-O(2)×3		2.73(3)		0.300×3
Ba(3)-O(3)×3		2.71(3)		0.317×3
{Ba(3)-O(4)×3		3.46(3)}*		
	mean	2.72	Σ	1.85
Si-O(1)		1.67(2)		0.883
Si-O(2)		1.53(2)		1.289
Si-O(3)		1.70(2)		0.814
Si-O(4)		1.63(2)		0.984
	mean	1.63	Σ	3.97
O-Si-O		103.9 ~ 114.8°		
Zn-O(1)		1.90(2)		0.589
Zn-O(2)		1.93(2)		0.543
Zn-O(3)		1.95(1)		0.514
Zn-O(4)		1.89(2)		0.605
	mean	1.92	Σ	2.25
O-Zn-O		98.2 ~ 116.2°		

* The mean bond lengths and bond valence sums of Ba(3) were calculated by excluding the long bonds.

The bond lengths/angles were calculated based on the cell parameters (a = 9.0850(9), c = 8.7147(11) Å) obtained from powder neutron data.

TABLE 3.8

SUMMARY OF SINGLE CRYSTAL DATA, INTENSITY MEASUREMENTS AND STRUCTURE REFINEMENT PARAMETERS FOR $BaCoSiO_4$

Crystal Data	
Crystal system	Hexagonal
Space group	$P6_3$
Unit cell Dimensions	a = 9.126(2), c = 8.683(4) Å
Volume	626.3(5) $Å^3$
Z	6
Crystal size	0.30 × 0.08 × 0.10 mm^3
Formula weight	288.4
Density(calc.)	4.587 Mg/m^3
Absorption coefficient	13.508 mm^{-1}
F(000)	774
Data collection	
Diffractometer	Siemens R3m/V
Radiation	AgKα (λ = 0.56086 Å)
Temperature (K)	300
Monochromator	Highly oriented graphite crystal
2θ range	5.0 to 65.0°
Scan type	2θ-θ
Scan speed	Variable; 1.50 to 14.65°/min. in ω
Scan range (ω)	1.20° plus Kα-separation
Standard reflections	2 2 2, 2 2 -2, -3 6 0, measured every 100 reflections
Index range	$-17 \leq h \leq 15$, $0 \leq k \leq 17$, $0 \leq l \leq 16$
Reflections collected	5080
Independent reflections	1631 (R_{int} = 4.75%)
Observed reflections	1062 ($F > 6.0\sigma(F)$)
Absorption correction	Semi-empirical
Min./Max. Transmission	0.2777 / 0.5233
Solution and Refinement	
System	Siemens SHELXTL PLUS (VMS)
Solution	Direct Methods and Fourier Difference
Refinement method	Full-Matrix Least-Squares
Quantity minimized	$\Sigma w(F_o-F_c)^2$

Absolute Structure	N/A
Extinction correction	χ = 0.00074(8), where $F^* = F\,[1 + 0.002\chi F^2/\sin(2\theta)]^{-1/4}$
Weighting scheme	$w^{-1} = \sigma^2(F) + 0.0008F^2$
Number of parameters refined	64
Final R indices (obs. data)	R = 3.48%, wR = 4.15%
R indices (all data)	R = 6.05%, wR = 5.83%
Goodness-of-fit	0.93
Largest and mean Δ/σ	0.012, 0.004
Data-to-parameter ratio	16.6:1
Largest difference peak	2.89 eÅ^{-3}
Largest difference hole	-4.04 eÅ^{-3}

TABLE 3.9

ATOMIC COORDINATES ($\times 10^4$) AND EQUIVALENT ISOTROPIC DISPLACEMENT COEFFICIENTS ($Å^2 \times 10^3$) FOR THE SINGLE CRYSTAL X-RAY REFINEMENT OF $BaCoSiO_4$. The estimated standard deviations on the last digits are given in brackets.

Atom	Site	x	y	z	U_{eq}*
Ba(1)	2a	0	0	2500#	12(1)
Ba(2)	2b	3333	6667	2197(1)	14(1)
Ba(3)	2b	6667	3333	2185(1)	16(1)
Si	6c	6588(2)	-118(2)	4303(3)	10(1)
Co	6c	6823(1)	6711(1)	5322(2)	12(1)
O(1)	6c	7635(6)	-861(6)	5211(9)	21(2)
O(2)	6c	4645(7)	-950(8)	4889(8)	21(2)
O(3)	6c	7612(6)	1950(6)	4459(3)	17(2)
O(4)	6c	7223(8)	6534(9)	7527(8)	30(2)

* $U_{eq} = 1/3\ (U_{11} + U_{22} + U_{33})$

Used to fix the origin in the $P6_3$ space group.

TABLE 3.10

ANISOTROPIC THERMAL PARAMETERS* ($Å^2 \times 10^3$) OF $BaCoSiO_4$

	U_{11}	U_{22}	U_{33}	U_{12}	U_{13}	U_{23}
Ba(1)	14(1)	14(1)	9(1)	7(1)	0	0
Ba(2)	15(1)	15(1)	12(1)	7(1)	0	0
Ba(3)	20(1)	20(1)	8(1)	10(1)	0	0
Si	10(1)	10(1)	9(1)	4(10)	2(1)	3(1)
Co	13(1)	12(1)	11(1)	7(1)	-1(1)	-2(1)
O(1)	20(2)	14(2)	31(2)	0(2)	-14(3)	0(3)
O(2)	15(2)	18(2)	31(4)	9(2)	13(2)	9(2)
O(3)	13(2)	14(2)	24(3)	5(2)	-7(2)	-1(2)
O(4)	37(3)	36(3)	10(2)	11(3)	3(2)	-5(2)

* The anisotropic displacement factor exponent takes the form: $-2\pi^2(h^2a^{*2}U_{11} + \ldots + 2hka^*b^*U_{12})$

TABLE 3.11#

SELECTED BOND LENGTHS (Å), BOND VALENCES (s) AND BOND ANGLES (°) IN THE $BaCoSiO_4$ STRUCTURE. The estimated standard deviations on the last digits are given in brackets

		l		s
Ba(1)-O(1)×3		2.744(7)		0.289(×3)
Ba(1)-O(1)×3		3.020(8)		0.137(×3)
Ba(1)-O(4)×3		2.900(9)		0.190(×3)
	mean	2.888	Σ	1.85
Ba(2)-O(2)×3		3.004(6)		0.143(×3)
Ba(2)-O(3)×3		3.013(7)		0.140(×3)
Ba(2)-O(4)×3		2.718(9)		0.310(×3)
	mean	2.912	Σ	1.78
Ba(3)-O(2)×3		2.745(5)		0.288(×3)
Ba(3)-O(3)×3		2.706(6)		0.321(×3)
{Ba(3)-O(4)×3		3.629(9)}*		
	mean	2.726	Σ	1.83
Si-O(1)		1.626(8)		0.995
Si-O(2)		1.623(6)		1.003
Si-O(3)		1.639(5)		0.960
Si-O(4)		1.620(7)		1.011
	mean	1.627	Σ	3.97
O-Si-O		104.9 ~ 112.6		
Co-O(1)		1.956(5)		0.490
Co-O(2)		1.952(6)		0.495
Co-O(3)		1.951(7)		0.497
Co-O(4)		1.971(7)		0.470
	mean	1.957	Σ	1.95
O-Co-O		99.1 ~ 123.5		

* The mean bond lengths and bond valence sums of Ba(3) were calculated by excluding the long bonds.

The bond lengths/angles were calculated based on the cell parameters obtained from single X-ray data.

CHAPTER 4

THE $Na_{0.5}K_{0.5}GaSiO_4$ COMPOUND

The compound $Na_{0.5}K_{0.5}GaSiO_4$ was found to crystallize with a ($\sqrt{3}\times$A, C) hexagonal unit-cell during the study of the (Na, K)$GaSiO_4$ system [Weber & Barbier, 1990] and it was then suggested that its structure could be a superstructure of kalsilite ($KAlSiO_4$). In this chapter, the compound $Na_{0.5}K_{0.5}GaSiO_4$ was re-investigated by powder X-ray diffraction and electron diffraction. Its crystal structure was refined by the Rietveld method using powder X-ray diffractometer data.

4.1 Powder X-ray and Electron Diffraction

The nature of the compound $Na_{0.5}K_{0.5}GaSiO_4$ was first characterized by powder X-ray diffraction using a Guinier-Hägg camera ($CuK_{\alpha 1}$ radiation, λ = 1.540598 Å). Its diffraction pattern was indexed on an hexagonal unit cell with a = 8.8894(6) and c = 8.4894(11) Å by means of the computer program LSUDF . The cell is a ($\sqrt{3}\times$A, C) superstructure of the basic (A, C) kalsilite cell, which is required by the presence of a few reflections of the type {hkl, h-k $\neq$ 3n}. It should be noted that the superstructure reflections are much stronger than those of the $BaTSiO_4$ (T = Co, Mg, Zn) compounds (cf. Tables 4.1 and 3.1)

The compound was also examined by electron diffraction using a Philips CM-12

transmission electron microscope operating at 120 kV and equipped with a double-tilt goniometer stage. The electron diffraction patterns confirmed the presence of a $\sqrt{3}\times A$ superstructure along the a-axis of the hexagonal cell and also showed the absence of a superstructure along the c axis (Fig. 4.1).

The results confirmed the previous work of Weber and Barbier [1990] and indicated that the compound $Na_{0.5}K_{0.5}GaSiO_4$ crystallized with the same kind of kalsilite superstructure as the compounds $BaTSiO_4$ (T = Co, Mg Zn) (cf. Chapter 3).

4.2 Structure Refinement

In order to refine the crystal structure of $Na_{0.5}K_{0.5}GaSiO_4$, powder X-ray data were collected on a Nicolet I2 automated diffractometer (Cu $K_{\alpha 1}$ = 1.5406 Å and Cu $K_{\alpha 2}$ = 1.5448 Å). The data were recorded at room temperature over the angular range $10° < 2\theta < 85°$. The profile refinement was carried out by means of a modified Rietveld program [Young & Wiles, 1982; Howard & Hill, 1985].

The refinement was started with the cell parameters determined from the Guinier-Hägg camera data (cf. Table 4.1) and the atomic positions determined in the $P6_3$ space group for the isostructural $BaCoSiO_4$ compound (cf. Chapter 3). The stuffed Na and K atoms were positioned on the 2a and 2b sites, and the Ga, Si, O atoms occupied three sets of general 6c sites. During the refinement, the structural parameters (unit-cell parameters, atom positions, temperature factors), scale factor and profile parameters were varied in a least-squares procedure until the calculated powder pattern, based on the structure model, best matched the observed pattern. The refinement was carried out by varying, in order, the scale factor, the background coefficients, the cell parameters, the

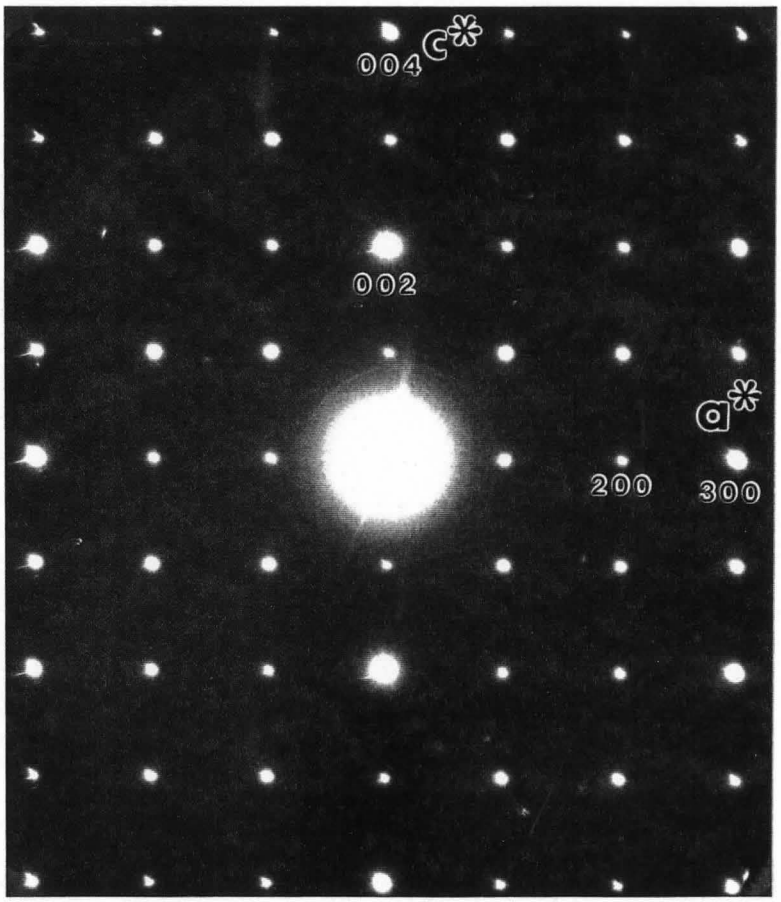

Fig. 4.1 Electron diffraction pattern of $Na_{0.5}K_{0.5}GaSiO_4$ along the [010] zone axis. Note the $\sqrt{3} \times A$ superstructure along the a-axis and the absence of superstructure along the c axis. The $\{00l,\ l = 2n+1\}$ reflections (forbidden in the $P6_3$ space group) appear by double diffraction.

atom positions, profile parameters and, at last, the temperature factors. The oxygen temperature factors were constrained to be equal except for that of O(4).

For the tetrahedral Ga and Si atoms, a complete ordering was assumed initially with Ga and Si occupying the Co and Si sites of the $BaCoSiO_4$ structure respectively (cf. Chapter 3). In the refinement, however, this model yielded a high temperature factor for the Ga site, suggesting that there might be a small amount of disorder between the Ga and Si atoms. By adjusting the occupancies of the two sites and refining the temperature factors, a result of 7.5 at% disordering (with a probable error of a few at%) was obtained.

For the stuffed Na and K atoms, refinements were tried for the following three models: (1) a totally disordered distribution with each site occupied by 50% Na and 50% K atoms; (2) an ordered distribution with K atoms in site 1, Na atoms in site 2 and an equal number of Na and K atoms in site 3; (3) a reversed distribution on site 2 and 3 as compared to model (2). Model(1) yielded a negative temperature factor for site 1, indicating that this site should be K-rich; model (3) yielded a negative temperature factor for site 3 and a very high temperature factor for site 2, showing that site 3 must be richer in K than site 2. Model(2) yielded the best results with reasonable temperature factors for the three sites and after adjusting the occupancies of the three (K, Na) sites and refining the temperature factors, an ordered distribution with 90% K and 10% Na in site 1, 100% Na in site 2 and 60% K plus 40% Na in site 3 was obtained (cf. Table 4.2).

The refinement converged smoothly to the following agreement indices: profile R = 8.47, weighted profile R_{wp} = 10.97 , Bragg R-factor R_B = 3.73 and expected R_e = 2.75. The quality of the refinement is good in terms of these R factors for a powder X-ray profile refinement. The final atomic positions, isotropic temperature factors and

occupancy factors are listed in Table 4.3 and the calculated, observed and difference profiles are shown in Fig. 4.2. Selected bond lengths, angles and valences are listed in Table 4.4.

Powder neutron diffraction data for $Na_{0.5}K_{0.5}GaSiO_4$ were also collected and refined by a local version of the Rietveld program. The structure obtained was very similar to the one obtained from powder X-ray diffraction data but it was impossible to determine the ordering of Na and K atoms because of their similar nuclear scattering lengths (0.367 and 0.363 $\times$ 10^{-12} cm respectively [Sears, 1984]). The calculated, observed and difference profiles are shown in Fig. 4.3. The superstructure reflections are also stronger compared to the neutron diffraction patterns of $BaTSiO_4$ (T = Mg, Zn).

4.3 Description of the $Na_{0.5}K_{0.5}GaSiO_4$ Structure

The structure of $Na_{0.5}K_{0.5}GaSiO_4$ projected along the c axis of the hexagonal cell is shown in Fig 4.4. Similar to the $BaTSiO_4$ (T = Co, Mg, Zn) structures, the tetrahedral framework of the $Na_{0.5}K_{0.5}GaSiO_4$ structure is constructed of six-membered rings of corner-shared tetrahedra which are pointing alternately up and down. All rings are identical with a ditrigonal shape when viewed along the c axis. The successive tetrahedral layers are stacked in a "staggered" way by sharing the O(4) oxygen atoms to form a three-dimensional framework. The interstices which are enclosed within the framework are "stuffed" by the Na and K atoms.

From the structural refinement results and bond lengths (cf. Table 4.3), it can be seen that the larger tetrahedra (T_1, pointing up) are mainly occupied by Ga atoms (92.5% Ga and 7.5% Si), while the smaller tetrahedra (T_2, pointing down) are mainly occupied

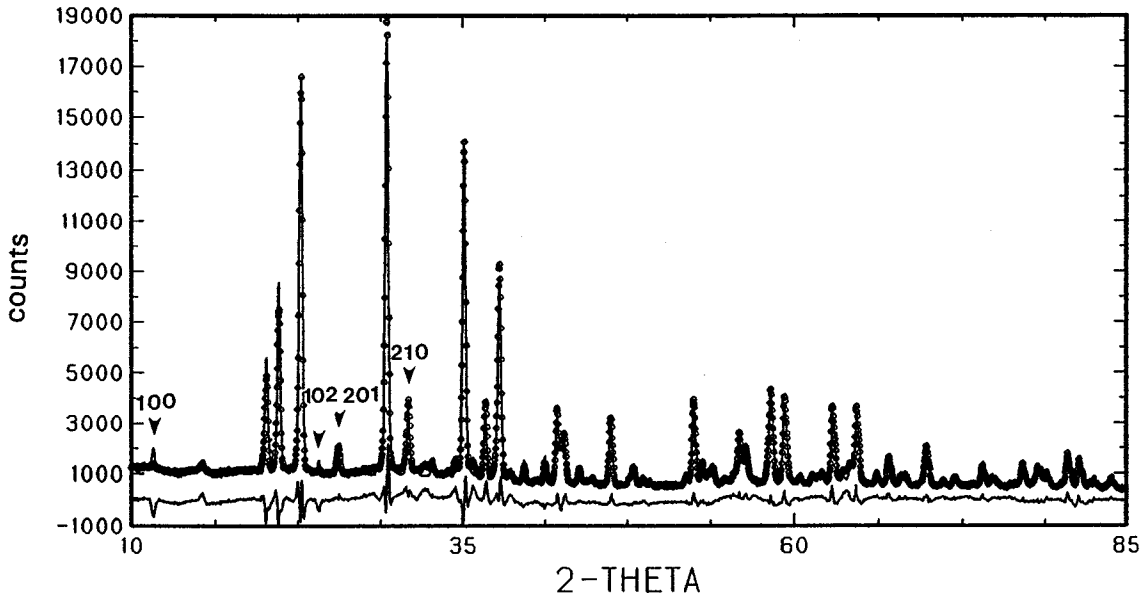

Fig. 4.2 Observed, calculated and difference (bottom) powder X-ray diffraction profiles for $Na_{0.5}K_{0.5}GaSiO_4$. The (↓) signs indicate the ($\sqrt{3}\times A$) superstructure reflections.

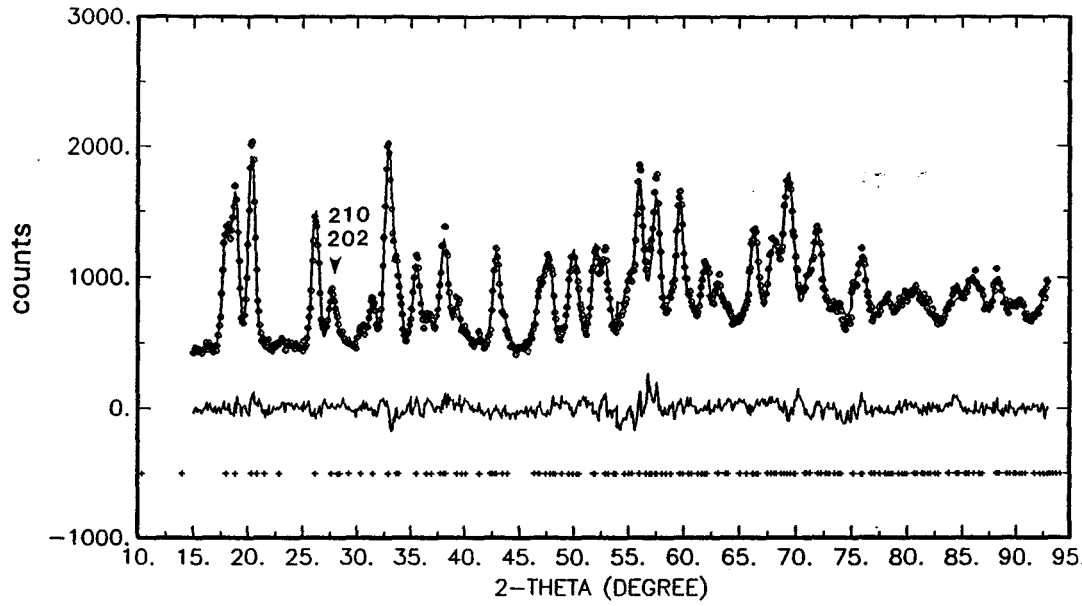

Fig. 4.3 Observed, calculated and difference (bottom) powder neutron diffraction profiles for $Na_{0.5}K_{0.5}GaSiO_4$. The (↓) signs indicate the ($\sqrt{3}\times A$) superstructure reflections. The lower resolution of the neutron diffractometer leads to a larger amount of perk overlap than in the X-ray pattern.

by Si atoms (92.5% Si and 7.5% Ga). The mean T_1-O (= 1.81 Å) and T_2-O (= 1.64 Å) bond lengths are consistent with the atomic distribution: the mean T_1-O bond is a little shorter than the expected Ga-O bond (= 1.85 Å) whereas the mean T_2-O bond is a little longer than the expected Si-O bond (= 1.62 Å).

The structural refinement also reveals a strong K/Na ordering on the three cavity sites, with M(1) mainly occupied by K atoms (90% K and 10% Na), M(2) filled by smaller Na atoms and M(3) occupied by a mixture of 60% K and 40% Na atoms. These three sites in the $Na_{0.5}K_{0.5}GaSiO_4$ structure are located on the three-fold axes of the framework with different coordinations: M(1) is surrounded by three O(1)s and three O(4)s at an average distance of 2.91 Å, M(2) is bounded to three O(2)s and three O(4)s at an average distance of 2.50 Å and M(3) is bounded to three O(2)s plus three O(3)s at an average distance of 2.73 Å (cf. Table 4.3). The coordinations of the cavity atoms are therefore somewhat different from those in the $BaTSiO_4$ structures where only Ba(3) is six-coordinated (cf. Chapter 3). From Fig. 4.4, it can be seen that the six-fold coordinations of the M(2) and M(3) sites in the $Na_{0.5}K_{0.5}GaSiO_4$ structure result from the tilting of the tetrahedra and the displacement of the M(2) (= 100% Na) atoms along the c-axis. The O(4) atoms are displaced towards the M(2) sites and away from the M(3) sites (M(3)-O(4) = 3.86 Å) while the small Na atoms in the M(2) sites move towards the O(2) atoms and away from the O(3) atoms (M(2)-O(3) = 3.73 Å). The mean bond lengths of the three sites (M(1)-O = 2.91 Å; M(3)-O = 2.73 Å; M(2)-O = 2.50 Å) are consistent with the proposed ordering (10% Na in site 1, 40% Na in site 3 and 100% Na in site 2) and the bond valence sums around M(2) and M(3) (0.99 and 0.96) are very close to the expected values. The slightly high bond valence sum around M(1) (1.27) is mainly due to the rather short M(1)-O(1) bonds (2.59 Å, cf. Table 4.4).

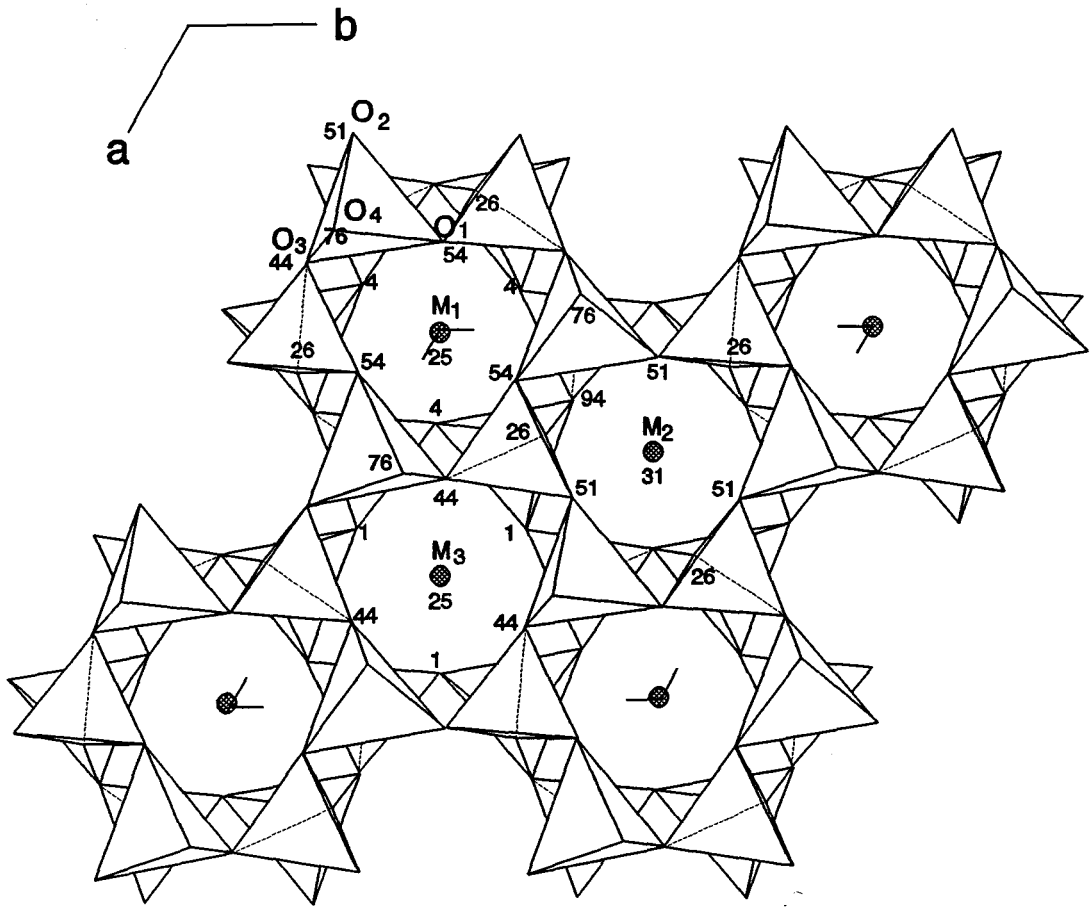

Fig. 4.4 The structure of $Na_{0.5}K_{0.5}GaSiO_4$ viewed along the c-axis. The larger TO_4 tetrahedra (pointing up) are mainly occupied by Ga atoms and the small TO_4 tetrahedra (pointing down) are mainly occupied by Si atoms. The distribution of Na and K atoms is in a strong ordering patten with 10% Na in M(1), 100% Na in M(2) and 40% Na in M(3). Atom heights are given in units of c/100.

The displacement of the O(4) atoms corresponds to the collapse of the tetrahedral framework, involving the tilting of the T_1 and T_2 tetrahedra around horizontal axes approximately parallel to the [110] direction (cf. Fig. 4.4). Like in the $BaTSiO_4$ structures, the degree of framework collapse can be qualitatively estimated from the difference (Δz) between $z_{O(1)}$ and $z_{O(2)}$ and the T_1-O(4)-T_2 angle: in the $Na_{0.5}K_{0.5}GaSiO_4$ structure, Δz is equal to 0.103 and the T_1-O(4)-T_2 angle is equal to 141.0(17), both indicating a greater collapse than in the $BaCoSiO_4$ structure.

As mentioned in Chapter 2, the lowest possible synthesis temperature was 925°C for the $Na_{0.5}K_{0.5}GaSiO_4$ compound which decomposed at about 875°C. The previous study of this compound [Barbier & Weber, 1990] showed that it crystallized with an hexagonal ($\sqrt{3}\times A$, C) cell even when recrystallized from a melt at 1100°C. These observations indicate that the kalsilite-like $Na_{0.5}K_{0.5}GaSiO_4$ structure is stable at high temperature only, probably up to the melting point. On the other hand, the synthesis temperature was high enough to cause a small degree of disordering of the tetrahedral Ga and Si atoms. A similar situation has been found in kalsilite ($KAlSiO_4$) for which the Al and Si tetrahedral atoms are perfectly ordered in the low temperature form with the space group $P6_3$ [Perrotta, 1965], but totally disordered in the high-temperature form at 925°C with the space group $P6_3/m$ [Kawahara, 1987].

TABLE 4.1

X-RAY POWDER DIFFRACTION PATTERN (GUINIER CAMERA) FOR $Na_{0.5}K_{0.5}GaSiO_4$ INDEXED ON A HEXAGONAL CELL WITH a = 8.8894(6) c = 8.4894(11) Å

h	k	l	d_{cal}(Å)	d_{obs}(Å)	I/I_o
1	1	0	4.4447	4.4373	25
0	0	2	4.2447	4.2394	18
1	1	1	3.9377	3.9333	77
1	1	2	3.0697	3.0688	100
2	1	0#	2.9097	2.9089	20
3	0	0	2.5662	2.5660	84
3	0	1	2.4564	2.4564	17
1	1	3	2.3871	2.3873	49
3	0	2	2.1960	2.1969	12
2	2	1	2.1499	2.1503	18
3	1	0#	2.1352	2.1357	8
0	0	4	2.1223	2.1233	13
2	2	2	1.9688	1.9691	17
2	2	3	1.7478	1.7480	25
4	1	1	1.6480	1.6483	20
3	2	2#	1.6306	1.6324	15
1	1	5	1.5861	1.5862	40
4	1	2	1.5621	1.5621	32
3	3	0	1.4816	1.4815	31
4	1	3	1.4446	1.4444	43
3	3	2	1.3988	1.3990	13
2	2	5	1.3492	1.3488	17
1	1	6	1.3482		
6	0	0	1.2831	1.2832	7
3	0	6	1.2390	1.2388	10
3	2	5#	1.2240	1.2242	9
4	1	5	1.1942		
2	2	6	1.1935	1.1938	21
5	2	2	1.1838	1.1836	17
5	2	3	1.1302	1.1301	13

Strong superstructure reflections of the type {hkl, h-k $\neq$ 3n} requiring a $\sqrt{3}\times$A a-axis.

TABLE 4.2

COMPARISON OF THE DISTRIBUTIONS AND TEMPERATURE FACTORS OF THE (Na, K) SITES IN $Na_{0.5}K_{0.5}GaSiO_4$ FOR DIFFERENT ORDERING SCHEMES

	Model(1)		Model(2)		Model(3)	
Atom	N(%)	B(Å^2)	N(%)	B(Å^2)	N(%)	B(Å^2)
K(1)	50	-0.6(4)	90	1.1(5)	100	1.3(4)
Na(1)	50	-0.6(4)	10	1.1(5)	0	-
Na(2)	50	5.5(7)	100	2.2(6)	50	6.1(7)
K(2)	50	5.5(7)	0	-	50	6.1(7)
K(3)	50	0.4(3)	60	1.0(3)	0	-
Na(3)	50	0.4(3)	40	1.0(3)	100	-2.2(3)

TABLE 4.3

THE FINAL ATOMIC POSITIONS, ISOTROPIC TEMPERATURE FACTORS AND OCCUPANCIES FOR THE X-RAY POWDER REFINEMENT OF $Na_{0.5}K_{0.5}GaSiO_4$. The estimated standard deviations on the last digits are given in brackets.

Atom	x	y	z	B(Å^2)	Occupancy
M(1)	0.0000	0.0000	0.250#	1.1(5)	10%Na+90%K
M(2)	0.3333	0.6667	0.306(2)	2.2(8)	100%Na
M(3)	0.6667	0.3333	0.247(2)	1.0(3)	40%Na+60%K
T(1)	0.6771(8)	0.6528(7)	0.556(2)	0.8(1)	92.5%Ga+7.5%Si
T(2)	0.660(2)	-0.032(2)	0.436(2)	1.0(2)	7.5%Ga+92.5%Si
O(1)	0.755(2)	0.890(2)	0.5413(8)	0.9(2)	
O(2)	0.4685(7)	0.926(2)	0.507(2)	0.9(2)	
O(3)	0.788(2)	0.190(2)	0.438(2)	0.9(2)	
O(4)	0.721(2)	0.619(2)	0.761(4)	1.5(5)	

Cell Parameters:	a = 8.8846(8) Å
	c = 8.4900(5) Å
Profile R-factor:	8.43%
Weighted profile R-factor:	10.96%
Bragg R-factor:	3.66%
Expected:	2.75%
Goodness-of-fit:	15.84
Number of data points (N):	2502
Number of parameters refined (P):	35

Used to fix the origin in the $P6_3$ space group.

TABLE 4.4

SELECTED BOND LENGTHS (Å), BOND STRENGTHS (s) AND BOND ANGLES (°) IN THE $Na_{0.5}K_{0.5}GaSiO_4$ STRUCTURE. The estimated standard deviations on the last digits are given in brackets.

		l	s(K)	s(Na)
M(1)-O(1)×3		3.11(2)	0.07×3	0.03×3
M(1)-O(1)×3		2.59(1)	0.29×3	0.12×3
M(1)-O(4)×3		3.04(2)	0.09×3	0.04×3
	mean	2.82	Σs 1.35 × 0.9 +	0.55 × 0.1 = 1.27
{M(2)-O(3)×3		3.73(2)}*		
M(2)-O(2)×3		2.63(2)		0.11×3
M(2)-O(4)×3		2.36(1)		0.22×3
	mean	2.50	Σs	0.99
{M(3)-O(4)×3		3.68(2)}*		
M(3)-O(2)×3		2.86(2)	0.14×3	0.059×3
M(3)-O(3)×3		2.60(2)	0.28×3	0.116×3
	mean	2.73	Σs 1.26 × 0.6 +	0.52 × 0.4 = 0.96
			s(Ga)	s(Si)
T1-O(1)		1.87(2)	0.69	0.52
T1-O(2)		1.74(2)	0.97	0.73
T1-O(3)		1.79(2)	0.85	0.64
T1-O(4)		1.84(3)	0.74	0.56
	mean	1.81	Σs 3.25 × 0.925 +	2.44 × 0.075 = 3.19
O-T1-O		105.1(7) ~ 112.7(7)		
T2-O(1)		1.60(2)	1.41	1.06
T2-O(2)		1.66(2)	1.22	0.91
T2-O(3)		1.71(2)	1.05	0.79
T2-O(4)		1.59(3)	1.46	1.10
	mean	1.64	Σs 5.14 × 0.075 +	3.86 × 0.925 = 3.96
O-T2-O		104.1(11) - 114.0(8)		
T_1-O(4)-T_2		141.0(17)		

* The mean bond lengths and bond valence sums of the M(2) and M(3) sites were calculated by excluding the long bonds.

CHAPTER 5

THE (Sr, Ca)$BeSiO_4$ COMPOUNDS

The compound $SrBeSiO_4$ has previously been reported to crystallize with an hexagonal unit-cell with parameters a = 4.853 Å, c = 8.189 Å and space group $P6_322$ [JCPDS #26-978], suggesting that its structure corresponds to the basic (A, C) kalsilite-type with a completely disordered distribution of the tetrahedral Be and Si atoms. The compound $CaBeSiO_4$ is known to crystallize with a monoclinic unit-cell with parameters a = 8.27, b = 14.24, c = 7.85 Å and $\gamma = 90°$ [JCPDS, #26-298], indicating that its structure is of the ($\sqrt{3}\times$A, 3×A, C) beryllonite ($NaBePO_4$)-type. This chapter deals with the study of the mixed compounds in the (Sr, Ca)$BeSiO_4$ system. All compounds were characterized by powder X-ray diffraction and a few of them, $Sr_{1-x}Ca_xBeSiO_4$ (x = 0.0 ~ 0.3), were also examined by electron diffraction. The crystal structures of $SrBeSiO_4$ and $Sr_{1-x}Ca_xBeSiO_4$ (x = 0.27) were refined by single crystal X-ray diffraction.

5.1 Powder X-ray and Electron Diffraction

The nature of the eleven compounds Sr_{1-x} Ca_xBeSiO_4 (x = 0.0, 0.1, ..., 0.9, 1.0) was characterized by powder X-ray diffraction using a Guinier-Hägg camera ($CuK_{\alpha 1}$ radiation, λ = 1.540598 Å). The powder patterns of the Sr-rich compounds (x = 0.0 ~ 0.4) were indexed on a ($\sqrt{3}\times$A, C) hexagonal unit-cell, indicating that their structure

is a superstructure of the basic (A, C) kalsilite cell. On the other hand, the powder patterns of the Ca-rich compounds ($x = 0.6 \sim 1.0$) were indexed on a ($\sqrt{3}\times A$, $3\times A$, C, $\gamma \approx 90°$) monoclinic cell, indicating the formation of a wide solid solution with a beryllonite-type structure. The cell parameters of the whole series of $Sr_{1-x}Ca_xBeSiO_4$ compounds are given in Table 5.3 but only the powder patterns of the hexagonal $SrBeSiO_4$ and $Sr_{0.7}Ca_{0.3}BeSiO_4$ compounds are given in Tables 5.1 and 5.2 showing a few weak reflections of the type {hkl, h-k $\neq$ 3n} requiring the $\sqrt{3}\times A$ superstructure. The relationship between the c parameter and the composition is illustrated in Fig. 5.1, showing i) a linear decrease with increasing Ca-content within the solid solution regions and ii) a discontinuity at $x = 0.5$ corresponding to a change in the structure-type and framework topology. A similar effect has previously been observed in related systems such as (Ca, Sr)Al_2O_4 [Barbier and Neuhausen, 1990] and (Na, K)$AlGeO_4$ [Barbier and Fleet, 1988].

The Sr-rich compounds $Sr_{1-x}Ca_xBeSiO_4$ ($x = 0.0 \sim 0.3$) were also examined by electron diffraction /microscopy using a Philips CM-12 transmission electron microscope. Interestingly, not only the presence of the $\sqrt{3}\times A$ superstructure in the basal plane of the hexagonal cell was confirmed but, also, a $4\times C$ superstructure along the c-axis was found for the composition $x = 0.0$ (Fig. 5.2a). With increasing Ca-content, the $4\times C$ superstructure was observed to become weaker ($x = 0.1$ and 0.2 - Figs. 5.2b and 5.2c) and eventually vanish completely for $x = 0.3$ (Fig. 5.2d). Lattice images of the $SrBeSiO_4$ compound clearly showed the superstructure along the c-axis (Fig. 5.3). However it was found by a careful inspection of the diffraction patterns that the $4\times C$ superstructure reflections were not all exactly aligned along the c^*-axis, indicating that the superstructure may be incommensurate with the ($\sqrt{3}\times A$, C) hexagonal sub-cell.

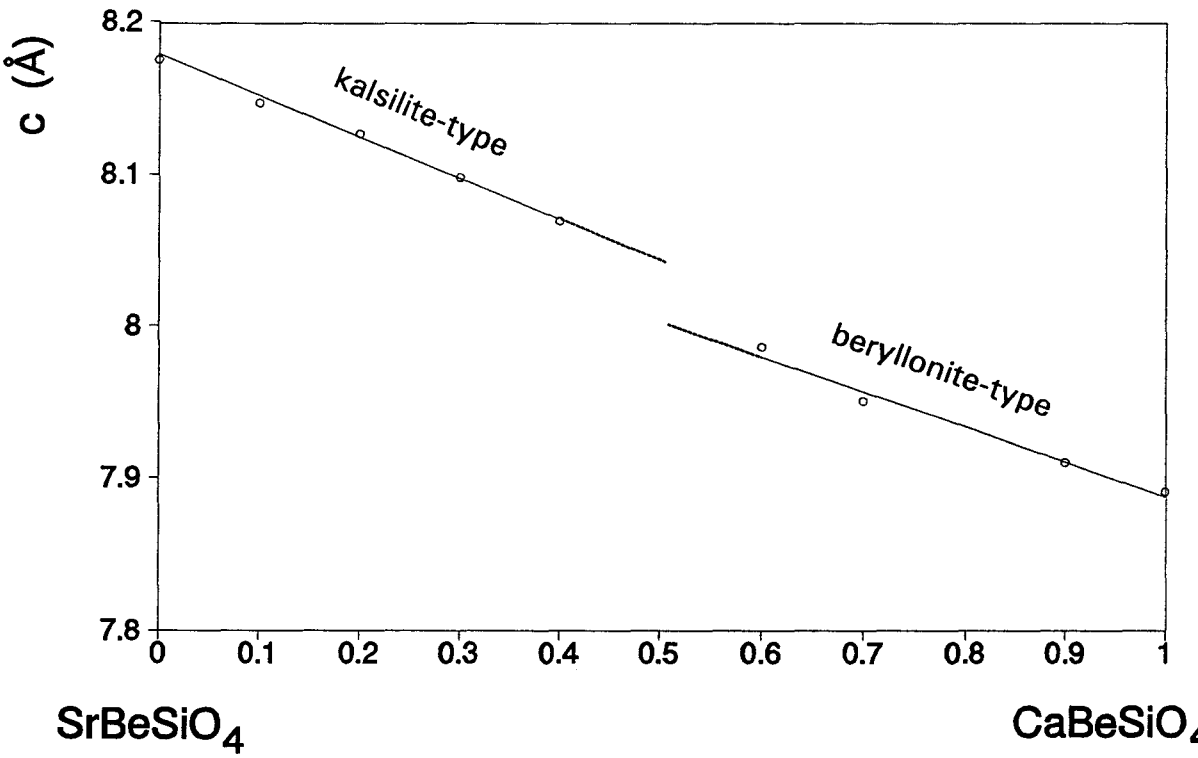

Fig. 5.1 Plot of the c-parameters vs compositions in the (Sr, Ca)$BeSiO_4$ system. The regions corresponding to the kalsilite-type and beryllonite-type structures are indicated.

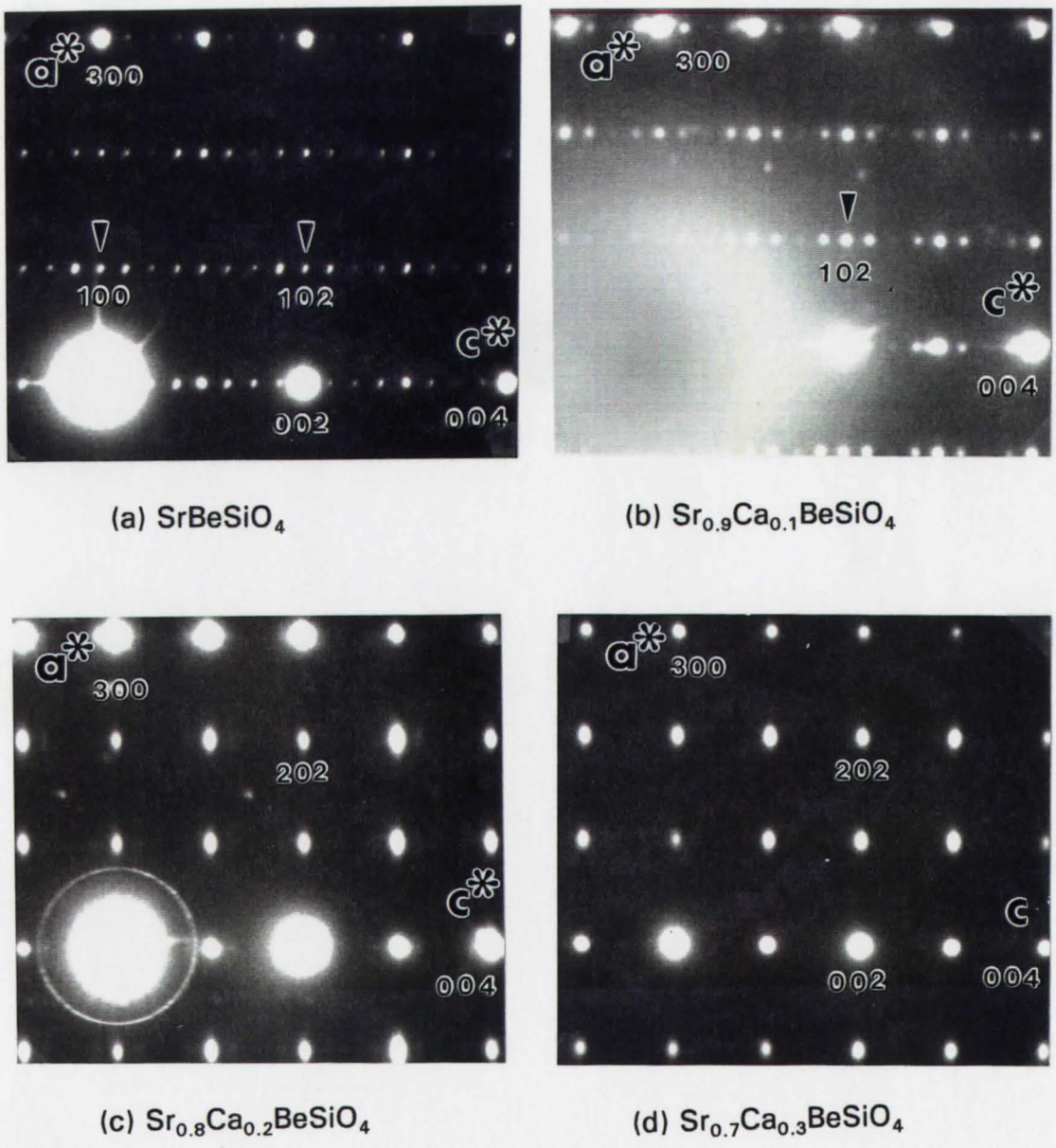

Fig. 5.2 [010] zone-axis electron diffraction patterns of (a) $SrBeSiO_4$ (indexed on the ($\sqrt{3}\times$A, C) sub-cell), (b) $Sr_{0.9}Ca_{0.1}BeSiO_4$, (c) $Sr_{0.8}Ca_{0.2}BeSiO_4$ and (d) $Sr_{0.7}Ca_{0.3}BeSiO_4$. Note that the 4C superstructure weakens and vanishes with increasing Ca-content. The $\{00l,\ l = 2n+1\}$ reflections (forbidden in the $P6_3$ space group) appear by double diffraction.

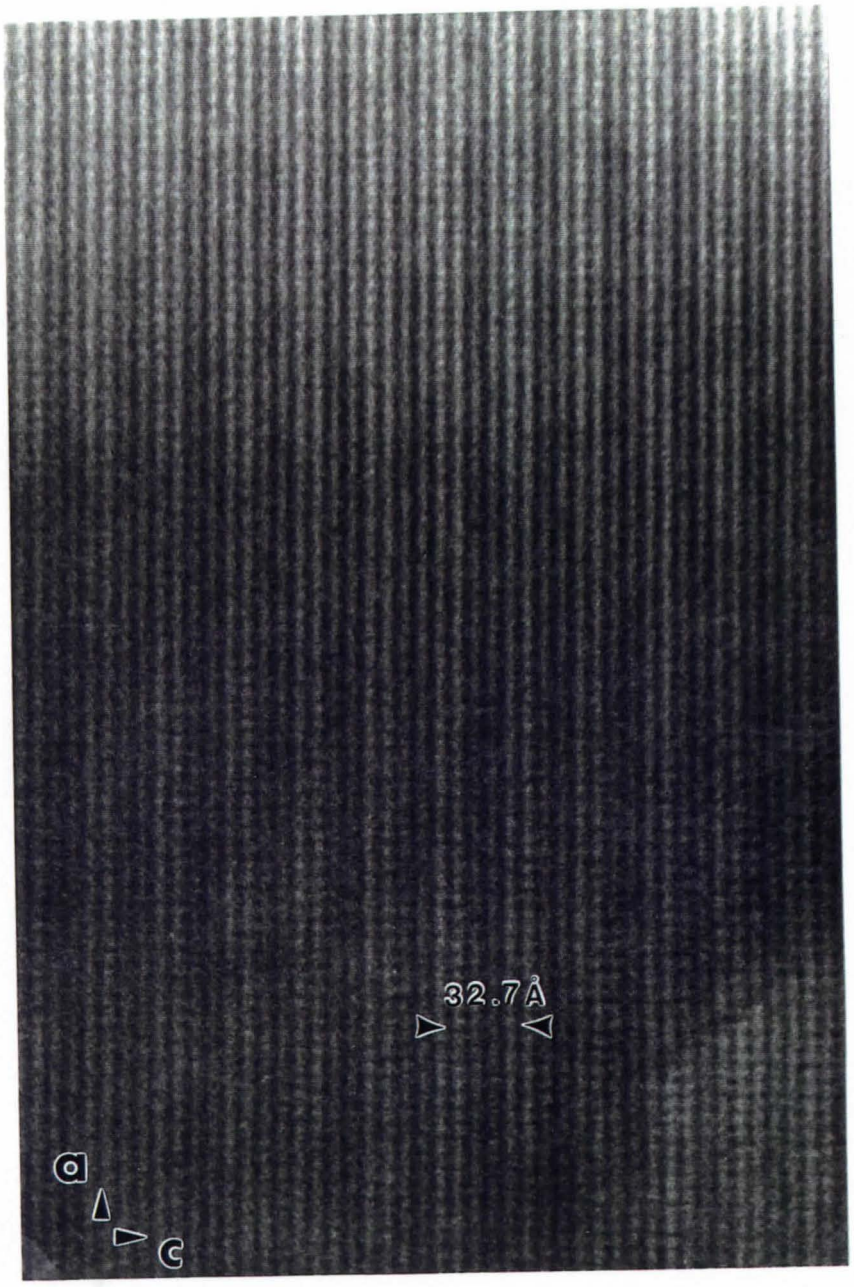

Fig. 5.3 High resolution image of $SrBeSiO_4$ viewed along the [010] zone-axis showing the 4×C superstructure.

In order to analyze their crystal structure and in an attempt to understand the origin of the 4×C superstructure, single crystals of $SrBeSiO_4$ and $Sr_{1-x}Ca_xBeSiO_4$ were grown and studied by X-ray diffraction.

5.2 Single Crystal X-ray Refinement of the $SrBeSiO_4$ Structure

Single crystal intensity data for $SrBeSiO_4$ were collected on a P_4 diffractometer using graphite-monochromatized MoKα radiation. The unit-cell constants determined from 42 single reflections within $9.70° \leq 2\theta \leq 24.65°$, a = 8.405(8) and c = 32.68(3) Å were consistent with the electron diffraction and X-ray precession data. The corresponding sub-cell obtained by rejecting the 4×C superstructure reflections had parameters a = 8.405(8) and c = 8.171(8) Å, in very close agreement with those refined from powder X-ray diffraction data (cf. Table 5.3).

Attempts were made to refine the $SrBeSiO_4$ structure by using the superstructure reflections both in the basal plane and along the c-axis. However, this was unsuccessful because the 4×C superstructure reflections were weak and incommensurate and only an average structure was refined using the ($\sqrt{3}$×A, C) sub-cell reflections. All crystal data, data collection parameters, and results of analysis are listed in Table 5.4. The structure was solved in the $P6_3$ space group by direct methods and successive Fourier syntheses. For consistency with the $BaTSiO_4$ (T = Co, Mg, Zn) structures (cf. chapter 3), the Sr(1) atom was chosen to fix the origin at (0, 0, 1/4). An ordered arrangement of the tetrahedral Be and Si atoms was also assumed initially and later confirmed during the refinement. Using 365 observed reflections ($F > 4.0\sigma(F)$), a full-matrix least-squares refinement was carried out with anisotropic temperature factors for all atoms, converging

to final agreement indices R = 0.043 and R_w = 0.061. The final atomic positions and equivalent isotropic displacement parameters are listed in Table 5.5 and the anisotropic thermal parameters are shown in Table 5.6. The relatively large errors on the atomic positions and temperature factors reflect the fact that they correspond to an average structure only. Selected bond lengths, bond angles and associated bond valences are given in Table 5.7.

5.3 Single Crystal X-ray Refinement of the $Sr_{1-x}Ca_xBeSiO_4$ Structure

The intensity data for a single crystal of $Sr_{1-x}Ca_xBeSiO_4$ were collected on a Siemens R3m/v diffractometer using graphite-monochromatized AgKα radiation. All crystal data, data collection parameters, and results of analysis are listed in Table 5.8. The unit cell constants (a = 8.3694(8) and c = 8.100(1) Å) determined from 27 reflections in the 2θ range 20.42 ~ 43.15° indicated a composition close to 30 at% Ca for this crystal as deduced from the Vegard's law behaviour of the (Sr, Ca)$BeSiO_4$ system (cf. Fig. 5.1). The structure was solved in the $P6_3$ space group by direct methods and successive Fourier syntheses. In order to be consistent with the other structures, the M(1) atom was chosen to fix the origin at (0, 0, 1/4). An ordered arrangement of the tetrahedral Be and Si atoms was also assumed initially and later confirmed during the refinement. Using 787 observed reflections ($F > 6.0\sigma(F)$), a full-matrix least-squares refinement was carried out with anisotropic temperature factors for all atoms, converging to final agreement indices R = 0.056 and R_w = 0.071. During the refinement, the Ca content was determined to be equal to 27(2)%, a value entirely consistent with the prediction from the cell parameters. The final atomic positions, equivalent isotropic

displacement and occupancy parameters are listed in Table 5.9 and the anisotropic thermal parameters are shown in Table 5.10. Selected bond lengths, bond angles and associated bond strengths are given in Table 5.11.

5.4 Description of the Structures

The structures of the $SrBeSiO_4$ and $Sr_{0.73}Ca_{0.27}BeSiO_4$ compounds projected along the c axis of the hexagonal cells are shown in Figs. 5.4 and 5.5. The two structures are basically identical except for slight shifts of atom positions (cf. Tables 5.5 and 5.9). Like in the $BaTSiO_4$ (T = Co, Mg, Zn) and $Na_{0.5}K_{0.5}GaSiO_4$ structures, the tetrahedral framework of the $SrBeSiO_4$ and $Sr_{0.73}Ca_{0.27}BeSiO_4$ structures are constructed of six-membered rings of corner-shared BeO_4 and SiO_4 tetrahedra which are pointing alternately up and down. All rings are identical with a ditrigonal shape when viewed along the c axis. The tetrahedral layers are stacked in a "staggered" arrangement by sharing the O(4) oxygen atoms to form a three-dimensional framework. The interstices enclosed within the framework are "stuffed" by the Sr atoms in the $SrBeSiO_4$ structure or Sr/Ca atoms in the $Sr_{0.73}Ca_{0.27}BeSiO_4$ structure.

The mean tetrahedral Be-O and Si-O bond lengths are similar (Be-O $\approx$ 1.63 Å, Si-O $\approx$ 1.60 Å, cf. Tables 5.7 and 5.11) but nevertheless, the final results showed completely ordered arrangements of Be and Si atoms in both the $SrBeSiO_4$ and $Sr_{0.73}Ca_{0.27}BeSiO_4$ structures (cf. Tables 5.5 and 5.9). A similar ordered distribution of Be/Si atoms can also be found in the tetrahedral framework of other compounds, such as $Na_2Be_2Si_3O_9$ [Ginderow, 1982].

Because of the different compositions of the two compounds, the geometries of

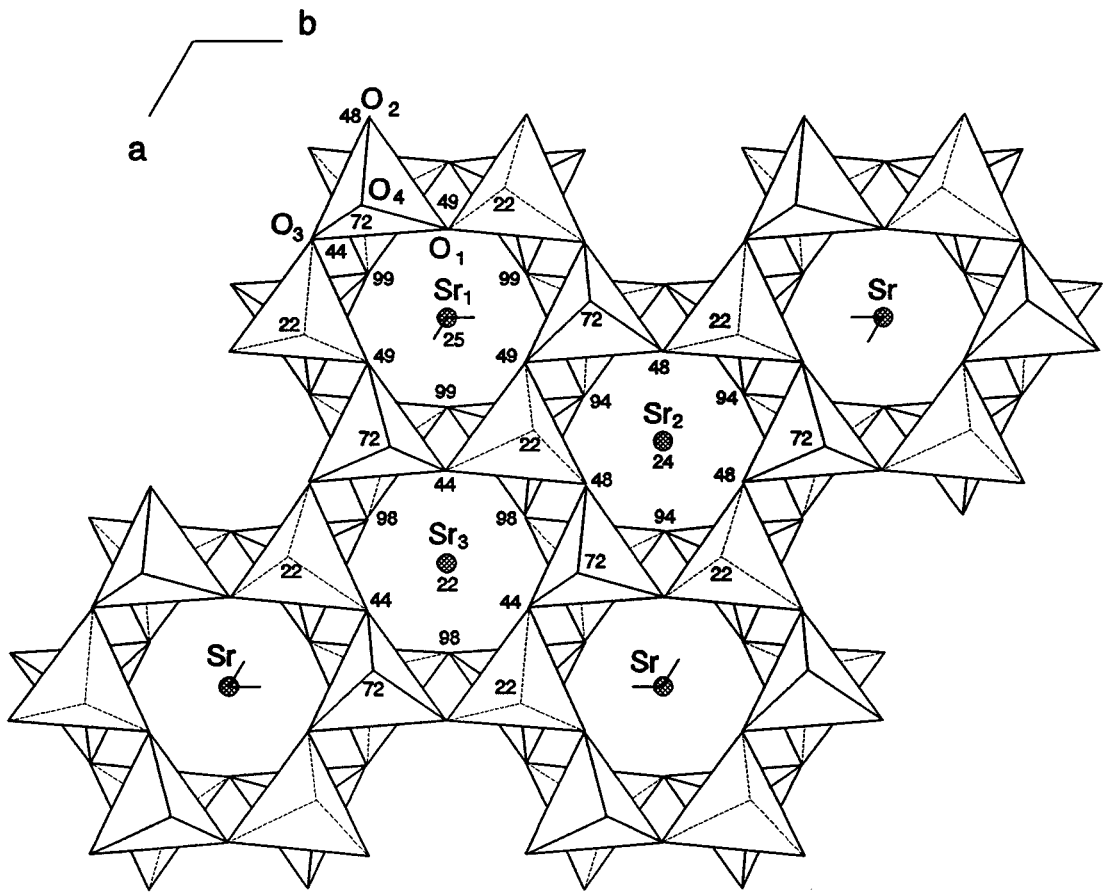

Fig. 5.4 The structure of $SrBeSiO_4$ viewed along the c-axis. The Si and Be atoms are fully ordered in the framework with SiO_4 tetrahedra pointing up and BeO_4 tetrahedra pointing down. The cavities are filled by Sr atoms. Atom heights are given in units of c/100.

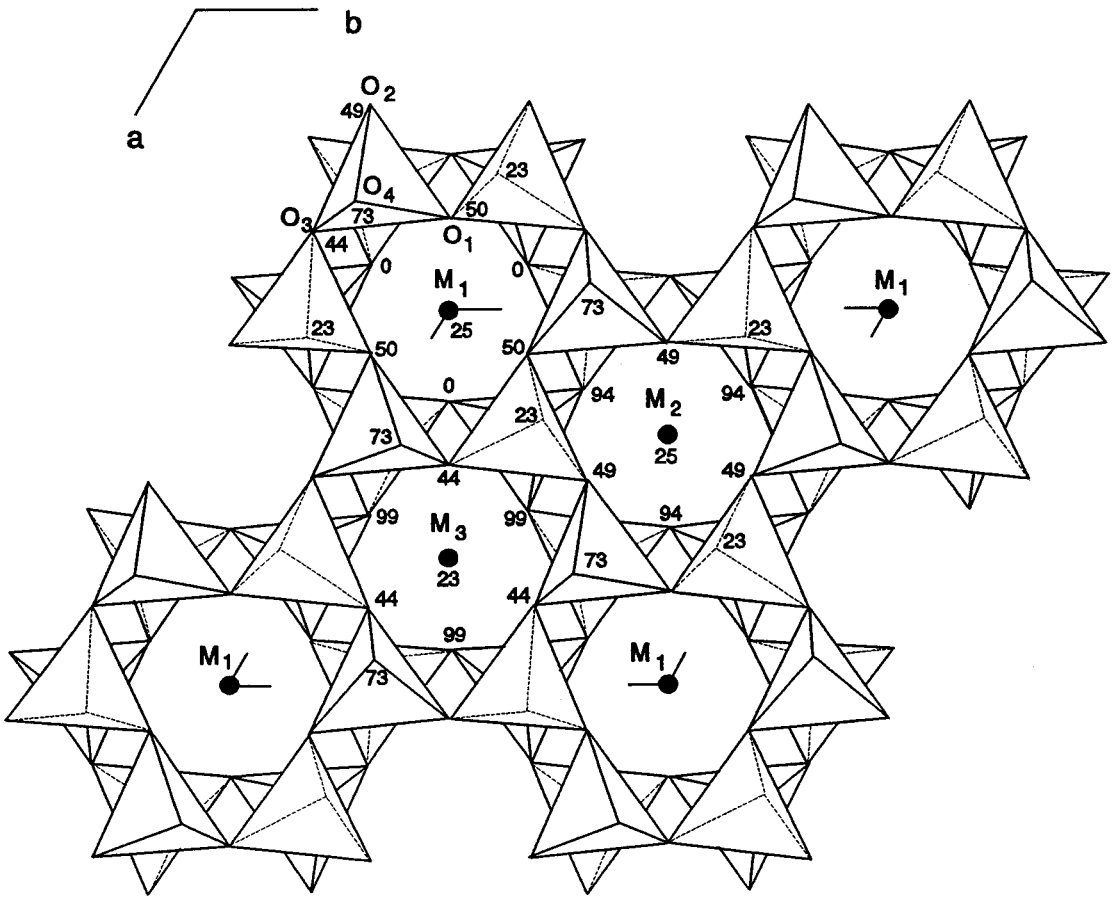

Fig. 5.5 The structure of $Sr_{0.73}Ca_{0.27}BeSiO_4$ viewed along the c-axis. The Si and Be atoms are fully ordered in the framework with SiO_4 tetrahedra pointing up and BeO_4 tetrahedra pointing down. The cavities are filled by Sr/Ca atoms with a tendency towards ordering (M(1) = 19 at% Ca, M(2) = 36 at% Ca, M(3) = 25 at% Ca). Atom heights are given in units of c/100. Note the shifts of the O(4) atoms towards the M(2) sites.

the cavity sites within the frameworks are different. In the $SrBeSiO_4$ structure, the three cavity sites are all occupied by Sr atoms only with, however, different coordinations: Sr(1) is nine-coordinated with a rather regular arrangement of six O(1)s plus three O(4)s at an average distance of 2.74 Å; Sr(2) is six-coordinated by three O(2)s and three O(4)s at a shorter average distance of 2.60 Å and in addition three O(2)s at a longer distance of 3.02 Å; and Sr(3) is also six-coordinated by three O(2)s and three O(3)s at a similar average distance of 2.59 Å. In the $Sr_{0.73}Ca_{0.27}BeSiO_4$ structure, the three sites are occupied by both Sr and Ca atoms with a rather uniform distribution. The refinement nevertheless revealed a certain tendency for Sr/Ca ordering with the Ca-content increasing from 19% in M(1) to 25% in M(3) and 36% in M(2). This ordering trend is similar to that observed in the $Na_{0.5}K_{0.5}GaSiO_4$ structure but much less pronounced (cf. Chapter 4) with the M(1) site accommodating the larger Sr (K) atoms and the M(2) site accommodating the smaller Ca (Na) atoms. Similar to the $SrBeSiO_4$ structure, the cavity sites have different coordination geometries: the Sr-rich M(1) site is nine-coordinated (six O(1)s plus three O(4)s with an average distance of 2.71 Å), while the M(2) and M(3) sites, richer in Ca, are only six-coordinated (three O(2)s plus three O(4)s at an average distance of 2.51 Å for M(2) and three O(2)s and three O(3)s at an average distance of 2.55 Å for M(3)). Although the coordination environments are irregular and the coordination numbers chosen somewhat arbitrarily, the corresponding average M-O distances are consistent with the Sr/Ca ordering, that is, they decrease as the Sr content decreases.

Comparing the structures of $SrBeSiO_4$ and $Sr_{1-x}Ca_xBeSiO_4$ (Figs. 5.4 and 5.5), it is clear that the latter is more collapsed than the former as shown by the displacement of the O(4) atom further away from its ideal position on the pseudo 3-fold axes. The

degree of framework collapse can be qualitatively estimated from the differences (Δz) between $z_{O(1)}$ and $z_{O(3)}$ and the Be-O(4)-Si angles: in the $SrBeSiO_4$ structure, Δz is equal to 0.055 and the Be-O(4)-Si angle is equal to 161.0(11), while in the $Sr_{0.73}Ca_{0.27}BeSiO_4$ structure, Δz is equal to 0.067 and the Be-O(4)-Si angle is equal to 149.1(10), showing that the framework of the latter structure is significantly more collapsed. The smaller average size of the (Sr, Ca) atoms forces the structure to reduce the cavity size by collapsing the framework to meet their bonding requirement. To accommodate large amounts of the smaller Ca atoms ($x > 0.5$ in $Sr_{1-x}Ca_xBeSiO_4$), a change of framework topology to the beryllonite ($NaBePO_4$)-type is required, accompanied by an abrupt decrease in the c-parameter (Fig. 5.1). The beryllonite-type structure is commonly adopted by compounds with small cavity atoms, such as $NaXYO_4$ (X=Al,Ga; Y=Si,Ge) [Barbier and Fleet, 1987, 1988] and $CaAl_2O_4$ [Hörkner and Müller-Buschbaum, 1976; Barbier and Neuhausen, 1990].

It should be noted that the valence sums for all the Sr atoms in the $SrBeSiO_4$ compound tend to be low ($\Sigma s(Sr) \approx 1.7$), especially for Sr(2) (cf. Table 5.7). This suggests that the coordinations of the Sr atoms are unsuitable, and that these atoms may undergo slight displacements along the c-axis to achieve a better bonding as observed for the Na atoms in the (Na, K)$GaSiO_4$ compounds (cf. Chapter 4). The approximate $4\times C$ superstructure of the $SrBeSiO_4$ compound could possibly originate from such modulated shifts of the Sr atoms along the c-axis. In contrast, in the $Sr_{0.73}Ca_{0.27}BeSiO_4$ structure, the valence sum for the Ca-rich M(2) site is definitely higher (1.87), this being chiefly due to the contribution of shorter M(2)-O(4) bonds resulting from the displacement of O(4) towards M(2). It therefore appears that, with increasing Ca-content, the framework of the $Sr_{1-x}Ca_xBeSiO_4$ structure becomes locked into a particular configuration which

satisfies the bonding requirement of, at least, the most Ca-rich site M(2). As a result, the incommensurate $4\times C$ superstructure vanishes rapidly with increasing x. It is also noteworthy that, like in other tridymite-derivative compounds, the temperature factors of the O(4) atoms in $SrBeSiO_4$ and $Sr_{0.73}Ca_{0.27}BeSiO_4$ are higher than those of other atoms, suggesting positional disorder of these O(4) atoms. However, the O(4) temperature factor is unusually high in the $SrBeSiO_4$ structure, probably as a result of O(4) displacements being associated with the formation of the ($\approx 4\times C$) superstructure.

TABLE 5.1

POWDER X-RAY DIFFRACTION PATTERN FOR $SrBeSiO_4$

h	k	l	d_{cal}(Å)	d_{obs}(Å)	I/I_o
1	1	0	4.2040	4.1979	32
1	1	1	3.7386	3.7350	22
1	1	2	2.9306	2.9310	100
3	0	0	2.4272	2.4274	48
3	0	1	2.3268	2.3270	9
1	1	3	2.2866	2.2861	3
2	0	3#	2.1816	2.1815	2
2	2	0	2.1020	2.1024	16
3	0	2	2.0870	2.0875	41
0	0	4	2.0437	2.0444	14
2	2	1	2.0358	2.0365	3
2	2	2	1.8693	1.8700	28
1	1	4	1.8380	1.8389	15
3	0	3	1.8124	1.8133	2
4	1	0	1.5890	1.5894	8
3	0	4	1.5633	1.5636	23
1	1	5	1.5238	1.5240	2
4	1	2	1.4810	1.4813	39
2	2	4	1.4653	1.4656	10
3	3	0	1.4013	1.4015	21
4	1	3	1.3726	1.3727	2
0	0	6	1.3625	1.3626	1
3	3	2	1.3256	1.3257	1
1	1	6	1.2961	1.2961	8
3	2	4#	1.2934	1.2936	1
2	2	5	1.2905	1.2907	2
4	1	4	1.2544	1.2544	15
2	1	6#	1.2210	1.2209	1
6	0	0	1.2135	1.2136	8
6	0	1	1.2004	1.2003	1
3	0	6	1.1881	1.1879	13
5	2	0	1.1660	1.1658	4
6	0	2	1.1634	1.1633	5
3	3	4	1.1557	1.1556	22
2	2	6	1.1433	1.1430	7
4	1	5	1.1395	1.1392	3
5	2	2	1.1213	1.1212	37
2	0	7#	1.1120	1.1121	2

Superstructure reflections of the type {hkl, h-k $\neq$ 3n} requiring a $\sqrt{3}\times$A axis.

TABLE 5.2

POWDER X-RAY DIFFRACTION PATTERN FOR $Sr_{0.7}Ca_{0.3}BeSiO_4$

h	k	l	d_{cal}(Å)	d_{obs}(Å)	I/I_o
1	1	0	4.1843	4.1820	19
1	1	1	3.7174	3.7167	24
1	1	2	2.9098	2.9106	100
3	0	0	2.4158	2.4162	41
3	0	1	2.3150	2.3154	14
2	1	2#	2.2689		
1	1	3	2.2683	2.2684	3
2	2	0	2.0922	2.0924	16
3	0	2	2.0746	2.0751	35
2	2	1	2.0257	2.0254	17
0	0	4	2.0246		
2	2	2	1.8587	1.8590	28
1	1	4	1.8224	1.8227	12
3	1	2#	1.8004	1.8008	3
3	0	3	1.8002		
4	0	2#	1.6538	1.6538	1
2	2	3	1.6536		
3	2	1#	1.6287	1.6300	4
2	1	4#	1.6281		
4	1	0	1.5815	1.5816	12
1	0	5#	1.5807		
4	1	1	1.5522		
3	0	4	1.5517	1.5518	24
1	1	5	1.5104	1.5104	4
4	1	2	1.4731	1.4731	41
2	2	4	1.4549	1.4549	3
3	3	0	1.3948	1.3947	22
2	1	5#	1.3942		
5	0	2#	1.3647		
4	1	3	1.3646	1.3645	3
4	2	1#	1.3505	1.3506	1
4	0	4#	1.3501		
5	1	1#	1.2852	1.2851	8
3	2	4#	1.2849		
2	2	5	1.2807	1.2807	2
6	0	0	1.2079		
4	0	5#	1.2075	1.2077	7

5	0	4#	1.1786		
3	0	6	1.1783	1.1781	9
5	2	0	1.1605		
3	2	5#	1.1602	1.1604	4
6	0	2	1.1575	1.1573	4
5	2	1	1.1488		
3	3	4	1.1486	1.1485	15
4	2	4#	1.1344	1.1344	5
2	2	6	1.1342		
4	1	5	1.1315	1.1312	2
3	1	6#	1.1205	1.1207	3

Superstructure reflections of the type {hkl, h-k $\neq$ 3n} requiring a $\sqrt{3}\times$A axis.

TABLE 5.3

UNIT-CELL PARAMETERS (Å) AND VOLUMES PER FORMULA UNIT (Å^3) FOR THE $Sr_{1-x}Ca_xBeSiO_4$ COMPOUNDS REFINED FROM X-RAY POWDER DIFFRACTION DATA

x	struc type	a	b	c	γ(°)	V	Quench temp(°C).
0.0	kal*	8.4080(4)	-	8.1749(5)		83.41	1200
0.1	kal	8.3936(5)	-	8.1467(6)		82.84	1200
0.2	kal	8.3818(3)	-	8.1267(5)		82.41	1200
0.3	kal	8.3687(6)	-	8.0982(8)		81.86	1200
0.4	kal	8.3535(6)	-	8.0692(8)		81.27	1200
0.5	mix	-	-	-	-	-	1200
0.6	ber**	8.286(3)	14.402(5)	7.986(9)	90	79.42	1200
0.7	ber	8.283(2)	14.31(1)	7.95(2)	90	78.52	1200
0.9	ber	8.22(1)	14.32(1)	7.910(3)	90	77.57	1200
1.0	ber	8.245(3)	14.218(3)	7.891(2)	90.25	77.09	1400

* kal = solid solution with a ($\sqrt{3}\times$A, C) kalsilite superstructure.
** ber = solid solution with beryllonite structure.

TABLE 5.4

SUMMARY OF SINGLE CRYSTAL DATA, INTENSITY MEASUREMENTS AND STRUCTURE REFINEMENT PARAMETERS FOR $SrBeSiO_4$

Crystal Data

Empirical Formula	$SrBeSiO_4$
Color; Habit	Colorless (001) plate
Crystal System	hexagonal
Space Group	$P6_3$
Unit Cell Dimensions (sub-cell)	a = 8.405(8) Å
	c = 8.171(8) Å
Volume	499.9(4) $Å^3$
Z	6
Formula weight	188.7
Density(calc.)	3.761 Mg/m^3
Absorption Coefficient	16.38 mm^{-1}
F(000)	528

Data Collection

Diffractometer Used	P_4
Radiation	MoKα (λ = 0.71073 Å)
Temperature (K)	298
Monochromator	Highly oriented graphite crystal
2θ Range	7.0 to 45.0°
Scan Type	ω
Scan Speed	Variable;10.00 to 15.00°/min. in ω
Scan Range (ω)	0.31°
Background Measurement	Stationary crystal and stationary counter at beginning and end of scan, each for 0.5% of total scan time
Standard Reflections	3 measured every 97 reflections
Index Ranges	$-10 \leq h \leq 2$, $-1 \leq k \leq 10$, $0 \leq l \leq 10$
Reflections Collected	4128
Reflections Collected (sub-cell)	1065
Independent Reflections (sub-cell)	410 (R_{int} =4.08%)
Observed Reflections (sub-cell)	365 ($F \geq 4.0\sigma(F)$)
Absorption Correction	Psi-scan

Solution and Refinement

System Used	Siemens SHELXTL PLUS (PC Version)
Solution	Direct Methods
Refinement Method	Full-Matrix Least-Squares
Quantity Minimized	$\Sigma w(F_o-F_c)^2$
Absolute Structure	N/A
Extinction Correction	χ = 0.014(2), where $F^* = F [1 + 0.002\chi F^2/\sin(2\theta)]^{-1/4}$
Weighting Scheme	$w^{-1} = \sigma^2(F) + 0.0012F^2$
Number of Parameters Refined	64
Final R Indices (obs. data)	R =4.34 %, wR =6.12 %
R Indices (all data)	R =4.91 %, wR =6.38 %
Goodness-of-Fit	1.28
Largest and Mean Δ/σ	0.035,0.009
Data-to-Parameter Ratio	5.7:1
Largest Difference Peak	1.37 eÅ^{-3}
Largest Difference Hole	-2.50 eÅ^{-3}

TABLE 5.5

ATOMIC COORDINATES* AND EQUIVALENT ISOTROPIC DISPLACEMENT COEFFICIENTS ($Å^2 \times 10^3$) FOR THE SINGLE CRYSTAL X-RAY REFINEMENT OF $SrBeSiO_4$. The estimated standard deviations on the last digits are given in brackets.

Atom	Site	x	y	z	U_{eq}**
Sr(1)	2a	0	0	0.2500#	12(1)
Sr(2)	2b	0.3333	0.6667	0.2394(3)	12(1)
Sr(3)	2b	0.6667	0.3333	0.2236(4)	13(1)
Si	6c	0.6739(4)	0.6636(3)	0.524(1)	8(1)
Be	6c	0.664(2)	0.993(2)	0.412(4)	20(7)
O(1)	6c	0.757(1)	0.879(1)	0.496(2)	30(4)
O(2)	6c	0.452(1)	0.909(1)	0.482(2)	17(3)
O(3)	6c	0.739(1)	0.213(2)	0.441(2)	37(5)
O(4)	6c	0.648(3)	0.955(2)	0.216(2)	83(11)

* Transformed by the matrix (010, 100, 00-1) to be consistent with the other compounds.
** $U_{eq} = 1/3\ (U_{11} + U_{22} + U_{33})$
# Used to fix the origin in the $P6_3$ space group.

TABLE 5.6

ANISOTROPIC DISPLACEMENT COEFFICIENTS ($Å^2 \times 10^3$) OF $SrBeSiO_4$

	U_{11}	U_{22}	U_{33}	U_{12}	U_{13}	U_{23}
Sr(1)	18(1)	18(1)	9(2)	9(1)	0	0
Sr(2)	10(1)	10(1)	17(2)	5(1)	0	0
Sr(3)	18(1)	18(1)	4(1)	9(1)	0	0
Si	10(1)	3(1)	8(3)	0(1)	2(1)	1(1)
Be	30(9)	19(8)	11(11)	13(7)	-4(6)	-7(6)
O(1)	17(4)	20(4)	18(5)	11(3)	1(3)	0(3)
O(2)	15(4)	26(4)	58(6)	17(3)	-1(4)	-6(4)
O(3)	31(5)	28(5)	66(10)	26(4)	40(5)	38(5)
O(4)	197(19)	62(9)	14(7)	84(11)	11(7)	16(6)

The anisotropic displacement exponent takes the form: $-2\pi^2(h^2a^{*2}U_{11} + \ldots + 2hka^*b^*U_{12})$

TABLE 5.7

SELECTED BOND LENGTHS (Å), ANGLES (°) AND VALENCES (s) IN THE $SrBeSiO_4$ STRUCTURE. The estimated standard deviations on the last digits are given in brackets.

		l		s
Sr(1)-O(1)×3		2.67(1)		0.23×3
Sr(1)-O(1)×3		2.74(1)		0.19×3
Sr(1)-O(4)×3		2.81(3)		0.16×3
	mean	2.74	Σ	1.74
Sr(2)-O(2)×3		2.65(1)		0.24×3
{Sr(2)-O(3)×3		3.02(1)}*		0.09×3}
Sr(2)-O(4)×3		2.55(2)		0.31×3
	mean	2.60	Σ	1.65
Sr(3)-O(2)×3		2.65(1)		0.24×3
Sr(3)-O(3)×3		2.527(9)		0.33×3
{Sr(3)-O(4)×3		3.10(1)}*		0.07×3}
	mean	2.59	Σ	1.71
Si-O(1)		1.60(1)		1.07
Si-O(2)		1.617(9)		1.02
Si-O(3)		1.59(1)		1.10
Si-O(4)		1.59(2)		1.10
	mean	1.60	Σ	4.29
O-Si-O		103.8(11) ~ 114.8(5)		
Be-O(1)		1.65(2)		0.48
Be-O(2)		1.65(2)		0.48
Be-O(3)		1.63(2)		0.51
Be-O(4)		1.62(4)		0.52
	mean	1.64	Σ	1.99
O-Be-O		106.9(18)-113.4(13)		
Si-O(4)-Be		161.0(11)		

* The mean bond lengths and valence sums are calculated by excluding the long bonds.

TABLE 5.8

SUMMARY OF SINGLE CRYSTAL DATA, INTENSITY MEASUREMENTS AND STRUCTURE REFINEMENT PARAMETERS FOR $Sr_{1-X}Ca_XBeSiO_4$

Crystal Data

Empirical Formula	$Sr_{1-X}Ca_XBeSiO_4$ (x = 0.27(2))
Color; Habit	Colorless (001) plate
Crystal size (mm)	0.05 × 0.35 × 0.31
Crystal System	Hexagonal
Space Group	$P6_3$
Unit Cell Dimensions	a = 8.3694(8) Å
	c = 8.1000(10) Å
Volume	491.4(3) $Å^3$
Z	6
Formula weight	176.0
Density(calc.)	3.569 Mg/m^3
Absorption Coefficient	12.775 mm^{-1}
F(000)	499.15

Data Collection

Diffractometer Used	Siemens R3m/V
Radiation	AgKα (λ = 0.56087 Å)
Temperature (K)	300
Monochromator	Highly oriented graphite crystal
2θ Range	7.0 to 45.0°
Scan Type	ω
Scan Speed	Variable; 2.00 to 29.30°/min. in ω
Scan Range (ω)	0.06°
Background Measurement	Stationary crystal and stationary counter at beginning and end of scan, each for 0.5% of total scan time
Standard Reflections	3 measured every 100 reflections
Index Ranges	$-17 \leq h \leq 14$, $0 \leq k \leq 17$, $0 \leq l \leq 16$
Reflections Collected	4528
Independent Reflections	1554 (R_{int} = 5.11%)
Observed Reflections	787 ($F > 6.0\sigma(F)$)
Absorption Correction	Psi-scan

Solution and Refinement

System Used	Siemens SHELXTL PLUS (PC Version)
Solution	Direct Methods
Refinement Method	Full-Matrix Least-Squares
Quantity Minimized	$\Sigma w(F_o-F_c)^2$
Absolute Structure	N/A
Extinction Correction	χ = 0.0003(3), where $F^* = F\,[1 + 0.002\chi F^2/\sin(2\theta)]^{-1/4}$
Weighting Scheme	$w^{-1} = \sigma^2(F) + 0.0015F^2$
Number of Parameters Refined	67
Final R Indices (obs. data)	R = 5.60 %, wR = 7.06 %
R Indices (all data)	R =8.84 %, wR =8.44 %
Goodness-of-Fit	1.18
Largest and Mean Δ/σ	0.000, 0.000
Data-to-Parameter Ratio	11.7:1
Largest Difference Peak	4.18 eÅ^{-3}
Largest Difference Hole	-3.13 eÅ^{-3}

TABLE 5.9

ATOMIC COORDINATES EQUIVALENT ISOTROPIC DISPLACEMENT COEFFICIENTS ($Å^2 \times 10^3$) AND OCCUPANCY FACTORS FOR THE SINGLE CRYSTAL X-RAY REFINEMENT OF $Sr_{0.73(2)}Ca_{0.27(2)}BeSiO_4$. The estimated standard deviations on the last digits are given in brackets.

Atom	site	x	y	z	U_{eq}*	Occupancy (±2%)
M(1)	2a	0	0	0.2500#	13(1)	81%Sr+19%Ca
M(2)	2b	0.3333	0.6667	0.2511(4)	23(1)	64%Sr+36%Ca
M(3)	2b	0.6667	0.3333	0.2289(3)	14(1)	75%Sr+25%Ca
Si	6c	0.6768(3)	0.6639(2)	0.5340(4)	10(1)	
Be	6c	0.663(2)	0.991(2)	0.420(1)	11(3)	
O(1)	6c	0.7578(6)	0.8811(6)	0.504(2)	19(2)	
O(2)	6c	0.4541(7)	0.9111(6)	0.491(1)	18(2)	
O(3)	6c	0.7950(9)	0.2098(9)	0.437(2)	37(3)	
O(4)	6c	0.639(2)	0.930(1)	0.228(1)	49(4)	

* $U_{eq} = 1/3\ (U_{11} + U_{22} + U_{33})$.
# Used to fix the origin in the $P6_3$ space group.

TABLE 5.10

ANISOTROPIC DISPLACEMENT COEFFICIENTS ($Å^2 \times 10^3$) OF $Sr_{1-x}Ca_xBeSiO_4$

	U_{11}	U_{22}	U_{33}	U_{12}	U_{13}	U_{23}
M(1)	12(1)	12(1)	14(1)	6(1)	0	0
M(2)	13(1)	13(1)	42(2)	7(1)	0	0
M(3)	12(1)	12(1)	17(1)	6(1)	0	0
Si	9(1)	9(1)	10(1)	4(1)	0(1)	0(1)
Be	15(4)	16(4)	6(3)	10(3)	-3(3)	-2(3)
O(1)	10(2)	10(2)	37(3)	5(2)	0(3)	-4(3)
O(2)	11(2)	7(2)	36(3)	5(1)	-4(2)	1(2)
O(3)	21(3)	13(2)	83(7)	12(2)	28(3)	21(3)
O(4)	87(7)	38(4)	21(3)	31(5)	23(4)	1(3)

The anisotropic displacement exponent takes the form: $-2\pi^2(h^2a^{*2}U_{11} + \ldots + 2hka^*b^*U_{12})$.

TABLE 5.11

SELECTED BOND LENGTHS (Å), BOND VALENCES (s) AND BOND ANGLES (°) IN THE $Sr_{1-x}Ca_xBeSiO_4$ STRUCTURE. The estimated standard deviations on the last digits are given in brackets.

		l	s(Sr)	s(Ca)
M(1)-O(1)×3		2.655(9)	0.234	0.156
M(1)-O(1)×3		2.705(10)	0.205	0.136
M(1)-O(4)×3		2.780(7)	0.167	0.111
	mean	2.714	Σ 1.818 × 0.810 +	1.209 × 0.190 = 1.70
M(2)-O(2)×3		2.631(9)	0.250	0.166
{M(2)-O(3)×3		3.135(10)}*	0.064	0.043}
M(2)-O(4)×3		2.408(5)	0.457	0.304
	mean	2.511	Σ 2.121 × 0.636 +	1.410 × 0.363 = 1.87
M(3)-O(2)×3		2.617(9)	0.260	0.173
M(3)-O(3)×3		2.486(9)	0.37	0.246
{M(3)-O(4)×3		3.269(14)}*	0.045	0.030}
	mean	2.553	Σ 1.890 × 0.753 +	1.257 × 0.246 = 1.73
Si-O(1)		1.609(5)	1.041	
Si-O(2)		1.614(3)	1.027	
Si-O(3)		1.603(8)	1.058	
Si-O(4)		1.622(10)	1.005	
	mean	1.612	Σ 4.13	
O-Si-O		104.5(5)-112.7(4)		
Be-O(1)		1.635(11)	0.503	
Be-O(2)		1.653(15)	0.479	
Be-O(3)		1.602(16)	0.550	
Be-O(4)		1.623(13)	0.520	
	mean	1.628	Σ 2.05	
O-Be-O		103.8(7)-115.0(6)		
Si-O(4)-Be		149.1(10)		

* The mean bond lengths and valence sums are calculated by excluding the long bonds.

CHAPTER 6

CONCLUSION

The silicate compounds $BaTSiO_4$ (T = Co, Mg, Zn), $Na_{0.5}K_{0.5}GaSiO_4$ and $Sr_{1-x}Ca_xBeSiO_4$ ($x = 0.0 \sim 0.4$) have been determined to crystallize with the same ($\sqrt{3}\times A$, C) superstructure of the hexagonal (A, C) kalsilite ($KAlSiO_4$) structure. In these compounds of general formula $MTSiO_4$, the Si and T (= Co, Mg, Zn, Ga, Be) atoms form the three-dimensional frameworks and the large M (= Ba, Na/K, Sr/Ca) atoms fill the cavities enclosed by the frameworks (cf. Chapters 3, 4, 5). The structural refinements of these framework silicates provide new insight into how the kalsilite-type framework accommodates cavity atoms of variable size.

The main features of the $\sqrt{3}\times A$ kalsilite superstructure are, firstly, the concerted displacements of the apical O(4) oxygen atoms from their ideal positions on the three-fold axes toward neighbouring M atoms and, secondly, the shifts of the cavity atoms along the c-axis of the hexagonal unit-cell. The O(4) displacements correspond to the tilting of the tetrahedra and the collapse of the framework around the M atoms. This collapse is necessary in order to meet the bonding requirement of these atoms and to relieve the strain in the Si-O(4)-T angles which are reduced to values of $140 \sim 160°$. Similar O(4) shifts are probably also the cause of the weak and diffuse $\sqrt{3}\times A$ superstructure occasionally observed in the natural compounds kalsilite [Smith and Sahama, 1957] and nepheline [Sahama, 1958, 1962]. However, no structure refinement has yet been carried out on these ordered alumino-silicate minerals.

Shifts along the c-axis of the cavity M atoms occur in all the $MTSiO_4$ structures studied in this work. These shifts remain minor for the Ba compounds (Chapter 3) but become more pronounced in the mixed compounds $Ca_{0.27}Sr_{0.73}BeSiO_4$ (Chapter 5) and, especially, $Na_{0.5}K_{0.5}GaSiO_4$ (Chapter 4). In both cases, the M(2) sites shift upwards (to larger z values) away from the O(3) atoms, thereby reducing their coordination from nine-fold to six-fold. This decrease in coordination number is entirely consistent with the observed concentration of the smaller Ca and Na atoms on the M(2) sites of the structures. The greater degree of ordering and the greater atomic shifts occurring in $Na_{0.5}K_{0.5}GaSiO_4$ are also consistent with the size difference being larger between the Na and K atoms than between the Ca and Sr atoms [Shannon, 1976].

Overall, the atomic displacements and framework distortions observed in the $MTSiO_4$ structures can be correlated with the relative sizes of the tetrahedral (T, Si) atoms and the cavity (M) atoms. In Table 6.1 are listed the average tetrahedral and cavity bond lengths, their ratios and the Si-O(4)-T angles for a number of refined structures of kalsilite-type compounds (i.e. with hexagonal symmetry and with the same UDUDUD framework topology). It appears from these data that the simple kalsilite structure (with a small (A, C) unit-cell and without concerted displacement of the O(4) atoms) only occurs for compounds, such as $KAlSiO_4$, $KLiSO_4$ and $KLiBeF_4$, with small <T-O>/<M-O> ratios. As this bond ratio increases, i.e., as the cavity atoms decrease in size relative to the tetrahedral atoms, atomic shifts are required in order to maintain proper bonding within the structure, resulting in the formation of the $\sqrt{3}\times A$ superstructure. It can be seen also that, as the <T-O>/<M-O> bond ratio increases, the degree of framework collapse also increases as shown by the reduction in the Si-O(4)-T angles. Therefore, the compounds containing relatively small atoms in their framework

cavities can be expected to be destabilized. This is indeed the case for the two compounds with the larger bond ratios in Table 6.1, i.e., $Na_{0.5}K_{0.5}GaSiO_4$ and $BaCoSiO_4$, which have been found to be stable at high temperature only, above approximately 900 and 1100°C respectively.

In conclusion, the variety of compounds synthesized and characterized in the present work significantly expands the structural family of kalsilite-like tridymite derivatives. It has been shown that the kalsilite-type framework, with a single UDUDUD ring topology, can accommodate a wide range of tetrahedral and cavity atoms through relatively minor atomic shifts and framework distortions.

TABLE 6.1

CORRELATION BETWEEN THE FRAMEWORK DISTORTION AND THE RELATIVE SIZES OF THE TETRAHEDRAL (T) AND CAVITY (M) ATOMS IN KALSILITE-TYPE STRUCTURES.

Compound	Unit-cell	T-O(Å) (mean)	M-O(Å) (mean)	T-O/M-O	Si-O(4)-T (°)	Ref.
$Na_{0.5}K_{0.5}GaSiO_4$	$\sqrt{3}A,C$	1.72(3)	2.71(2)	0.637	141.0	[1]
$BaCoSiO_4$	$\sqrt{3}A,C$	1.792(8)	2.842(9)	0.631	148.6	[2]
$Sr_{0.73}Ca_{0.27}BeSiO_4$	$\sqrt{3}A,C$	1.62(2)	2.59(1)	0.625	149.1	[3]
$BaZnSiO_4$	$\sqrt{3}A,C$	1.775(15)	2.85(2)	0.622	156.1	[2]
$BaMgSiO_4$	$\sqrt{3}A,C$	1.775(15)	2.86(2)	0.621	157.9	[2]
$SrBeSiO_4$*	$\sqrt{3}A,4C$	1.62(4)	2.64(3)	0.614	161.0	[3]
$BaZnGeO_4$**	$\sqrt{3}A,4C$	1.83(7)	3.01(6)	0.608	-	[4]
$BaAl_2O_4$#	2A,C	1.757	2.932	0.599	<161.9>	[5]
$KLiSO_4$	A,C	1.716(6)	2.960(3)	0.593	-	[6]
$KLiBeF_4$	A,C	1.69	2.87	0.589	-	[7]
$KAlSiO_4$	A,C	1.677	2.896	0.579	163	[8]

* Average structure (cf. Chapter 5).

** Average structure with large errors on atomic coordinates and bond distances.

Very weak (2×A,C) kalsilite superstructure, no esd's given in the original structure refinement.

References: [1] Chapter 4; [2] Chapter 3; [3] Chapter 5; [4] Iijima et al., 1982; [5] Hörkner et al., 1979; [6] Schulz et al., 1985; [7] Roy et al.; 1972; [8] Perrotta et al., 1965.

REFERENCES

R.N. Abbott, Jr., Am. Miner. 69, 449-457 (1984).

D. Altermatt and I.D. Brown, Acta Crystallogr. B41, 244-247 (1985).

J. Barbier and M.E. Fleet, J. Solid State Chem. 71, 361-370 (1987).

J. Barbier and M.E. Fleet, Phys. Chem. Minerals 16, 176-285 (1988).

J. Barbier and J. Neuhausen, Eur. J. Mineral. 2, 273-282 (1990).

C. Do Dinh and A. Durif, Bull. Soc. Fr. Minéral. Cristallogr. 87, 108-110 (1964).
W.A. Dollase, Acta Crystallogr. 23, 617-623 (1967).

P.D. Ginderow, F. Cesbron and M-C Sichère, Acta Crystallogr. B38, 62-66 (1982).

G. Guiseppetti and C. Tadini, Tschermaks Min. Petr. Mitt. 20, 2-12 (1973).

C.M.B. Henderson and J. Roux, Contrib. Mineral. Petrol. 61, 279-298 (1977).

C.M.B. Henderson and D. Taylor, Mineral. Mag. 45, 111-127 (1982).

C.M.B. Henderson and A.B. Thompson, Am. Min. 65, 970-980 (1980).

W. Hörkner and HK. Müller-Buschbaum, J. Inorg. Nucl. Chem. 38, 983-984 (1976).

W. Hörkner and HK. Müller-Buschbaum, Z. Anorg. Allg. Chem. 451, 40-44 (1979).

C.J. Howard and R.J. Hill, AAEC report No. 000# (1985).

K. Iijima, F. Marumo and H. Takei, Acta Crystallogr. B38, 1112-1116 (1982).

A. Kawahara, Y. Andou, F. Marumo and M. Okuno, Miner. J. 13(5), 260-270 (1987).

G. Lampert and R. Böhme, Z. Kristallogr. 176, 29-33 (1986).

F. Liebau, "Structural Chemistry of Silicates", Springer-Verlag, Berlin/Heidelberg/New York / Tokyo (1985).

Y.A. Malinovskii, Sov. Phys. Dokl. 29(9), 706-708 (1984).

S. Merlino: Feldspathoids, Their Average and Real Structure. In W.L. Brown ed, Feldspars and Feldspathoids, NATO ASI Series, C137. Reidel , Dordrecht, Holland (1985).

A.J. Perrotta and J.V. Smith, Mineral. Mag. 35, 588-595 (1965).

H.M. Rietveld, Acta Crystallogr. 22, 151-152 (1967).

H.M. Rietveld, J. Appl. Cryst. 2, 65-71 (1969).

J.L. Roy and S. Aléonard, Acta Crystallogr. B28, 1383-1385 (1972).

H.Schulz, U. Zucher and R. Frech, Acta Crystallogr. B41, 21-26 (1985).

A.R. Schulze and HK. Müller-Buschbaum, Z. Anorg. Allg. Chem. 475, 205-210 (1981).

V.F. Sears: Thermal Neutron Scattering Lengths and Cross-sections for Condensed Matter Research", Atomic Energy of Canada Limited, Report AECL-8490 (1984).

R.D. Shannon, Acta Crystallogr. A32, 751-767 (1976).

W.B. Simmons, Jr. and D.R. Peacor, Am. Miner. 57, 1711-1719 (1972).

J.V. Smith and O. F. Tuttle, Am. J. Sci 255, 282-305 (1957).

H. Takei, S.Tsunekawa and M. Maeda, J. Mat. Sci. 15, 2612-2618 (1980).

H. Takei, J. Appl. Crystallogr. 13, 400-401 (1980).

D. Taylor, M.J. Dempsey and C.M.B. Henderson, Bull. Minéral. 108, 643-652 (1985).

C.W. Tompson, D.F.R. Mildner, M. Mehregang, J. Sudol, R. Berliner, and W. B. Yelton, J. Appl. Crystallogr. 17, 385-394 (1984).

O. F. Tuttle and J.V. Smith, Am. J. Sci 256, 571-589 (1958).

J.W. Visser, J. Appl. Crystallogr. 2, 89-95 (1969).

J. Weber and J. Barbier: Synthesis, Structures and Crystal Chemistry in (Na, K)$GaSiO_4$ and (Ca, Ba)Al_2O_4, Senior thesis, McMaster University (1990).

A.R. West: Solid State Chemistry, Chichester . New York . Brisbane . Toronto . Singapore: John Wiley & Sons (1988).

R.A. Young & D.B. Wiles, J. Appl. Crystallogr.15, 430-438 (1982).

APPENDIX

OBSERVED AND CALCULATED STRUCTURE FACTORS

The following tables contain the observed (F_o) and calculated ($|F_c|$) structure factors for the three single crystal structure determinations ($BaCoSiO_4$ and $Sr_{1-x}Ca_xBeSiO_4$, x = 0.0 and 0.27). A negative standard deviation (s) indicates that the reflection was treated as unobserved during the refinement.

Observed and calculated structure factors for $BaCoSiO_4$

h	k	l	10Fo	10Fc	10s	h	k	l	10Fo	10Fc	10s	h	k	l	10Fo	10Fc	10s	h	k	l	10Fo	10Fc	10s	h	k	l	10Fo	10Fc	10s
0	1	0	151	69	-4	-9	11	0	94	79	-26	-7	15	0	141	148	19	0	7	1	109	87	16	-7	13	1	83	66	-36
-1	2	0	1569	1618	12	-8	11	0	127	119	17	-6	15	0	756	762	35	-7	8	1	299	311	8	-6	13	1	161	138	24
0	2	0	157	161	7	-7	11	0	567	582	9	-5	15	0	71	90	-31	-6	8	1	153	136	15	-5	13	1	150	125	24
-2	3	0	289	288	4	-6	11	0	63	50	-24	-4	15	0	163	146	18	-5	8	1	62	70	-25	-4	13	1	104	89	-30
-1	3	0	303	304	6	-5	11	0	163	179	11	-3	15	0	657	656	18	-4	8	1	203	208	15	-3	13	1	127	89	-30
0	3	0	3783	4044	40	-4	11	0	803	844	15	-2	15	0	114	90	-31	-3	8	1	220	227	8	-2	13	1	119	104	-20
-3	4	0	232	226	10	-3	11	0	42	21	-25	-1	15	0	48	83	-28	-2	8	1	89	112	-21	-1	13	1	65	54	-32
-2	4	0	1616	1619	12	-2	11	0	68	112	-28	0	15	0	512	486	21	-1	8	1	424	440	11	0	13	1	68	66	-25
-1	4	0	518	519	4	-1	11	0	512	527	7	-14	16	0	298	281	22	0	8	1	155	155	11	-13	14	1	136	107	20
0	4	0	189	193	11	0	11	0	42	29	-21	-13	16	0	135	112	-27	-8	9	1	158	170	12	-12	14	1	136	105	-23
-4	5	0	1117	1150	22	-11	12	0	57	83	-32	-12	16	0	73	54	-32	-7	9	1	80	71	-23	-11	14	1	48	82	-29
-3	5	0	92	64	13	-10	12	0	241	250	23	-11	16	0	365	361	18	-6	9	1	144	137	20	-10	14	1	89	95	-27
-2	5	0	289	288	5	-9	12	0	1120	1153	21	-10	16	0	235	198	19	-5	9	1	210	214	9	-9	14	1	133	101	-25
-1	5	0	1578	1599	26	-8	12	0	111	124	-27	-9	16	0	66	5	-27	-4	9	1	110	92	15	-8	14	1	77	27	-29
0	5	0	203	198	13	-7	12	0	263	266	9	-8	16	0	345	349	34	-3	9	1	119	138	14	-7	14	1	102	96	-30
-5	6	0	255	253	6	-6	12	0	1280	1340	15	-7	16	0	211	197	30	-2	9	1	249	250	13	-6	14	1	186	164	25
-4	6	0	424	424	7	-5	12	0	155	152	14	-6	16	0	56	41	-28	-1	9	1	160	174	12	-5	14	1	67	76	-28
-3	6	0	3350	3636	43	-4	12	0	209	212	19	-5	16	0	315	327	21	0	9	1	92	52	-22	-4	14	1	171	169	19
-2	6	0	221	229	7	-3	12	0	1107	1152	13	-4	16	0	208	218	14	-9	10	1	183	201	13	-3	14	1	153	121	18
-1	6	0	298	297	6	-2	12	0	131	129	18	-3	16	0	78	30	-31	-8	10	1	218	208	10	-2	14	1	138	82	-23
0	6	0	2466	2610	54	-1	12	0	71	102	-29	-2	16	0	249	238	26	-7	10	1	44	66	-24	-1	14	1	106	89	-31
-6	7	0	124	124	16	0	12	0	973	980	12	-12	17	0	51	27	-31	-6	10	1	146	167	13	0	14	1	119	50	-22
-5	7	0	968	997	7	-12	13	0	92	72	-31	-11	17	0	46	53	-27	-5	10	1	292	289	9	-14	15	1	51	83	-30
-4	7	0	251	268	8	-11	13	0	419	439	9	-10	17	0	253	237	17	-4	10	1	82	84	-25	-13	15	1	85	52	-33
-3	7	0	49	65	-21	-10	13	0	175	165	21	-9	17	0	95	27	-35	-3	10	1	145	125	-25	-12	15	1	49	62	-29
-2	7	0	1125	1187	6	-9	13	0	62	32	-28	-8	17	0	76	71	-29	-2	10	1	248	260	8	-11	15	1	179	148	17
-1	7	0	401	410	8	-8	13	0	506	519	15	-7	17	0	379	351	14	-1	10	1	73	97	-25	-10	15	1	97	25	-29
0	7	0	41	126	-21	-7	13	0	225	220	10	-6	17	0	46	11	-26	0	10	1	119	93	15	-9	15	1	94	15	-30
-7	8	0	1090	1134	19	-6	13	0	43	20	-26	-5	17	0	54	24	-31	-10	11	1	140	138	17	-8	15	1	191	180	15
-6	8	0	79	59	-25	-5	13	0	522	541	17	0	1	1	30	44	-15	-9	11	1	172	163	13	-7	15	1	54	61	-27
-5	8	0	187	185	11	-4	13	0	263	268	14	-1	2	1	1030	961	21	-8	11	1	38	34	-22	-6	15	1	43	10	-25
-4	8	0	808	851	9	-3	13	0	64	61	-29	0	2	1	132	126	10	-7	11	1	266	287	9	-5	15	1	146	167	18
-3	8	0	33	32	-19	-2	13	0	506	514	10	-2	3	1	40	78	-19	-6	11	1	175	162	22	-4	15	1	97	75	-31
-2	8	0	187	184	11	-1	13	0	248	261	12	-1	3	1	80	83	-17	-5	11	1	40	29	-24	-3	15	1	83	39	-36
-1	8	0	816	833	18	0	13	0	130	142	-23	0	3	1	826	753	20	-4	11	1	166	170	11	-2	15	1	123	132	-43
0	8	0	183	179	12	-13	14	0	327	315	11	-3	4	1	364	359	6	-3	11	1	104	104	-19	-1	15	1	59	55	-35
-8	9	0	116	156	19	-12	14	0	50	43	-29	-2	4	1	943	900	9	-2	11	1	119	87	18	0	15	1	47	2	-24
-7	9	0	399	409	6	-11	14	0	129	99	-29	-1	4	1	107	103	11	-1	11	1	137	121	22	-14	16	1	67	57	-36
-6	9	0	1821	1960	14	-10	14	0	509	511	15	0	4	1	176	170	6	0	11	1	116	130	18	-13	16	1	90	62	-31
-5	9	0	161	169	10	-9	14	0	90	30	-30	-4	5	1	771	749	21	-11	12	1	163	154	17	-12	16	1	168	106	17
-4	9	0	245	255	8	-8	14	0	93	50	-30	-3	5	1	260	253	9	-10	12	1	55	75	-31	-11	16	1	106	90	-27
-3	9	0	1811	1950	18	-7	14	0	366	386	8	-2	5	1	209	206	9	-9	12	1	41	40	-23	-10	16	1	67	59	-28
-2	9	0	193	191	9	-6	14	0	45	9	-27	-1	5	1	554	544	12	-8	12	1	171	182	13	-9	16	1	117	90	-32
-1	9	0	110	132	-26	-5	14	0	47	85	-28	0	5	1	225	230	8	-7	12	1	115	104	-20	-8	16	1	135	73	22
0	9	0	1705	1780	11	-4	14	0	378	379	11	-5	6	1	201	201	9	-6	12	1	51	26	-24	-7	16	1	103	57	-29
-9	10	0	109	127	-25	-3	14	0	116	72	-22	-4	6	1	186	191	8	-5	12	1	193	201	13	-6	16	1	107	80	-28
-8	10	0	852	869	6	-2	14	0	106	106	-30	-3	6	1	77	57	-23	-4	12	1	74	72	-28	-5	16	1	81	75	-30
-7	10	0	243	262	15	-1	14	0	462	441	20	-2	6	1	262	273	10	-3	12	1	45	42	-27	-4	16	1	54	53	-29
-6	10	0	57	50	-25	0	14	0	74	42	-31	-1	6	1	192	186	14	-2	12	1	194	197	15	-3	16	1	142	79	-33
-5	10	0	840	879	7	-14	15	0	48	56	-28	0	6	1	271	285	5	-1	12	1	123	92	-27	-2	16	1	80	49	-31
-4	10	0	322	330	10	-13	15	0	242	228	23	-6	7	1	240	248	10	0	12	1	50	9	-23	-12	17	1	88	98	-31
-3	10	0	104	106	-20	-12	15	0	673	663	17	-5	7	1	349	353	6	-12	13	1	146	153	20	-11	17	1	80	5	-29
-2	10	0	668	704	9	-11	15	0	120	108	-25	-4	7	1	90	51	-25	-11	13	1	155	161	-32	-10	17	1	99	88	-36
-1	10	0	312	324	10	-10	15	0	235	212	18	-3	7	1	233	235	9	-10	13	1	46	77	-27	-9	17	1	115	103	-32
0	10	0	45	87	-22	-9	15	0	782	778	27	-2	7	1	335	334	5	-9	13	1	146	148	17	-8	17	1	87	12	-30
-10	11	0	520	536	7	-8	15	0	90	91	-30	-1	7	1	104	86	-27	-8	13	1	114	126	-21	-7	17	1	46	53	-26

Observed and calculated structure factors for $BaCoSiO_4$

h	k	l	10Fo	10Fc	10s	h	k	l	10Fo	10Fc	10s	h	k	l	10Fo	10Fc	10s	h	k	l	10Fo	10Fc	10s	h	k	l	10Fo	10Fc	10s
-6	17	1	67	80	-34	-1	10	2	177	193	20	-10	15	2	80	112	-31	-7	8	3	554	572	7	-6	13	3	155	139	18
-5	17	1	67	30	-30	0	10	2	41	43	-21	-9	15	2	288	296	14	-6	8	3	275	269	9	-5	13	3	278	274	15
0	0	2	693	623	7	-10	11	2	997	1032	14	-8	15	2	172	183	-35	-5	8	3	46	70	-28	-4	13	3	42	38	-24
0	1	2	268	237	5	-9	11	2	196	196	12	-7	15	2	105	80	-27	-4	8	3	641	638	6	-3	13	3	47	67	-28
-1	2	2	3608	3394	41	-8	11	2	238	252	10	-6	15	2	308	302	13	-3	8	3	263	260	17	-2	13	3	176	197	15
0	2	2	371	355	4	-7	11	2	1163	1215	13	-5	15	2	152	150	19	-2	8	3	109	124	16	-1	13	3	48	57	-29
-2	3	2	571	525	4	-6	11	2	232	230	9	-4	15	2	116	100	-25	-1	8	3	634	658	7	0	13	3	64	36	-26
-1	3	2	470	436	11	-5	11	2	221	237	12	-3	15	2	266	278	14	0	8	3	258	266	8	-13	14	3	161	147	26
0	3	2	1717	1586	28	-4	11	2	931	963	16	-2	15	2	161	142	25	-8	9	3	92	96	-24	-12	14	3	172	135	20
-3	4	2	249	239	6	-3	11	2	212	226	15	-1	15	2	119	99	-33	-7	9	3	77	86	-25	-11	14	3	190	209	15
-2	4	2	2824	2761	11	-2	11	2	240	217	15	0	15	2	258	247	11	-6	9	3	138	101	21	-10	14	3	198	182	14
-1	4	2	185	181	7	-1	11	2	976	1003	14	-13	16	2	65	35	-29	-5	9	3	158	132	15	-9	14	3	225	215	12
0	4	2	271	273	6	0	11	2	207	191	11	-12	16	2	130	112	-27	-4	9	3	77	79	-30	-8	14	3	139	145	22
-4	5	2	2630	2633	27	-11	12	2	215	218	12	-11	16	2	446	433	27	-3	9	3	144	145	12	-7	14	3	224	219	16
-3	5	2	311	292	11	-10	12	2	108	137	-29	-10	16	2	82	111	-33	-2	9	3	219	237	9	-6	14	3	273	247	10
-2	5	2	261	249	6	-9	12	2	468	476	8	-9	16	2	114	97	-34	-1	9	3	213	210	10	-5	14	3	136	123	21
-1	5	2	2201	2202	43	-8	12	2	243	236	10	-8	16	2	510	498	22	0	9	3	45	48	-23	-4	14	3	243	226	25
0	5	2	400	406	7	-7	12	2	168	175	17	-7	16	2	67	108	-30	-9	10	3	182	160	16	-3	14	3	202	206	16
-5	6	2	345	365	6	-6	12	2	392	400	7	-6	16	2	56	35	-34	-8	10	3	420	434	7	-2	14	3	51	79	-30
-4	6	2	242	244	7	-5	12	2	232	222	11	-5	16	2	500	474	17	-7	10	3	99	119	-22	-1	14	3	157	163	19
-3	6	2	524	508	19	-4	12	2	172	150	16	-4	16	2	109	119	-30	-6	10	3	174	159	23	0	14	3	169	170	17
-2	6	2	207	204	8	-3	12	2	462	461	7	-3	16	2	46	33	-27	-5	10	3	452	470	15	-14	15	3	70	35	-31
-1	6	2	251	251	8	-2	12	2	193	206	14	-11	17	2	145	128	24	-4	10	3	55	48	-24	-13	15	3	51	46	-29
0	6	2	938	941	17	-1	12	2	140	115	17	-10	17	2	495	464	21	-3	10	3	126	121	-22	-12	15	3	58	50	-29
-6	7	2	237	233	8	0	12	2	368	350	7	-9	17	2	136	128	-24	-2	10	3	404	425	11	-11	15	3	101	69	-32
-5	7	2	2069	2123	15	-12	13	2	153	140	-26	-8	17	2	122	127	-27	-1	10	3	44	61	-26	-10	15	3	45	58	-26
-4	7	2	165	173	11	-11	13	2	721	720	23	-7	17	2	371	366	14	0	10	3	127	139	16	-9	15	3	44	30	-26
-3	7	2	130	112	13	-10	13	2	95	81	-31	-6	17	2	121	112	-31	-10	11	3	293	296	9	-8	15	3	104	110	-32
-2	7	2	1945	2018	27	-9	13	2	148	131	24	0	1	3	168	153	7	-9	11	3	260	250	9	-7	15	3	47	60	-28
-1	7	2	169	185	10	-8	13	2	836	844	18	-1	2	3	1169	1059	15	-8	11	3	204	209	14	-6	15	3	103	10	-26
0	7	2	147	139	11	-7	13	2	135	123	18	0	2	3	275	240	5	-7	11	3	414	420	10	-5	15	3	174	130	22
-7	8	2	1425	1477	16	-6	13	2	150	112	16	-2	3	3	137	136	10	-6	11	3	228	246	12	-4	15	3	131	91	-31
-6	8	2	231	240	10	-5	13	2	832	836	20	-1	3	3	89	46	-22	-5	11	3	176	196	12	-3	15	3	64	28	-28
-5	8	2	267	274	16	-4	13	2	178	171	13	0	3	3	563	515	13	-4	11	3	389	397	7	-2	15	3	118	93	-31
-4	8	2	1808	1863	20	-3	13	2	53	53	-27	-3	4	3	240	220	7	-3	11	3	257	262	9	-1	15	3	137	107	-29
-3	8	2	281	288	8	-2	13	2	670	680	17	-2	4	3	1126	1080	10	-2	11	3	156	47	-40	-13	16	3	79	40	-30
-2	8	2	367	391	8	-1	13	2	140	154	20	-1	4	3	52	58	-20	-1	11	3	307	315	12	-12	16	3	61	91	-36
-1	8	2	1599	1655	23	0	13	2	88	67	-24	0	4	3	113	118	12	0	11	3	212	231	10	-11	16	3	145	150	-31
0	8	2	274	283	8	-13	14	2	587	580	23	-4	5	3	1015	991	10	-11	12	3	98	91	-27	-10	16	3	84	23	-31
-8	9	2	280	293	8	-12	14	2	148	120	18	-3	5	3	261	265	13	-10	12	3	72	34	-29	-9	16	3	124	75	-26
-7	9	2	199	207	10	-11	14	2	190	186	15	-2	5	3	134	119	12	-9	12	3	57	35	-30	-8	16	3	160	137	18
-6	9	2	657	677	11	-10	14	2	594	591	18	-1	5	3	939	927	20	-8	12	3	136	125	18	-7	16	3	71	35	-34
-5	9	2	486	359	-107	-9	14	2	120	125	-23	0	5	3	175	166	12	-7	12	3	138	107	18	-6	16	3	104	44	-33
-4	9	2	158	175	11	-8	14	2	94	131	-29	-5	6	3	241	224	15	-6	12	3	40	17	-23	-5	16	3	157	136	18
-3	9	2	658	680	19	-7	14	2	775	778	20	-4	6	3	180	174	9	-5	12	3	131	117	17	-4	16	3	105	18	-33
-2	9	2	239	243	8	-6	14	2	194	183	12	-3	6	3	40	48	-23	-4	12	3	142	129	23	-3	16	3	51	62	-30
-1	9	2	215	203	16	-5	14	2	180	176	19	-2	6	3	169	158	10	-3	12	3	42	27	-24	-11	17	3	142	121	23
0	9	2	445	453	6	-4	14	2	712	707	26	-1	6	3	193	205	12	-2	12	3	156	156	19	-10	17	3	135	109	-27
-9	10	2	182	182	13	-3	14	2	198	199	17	0	6	3	207	205	8	-1	12	3	142	156	18	-9	17	3	163	141	20
-8	10	2	1074	1123	12	-2	14	2	173	166	15	-6	7	3	147	153	13	0	12	3	104	38	-25	-8	17	3	155	130	18
-7	10	2	180	193	12	-1	14	2	471	460	19	-5	7	3	695	706	7	-12	13	3	160	142	19	-7	17	3	121	108	-32
-6	10	2	158	159	12	0	14	2	167	148	20	-4	7	3	116	70	-24	-11	13	3	206	229	20	-6	17	3	185	177	24
-5	10	2	1303	1350	21	-14	15	2	152	120	-29	-3	7	3	182	164	12	-10	13	3	48	63	-29	0	0	4	3870	3602	18
-4	10	2	188	209	11	-13	15	2	90	123	-31	-2	7	3	678	686	16	-9	13	3	108	118	-27	0	1	4	937	775	135
-3	10	2	73	71	-24	-12	15	2	305	285	22	-1	7	3	100	88	-21	-8	13	3	250	263	15	-1	2	4	2011	1841	21
-2	10	2	1284	1335	14	-11	15	2	191	177	15	0	7	3	128	136	12	-7	13	3	45	41	-27	0	2	4	560	507	8

Observed and calculated structure factors for $BaCoSiO_4$

h	k	l	10Fo	10Fc	10s	h	k	l	10Fo	10Fc	10s	h	k	l	10Fo	10Fc	10s	h	k	l	10Fo	10Fc	10s	h	k	l	10Fo	10Fc	10s
-2	3	4	273	259	8	-6	11	4	123	116	18	-4	15	4	124	98	-29	-5	9	5	162	127	14	-9	14	5	165	146	16
-1	3	4	543	506	6	-5	11	4	191	193	14	-3	15	4	459	448	19	-4	9	5	62	9	-25	-8	14	5	75	60	-31
0	3	4	2418	2293	26	-4	11	4	833	844	14	-2	15	4	51	67	-30	-3	9	5	70	47	-28	-7	14	5	220	227	12
-3	4	4	530	508	7	-3	11	4	132	113	17	-1	15	4	52	38	-30	-2	9	5	310	321	13	-6	14	5	176	169	18
-2	4	4	1812	1724	21	-2	11	4	191	167	12	-13	16	4	215	202	15	-1	9	5	100	104	-25	-5	14	5	50	41	-30
-1	4	4	845	820	13	-1	11	4	590	598	11	-12	16	4	125	96	-33	0	9	5	49	13	-21	-4	14	5	210	215	19
0	4	4	577	555	12	0	11	4	109	91	-27	-11	16	4	395	363	20	-9	10	5	214	225	12	-3	14	5	163	129	21
-4	5	4	1463	1429	25	-11	12	4	90	79	-37	-10	16	4	286	272	22	-8	10	5	441	445	7	-2	14	5	74	18	-29
-3	5	4	426	415	5	-10	12	4	278	288	10	-9	16	4	146	107	24	-7	10	5	168	146	14	-1	14	5	193	181	17
-2	5	4	501	505	5	-9	12	4	742	747	16	-8	16	4	362	364	13	-6	10	5	275	275	11	0	14	5	140	123	-27
-1	5	4	1665	1607	20	-8	12	4	134	161	18	-7	16	4	245	260	13	-5	10	5	468	479	13	-13	15	5	52	28	-31
0	5	4	208	203	12	-7	12	4	219	212	11	-6	16	4	179	180	19	-4	10	5	83	53	-25	-12	15	5	73	34	-31
-5	6	4	330	339	7	-6	12	4	858	867	28	-5	16	4	340	332	12	-3	10	5	187	184	20	-11	15	5	131	83	-26
-4	6	4	531	522	5	-5	12	4	177	181	13	-4	16	4	207	203	15	-2	10	5	426	447	7	-10	15	5	52	17	-30
-3	6	4	2107	2114	24	-4	12	4	205	202	22	-3	16	4	188	160	16	-1	10	5	94	34	-28	-9	15	5	71	38	-31
-2	6	4	495	497	13	-3	12	4	725	749	17	-9	17	4	78	18	-29	0	10	5	190	190	12	-8	15	5	134	145	-27
-1	6	4	447	446	13	-2	12	4	92	103	-26	-8	17	4	112	61	-35	-10	11	5	337	330	9	-7	15	5	122	16	-34
0	6	4	1542	1567	11	-1	12	4	131	131	-31	0	1	5	97	105	-17	-9	11	5	149	143	23	-6	15	5	45	11	-26
-6	7	4	286	290	8	0	12	4	642	635	12	-1	2	5	1438	1347	12	-8	11	5	171	157	17	-5	15	5	207	183	19
-5	7	4	1182	1184	8	-12	13	4	122	121	-29	0	2	5	40	20	-19	-7	11	5	383	400	17	-4	15	5	46	21	-26
-4	7	4	534	539	6	-11	13	4	483	476	11	-2	3	5	36	27	-21	-6	11	5	120	142	-21	-3	15	5	83	14	-30
-3	7	4	485	496	11	-10	13	4	283	292	11	-1	3	5	120	95	14	-5	11	5	155	145	15	-2	15	5	130	142	-30
-2	7	4	1298	1306	29	-9	13	4	191	183	14	0	3	5	249	238	7	-4	11	5	378	375	9	-12	16	5	168	157	18
-1	7	4	564	560	7	-8	13	4	549	543	13	-3	4	5	442	440	10	-3	11	5	218	214	11	-11	16	5	189	170	16
0	7	4	467	475	7	-7	13	4	302	308	18	-2	4	5	1211	1156	7	-2	11	5	57	63	-26	-10	16	5	64	81	-38
-7	8	4	1122	1150	7	-6	13	4	238	239	12	-1	4	5	96	89	-21	-1	11	5	318	322	12	-9	16	5	166	147	22
-6	8	4	233	229	9	-5	13	4	573	586	10	0	4	5	203	196	10	0	11	5	166	162	14	-8	16	5	142	146	22
-5	8	4	207	220	12	-4	13	4	330	347	10	-4	5	5	998	989	10	-11	12	5	73	60	-29	-7	16	5	46	47	-27
-4	8	4	1048	1060	12	-3	13	4	202	211	13	-3	5	5	299	295	7	-10	12	5	99	95	-29	-6	16	5	100	109	-34
-3	8	4	183	181	10	-2	13	4	530	536	9	-2	5	5	271	267	8	-9	12	5	65	29	-31	-5	16	5	155	145	21
-2	8	4	134	129	14	-1	13	4	303	308	10	-1	5	5	954	941	17	-8	12	5	192	187	16	-4	16	5	60	59	-36
-1	8	4	983	990	17	0	13	4	275	275	13	0	5	5	335	335	9	-7	12	5	63	39	-30	0	0	6	2215	2117	19
0	8	4	197	206	10	-13	14	4	383	360	18	-5	6	5	227	243	9	-6	12	5	53	26	-32	0	1	6	606	585	4
-8	9	4	287	286	8	-12	14	4	85	51	-33	-4	6	5	118	113	-20	-5	12	5	114	134	-27	-1	2	6	1392	1325	11
-7	9	4	487	488	11	-11	14	4	58	65	-35	-3	6	5	47	41	-24	-4	12	5	55	76	-27	0	2	6	727	699	9
-6	9	4	1182	1202	13	-10	14	4	528	522	16	-2	6	5	149	161	14	-3	12	5	68	59	-30	-2	3	6	889	865	10
-5	9	4	143	144	14	-9	14	4	85	84	-42	-1	6	5	120	128	16	-2	12	5	191	196	23	-1	3	6	797	788	6
-4	9	4	332	337	7	-8	14	4	117	110	-27	0	6	5	141	144	18	-1	12	5	94	74	-30	0	3	6	2172	2092	20
-3	9	4	1162	1190	15	-7	14	4	442	454	18	-6	7	5	249	250	11	0	12	5	47	31	-24	-3	4	6	578	562	10
-2	9	4	244	252	9	-6	14	4	69	28	-30	-5	7	5	736	725	6	-12	13	5	217	207	26	-2	4	6	1262	1217	19
-1	9	4	202	190	12	-5	14	4	107	65	-32	-4	7	5	106	93	-23	-11	13	5	245	239	25	-1	4	6	499	499	9
0	9	4	1106	1125	8	-4	14	4	435	429	16	-3	7	5	269	270	8	-10	13	5	53	75	-30	0	4	6	528	529	6
-9	10	4	261	254	10	-3	14	4	49	45	-29	-2	7	5	742	734	13	-9	13	5	170	184	16	-4	5	6	1162	1144	8
-8	10	4	889	893	14	-2	14	4	116	102	-30	-1	7	5	122	138	17	-8	13	5	303	288	12	-3	5	6	618	601	6
-7	10	4	459	466	8	-1	14	4	423	436	26	0	7	5	168	165	11	-7	13	5	152	109	20	-2	5	6	532	525	8
-6	10	4	283	283	12	0	14	4	59	39	-25	-7	8	5	563	573	11	-6	13	5	225	224	25	-1	5	6	1077	1067	28
-5	10	4	920	935	17	-14	15	4	116	69	-32	-6	8	5	188	176	12	-5	13	5	294	295	21	0	5	6	723	719	5
-4	10	4	475	498	16	-13	15	4	172	168	18	-5	8	5	86	83	-25	-4	13	5	120	126	-31	-5	6	6	604	597	6
-3	10	4	375	385	13	-12	15	4	463	453	20	-4	8	5	596	597	7	-3	13	5	121	132	-29	-4	6	6	571	570	10
-2	10	4	777	795	9	-11	15	4	118	86	-27	-3	8	5	223	216	9	-2	13	5	232	219	14	-3	6	6	1479	1473	25
-1	10	4	315	328	9	-10	15	4	209	211	16	-2	8	5	112	109	-19	-1	13	5	45	23	-26	-2	6	6	432	436	6
0	10	4	338	335	7	-9	15	4	536	521	18	-1	8	5	586	597	8	0	13	5	115	99	-25	-1	6	6	509	508	11
-10	11	4	622	627	7	-8	15	4	45	54	-26	0	8	5	265	253	9	-13	14	5	162	164	21	0	6	6	1486	1481	20
-9	11	4	87	84	-28	-7	15	4	155	148	24	-8	9	5	48	29	-25	-12	14	5	86	46	-32	-6	7	6	507	505	7
-8	11	4	126	85	20	-6	15	4	500	502	15	-7	9	5	65	35	-28	-11	14	5	120	138	-27	-5	7	6	999	997	10
-7	11	4	695	702	12	-5	15	4	121	97	-23	-6	9	5	99	103	-27	-10	14	5	190	205	15	-4	7	6	371	365	8

Observed and calculated structure factors for $BaCoSiO_4$

h	k	l	10Fo	10Fc	10s	h	k	l	10Fo	10Fc	10s	h	k	l	10Fo	10Fc	10s	h	k	l	10Fo	10Fc	10s	h	k	l	10Fo	10Fc	10s
-3	7	6	326	345	9	-10	13	6	127	101	-22	0	5	7	146	128	13	-7	12	7	121	74	-30	-3	5	8	597	592	6
-2	7	6	954	961	12	-9	13	6	209	224	17	-5	6	7	187	194	12	-6	12	7	44	8	-26	-2	5	8	600	606	7
-1	7	6	353	355	8	-8	13	6	498	489	20	-4	6	7	114	115	-25	-5	12	7	152	130	19	-1	5	8	1267	1258	23
0	7	6	276	289	11	-7	13	6	130	128	-24	-3	6	7	122	29	-41	-4	12	7	101	111	-30	0	5	8	436	426	7
-7	8	6	785	782	6	-6	13	6	171	183	16	-2	6	7	57	70	-30	-3	12	7	61	22	-28	-5	6	8	527	545	10
-6	8	6	479	489	9	-5	13	6	473	454	12	-1	6	7	150	154	14	-2	12	7	156	137	20	-4	6	8	651	650	13
-5	8	6	515	522	8	-4	13	6	102	64	-29	0	6	7	40	43	-20	-1	12	7	103	119	-34	-3	6	8	316	316	12
-4	8	6	868	873	14	-3	13	6	166	175	16	-6	7	7	46	57	-27	0	12	7	71	43	-31	-2	6	8	598	597	7
-3	8	6	543	553	6	-2	13	6	383	383	12	-5	7	7	479	486	7	-12	13	7	171	121	18	-1	6	8	601	596	7
-2	8	6	616	634	9	-1	13	6	131	82	-28	-4	7	7	65	49	-29	-11	13	7	156	166	20	0	6	8	262	254	9
-1	8	6	792	800	14	0	13	6	59	39	-27	-3	7	7	114	81	-22	-10	13	7	106	22	-32	-6	7	8	416	410	9
0	8	6	441	451	11	-13	14	6	325	317	10	-2	7	7	455	469	7	-9	13	7	76	88	-32	-5	7	8	1082	1066	18
-8	9	6	372	372	8	-12	14	6	252	229	14	-1	7	7	94	78	-28	-8	13	7	227	207	20	-4	7	8	623	617	14
-7	9	6	240	241	10	-11	14	6	240	245	13	0	7	7	96	79	-26	-7	13	7	124	44	-37	-3	7	8	570	573	7
-6	9	6	1112	1124	15	-10	14	6	343	338	14	-7	8	7	390	392	13	-6	13	7	147	103	19	-2	7	8	1099	1097	11
-5	9	6	562	567	11	-9	14	6	240	238	12	-6	8	7	207	211	13	-5	13	7	221	209	16	-1	7	8	612	627	14
-4	9	6	393	385	16	-8	14	6	225	236	18	-5	8	7	63	12	-30	-4	13	7	45	44	-26	0	7	8	505	515	11
-3	9	6	1115	1129	16	-7	14	6	420	410	22	-4	8	7	428	439	11	-3	13	7	50	36	-30	-7	8	8	904	906	7
-2	9	6	404	400	8	-6	14	6	320	329	10	-3	8	7	160	164	15	-2	13	7	161	145	20	-6	8	8	406	417	14
-1	9	6	399	409	8	-5	14	6	276	275	12	-2	8	7	93	51	-33	-1	13	7	57	55	-34	-5	8	8	414	416	8
0	9	6	864	865	11	-4	14	6	402	384	17	-1	8	7	423	436	10	0	13	7	64	12	-25	-4	8	8	996	996	13
-9	10	6	277	281	20	-3	14	6	277	273	18	0	8	7	195	167	11	-13	14	7	117	112	-33	-3	8	8	385	394	13
-8	10	6	591	605	9	-2	14	6	185	192	18	-8	9	7	155	123	16	-12	14	7	129	90	-38	-2	8	8	332	326	11
-7	10	6	139	130	18	-1	14	6	283	276	29	-7	9	7	69	78	-29	-11	14	7	158	137	22	-1	8	8	910	910	21
-6	10	6	318	337	9	0	14	6	223	207	12	-6	9	7	69	38	-27	-10	14	7	167	138	24	0	8	8	371	370	7
-5	10	6	704	703	13	-13	15	6	160	125	25	-5	9	7	54	72	-33	-9	14	7	191	181	24	-8	9	8	421	428	14
-4	10	6	165	149	17	-12	15	6	403	389	12	-4	9	7	121	65	-24	-8	14	7	122	83	-29	-7	9	8	557	552	17
-3	10	6	225	220	16	-11	15	6	190	193	16	-3	9	7	131	77	-24	-7	14	7	171	164	21	-6	9	8	230	202	13
-2	10	6	677	692	9	-10	15	6	134	105	-25	-2	9	7	203	200	14	-6	14	7	180	191	24	-5	9	8	322	322	9
-1	10	6	241	248	19	-9	15	6	456	454	17	-1	9	7	139	146	18	-5	14	7	62	62	-36	-4	9	8	478	478	13
0	10	6	182	160	14	-8	15	6	249	251	15	0	9	7	50	42	-25	-4	14	7	180	159	17	-3	9	8	219	197	11
-10	11	6	540	532	11	-7	15	6	170	162	23	-9	10	7	140	122	18	-3	14	7	133	131	-24	-2	9	8	370	389	14
-9	11	6	385	369	18	-6	15	6	491	463	19	-8	10	7	327	319	12	-2	14	7	71	93	-30	-1	9	8	367	359	8
-8	11	6	394	412	11	-5	15	6	201	192	18	-7	10	7	73	69	-31	-1	14	7	142	135	23	0	9	8	231	236	11
-7	11	6	623	607	20	-4	15	6	193	194	18	-6	10	7	105	126	-34	-12	15	7	66	35	-31	-9	10	8	360	367	11
-6	11	6	407	400	8	-3	15	6	394	384	15	-5	10	7	329	326	14	-11	15	7	66	97	-39	-8	10	8	728	716	21
-5	11	6	333	334	12	-2	15	6	186	176	17	-4	10	7	53	20	-27	-10	15	7	63	58	-37	-7	10	8	487	482	10
-4	11	6	522	539	9	-10	16	6	62	17	-30	-3	10	7	60	59	-27	-9	15	7	47	40	-27	-6	10	8	396	378	9
-3	11	6	389	392	8	-9	16	6	195	162	32	-2	10	7	294	307	12	-8	15	7	84	101	-31	-5	10	8	768	785	11
-2	11	6	332	336	14	-8	16	6	310	290	17	-1	10	7	106	64	-29	-7	15	7	74	22	-32	-4	10	8	501	513	8
-1	11	6	541	535	16	-7	16	6	51	58	-31	0	10	7	119	100	-22	-6	15	7	53	16	-30	-3	10	8	408	418	9
0	11	6	344	342	15	-6	16	6	139	85	-23	-10	11	7	222	219	14	-5	15	7	112	127	-33	-2	10	8	723	719	9
-11	12	6	320	328	12	0	1	7	63	70	-25	-9	11	7	194	199	22	-4	15	7	55	63	-31	-1	10	8	409	410	10
-10	12	6	145	150	22	-1	2	7	697	676	15	-8	11	7	172	145	17	-3	15	7	54	24	-32	0	10	8	378	375	11
-9	12	6	725	697	20	0	2	7	141	110	15	-7	11	7	277	292	15	0	0	8	434	428	11	-10	11	8	601	597	10
-8	12	6	313	316	12	-2	3	7	97	79	-24	-6	11	7	177	159	23	0	1	8	818	809	6	-9	11	8	221	245	17
-7	12	6	288	273	13	-1	3	7	117	107	18	-5	11	7	150	141	23	-1	2	8	1546	1545	9	-8	11	8	238	237	19
-6	12	6	677	690	9	0	3	7	80	77	-23	-4	11	7	265	293	26	0	2	8	682	679	8	-7	11	8	675	677	19
-5	12	6	264	282	11	-3	4	7	191	175	17	-3	11	7	207	210	14	-2	3	8	514	506	7	-6	11	8	281	285	17
-4	12	6	243	249	17	-2	4	7	647	648	7	-2	11	7	45	51	-26	-1	3	8	700	696	10	-5	11	8	318	318	10
-3	12	6	684	686	16	-1	4	7	88	49	-28	-1	11	7	231	241	16	0	3	8	327	324	7	-4	11	8	666	655	17
-2	12	6	307	310	17	0	4	7	95	85	-19	0	11	7	167	158	15	-3	4	8	631	627	8	-3	11	8	278	282	15
-1	12	6	254	249	19	-4	5	7	626	611	6	-11	12	7	46	48	-26	-2	4	8	1411	1397	11	-2	11	8	323	318	13
0	12	6	583	571	22	-3	5	7	138	158	16	-10	12	7	45	31	-26	-1	4	8	799	809	10	-1	11	8	565	554	17
-12	13	6	215	205	16	-2	5	7	137	148	17	-9	12	7	99	19	-31	0	4	8	652	651	10	0	11	8	234	229	12
-11	13	6	411	401	24	-1	5	7	601	596	11	-8	12	7	122	137	-26	-4	5	8	1317	1291	13	-11	12	8	195	190	21

Observed and calculated structure factors for $BaCoSiO_4$

h	k	l	10Fo	10Fc	10s	h	k	l	10Fo	10Fc	10s	h	k	l	10Fo	10Fc	10s	h	k	l	10Fo	10Fc	10s	h	k	l	10Fo	10Fc	10s
-10	12	8	351	353	11	-5	6	9	172	156	23	-6	12	9	98	18	-32	0	7	10	433	445	9	-6	13	10	271	257	18
-9	12	8	193	171	16	-4	6	9	90	57	-30	-5	12	9	165	139	-30	-7	8	10	303	298	11	-5	13	10	199	160	23
-8	12	8	305	304	23	-3	6	9	43	26	-25	-4	12	9	83	70	-31	-6	8	10	432	432	15	-4	13	10	237	238	15
-7	12	8	337	317	9	-2	6	9	207	209	14	-3	12	9	47	37	-27	-5	8	10	473	481	8	-3	13	10	257	259	21
-6	12	8	228	205	15	-1	6	9	48	64	-29	-2	12	9	143	107	-29	-4	8	10	267	271	12	-2	13	10	124	148	-32
-5	12	8	294	313	15	0	6	9	43	25	-22	-1	12	9	119	66	-33	-3	8	10	467	463	8	-7	14	10	136	130	-28
-4	12	8	325	325	14	-6	7	9	122	128	-24	0	12	9	52	22	-27	-2	8	10	500	523	20	0	1	11	93	37	-28
-3	12	8	172	172	19	-5	7	9	177	169	15	-12	13	9	91	84	-35	-1	8	10	272	257	12	-1	2	11	225	239	14
-2	12	8	207	210	17	-4	7	9	85	14	-30	-11	13	9	111	69	-43	0	8	10	413	403	10	0	2	11	85	59	-27
-1	12	8	280	251	13	-3	7	9	158	128	19	-10	13	9	48	19	-28	-8	9	10	410	405	11	-2	3	11	74	63	-30
0	12	8	153	128	19	-2	7	9	155	167	16	-9	13	9	57	74	-31	-7	9	10	405	405	16	-1	3	11	72	103	-30
-12	13	8	222	208	20	-1	7	9	43	38	-25	-8	13	9	52	85	-31	-6	9	10	860	850	16	0	3	11	75	26	-26
-11	13	8	425	427	27	0	7	9	47	27	-24	-7	13	9	78	56	-33	-5	9	10	490	503	21	-3	4	11	45	36	-26
-10	13	8	313	299	27	-7	8	9	151	131	-42	-6	13	9	51	66	-30	-4	9	10	414	421	10	-2	4	11	235	235	15
-9	13	8	251	250	14	-6	8	9	88	85	-40	-5	13	9	127	87	-28	-3	9	10	850	850	22	-1	4	11	110	56	-28
-8	13	8	475	465	12	-5	8	9	88	42	-31	-4	13	9	71	48	-35	-2	9	10	414	430	11	0	4	11	90	80	-27
-7	13	8	334	344	11	-4	8	9	134	109	-40	-3	13	9	58	23	-36	-1	9	10	359	374	10	-4	5	11	247	230	18
-6	13	8	306	307	12	-3	8	9	150	107	22	-2	13	9	66	50	-40	0	9	10	716	703	14	-3	5	11	53	47	-29
-5	13	8	518	515	20	-2	8	9	61	2	-33	-1	13	9	49	8	-28	-9	10	10	348	330	24	-2	5	11	70	72	-34
-4	13	8	353	364	15	-1	8	9	143	145	22	-11	14	9	55	30	-33	-8	10	10	249	242	13	-1	5	11	226	225	13
-3	13	8	271	247	14	0	8	9	59	43	-24	-10	14	9	54	54	-31	-7	10	10	327	330	10	0	5	11	82	85	-29
-2	13	8	468	452	28	-8	9	9	156	146	18	-9	14	9	69	94	-38	-6	10	10	394	393	16	-5	6	11	75	63	-29
-1	13	8	338	337	25	-7	9	9	46	45	-26	-8	14	9	48	35	-28	-5	10	10	267	238	18	-4	6	11	76	79	-30
0	13	8	310	279	19	-6	9	9	84	38	-30	-7	14	9	58	46	-32	-4	10	10	381	380	16	-3	6	11	47	18	-27
-12	14	8	168	159	22	-5	9	9	113	101	-28	-6	14	9	92	116	-33	-3	10	10	378	359	9	-2	6	11	75	86	-31
-11	14	8	176	176	19	-4	9	9	64	60	-33	-5	14	9	62	32	-31	-2	10	10	223	223	18	-1	6	11	104	107	-31
-10	14	8	456	423	13	-3	9	9	59	16	-33	-4	14	9	69	64	-37	-1	10	10	376	380	10	0	6	11	87	22	-28
-9	14	8	229	202	18	-2	9	9	173	170	17	-3	14	9	87	68	-36	0	10	10	306	294	11	-6	7	11	52	73	-30
-8	14	8	230	214	23	-1	9	9	53	51	-29	0	0	10	1581	1578	15	-10	11	10	143	164	-25	-5	7	11	164	174	20
-7	14	8	447	442	18	0	9	9	142	16	-42	0	1	10	651	659	7	-9	11	10	305	296	11	-4	7	11	95	40	-30
-6	14	8	161	152	24	-9	10	9	156	123	22	-1	2	10	419	413	10	-8	11	10	327	339	13	-3	7	11	147	79	20
-5	14	8	189	158	19	-8	10	9	156	120	18	0	2	10	650	646	6	-7	11	10	205	189	23	-2	7	11	192	182	15
-4	14	8	433	406	15	-7	10	9	87	36	-32	-2	3	10	692	693	7	-6	11	10	325	326	14	-1	7	11	115	57	-28
-3	14	8	166	170	22	-6	10	9	64	101	-36	-1	3	10	698	699	7	-5	11	10	333	339	15	0	7	11	54	52	-26
-2	14	8	199	191	19	-5	10	9	122	119	-28	0	3	10	1379	1392	12	-4	11	10	246	240	13	-7	8	11	186	155	27
-10	15	8	273	274	14	-4	10	9	58	22	-29	-3	4	10	589	596	13	-3	11	10	335	322	13	-6	8	11	144	129	22
-9	15	8	151	127	22	-3	10	9	49	29	-29	-2	4	10	389	387	11	-2	11	10	360	352	16	-5	8	11	69	76	-30
-8	15	8	161	157	19	-2	10	9	125	128	-34	-1	4	10	636	640	7	-1	11	10	200	190	19	-4	8	11	178	163	16
-7	15	8	249	230	21	-1	10	9	116	54	-27	0	4	10	610	606	7	0	11	10	332	312	15	-3	8	11	60	115	-35
-6	15	8	99	116	-34	0	10	9	102	46	-32	-4	5	10	326	338	17	-11	12	10	308	308	14	-2	8	11	67	38	-35
-5	15	8	169	187	20	-10	11	9	64	76	-31	-3	5	10	574	560	7	-10	12	10	277	263	19	-1	8	11	170	181	20
0	1	9	87	118	-35	-9	11	9	93	98	-37	-2	5	10	546	551	10	-9	12	10	556	533	24	0	8	11	57	55	-30
-1	2	9	333	337	9	-8	11	9	86	54	-31	-1	5	10	361	388	9	-8	12	10	354	344	20	-8	9	11	125	112	-29
0	2	9	41	32	-20	-7	11	9	79	112	-32	0	5	10	567	565	10	-7	12	10	314	328	15	-7	9	11	58	48	-31
-2	3	9	66	35	-31	-6	11	9	46	49	-26	-5	6	10	580	577	7	-6	12	10	564	560	17	-6	9	11	48	7	-28
-1	3	9	93	61	-26	-5	11	9	46	62	-27	-4	6	10	619	600	11	-5	12	10	290	306	12	-5	9	11	70	54	-31
0	3	9	71	10	-24	-4	11	9	64	88	-29	-3	6	10	1188	1179	19	-4	12	10	265	269	18	-4	9	11	106	71	-38
-3	4	9	190	195	14	-3	11	9	120	110	-36	-2	6	10	506	506	9	-3	12	10	555	532	29	-3	9	11	66	27	-30
-2	4	9	300	295	9	-2	11	9	157	92	18	-1	6	10	514	515	9	-2	12	10	300	306	17	-2	9	11	70	70	-36
-1	4	9	42	20	-24	-1	11	9	52	73	-31	0	6	10	1068	1066	14	-1	12	10	235	237	16	-1	9	11	138	90	-33
0	4	9	42	44	-21	0	11	9	77	84	-28	-6	7	10	509	515	12	0	12	10	478	465	14	0	9	11	60	35	-26
-4	5	9	249	252	12	-11	12	9	125	73	-33	-5	7	10	305	294	13	-11	13	10	179	148	19	-9	10	11	101	119	-33
-3	5	9	98	79	-31	-10	12	9	54	62	-32	-4	7	10	505	508	8	-10	13	10	249	258	18	-8	10	11	144	134	24
-2	5	9	110	105	-32	-9	12	9	87	12	-31	-3	7	10	466	454	22	-9	13	10	286	278	12	-7	10	11	80	55	-33
-1	5	9	224	218	20	-8	12	9	151	138	20	-2	7	10	302	297	11	-8	13	10	216	191	15	-6	10	11	65	47	-30
0	5	9	141	136	18	-7	12	9	73	74	-35	-1	7	10	496	495	10	-7	13	10	294	286	26	-5	10	11	159	128	21

Observed and calculated structure factors for $BaCoSiO_4$

h	k	l	10Fo	10Fc	10s	h	k	l	10Fo	10Fc	10s	h	k	l	10Fo	10Fc	10s	h	k	l	10Fo	10Fc	10s	h	k	l	10Fo	10Fc	10s
-4	10	11	86	52	-33	-3	6	12	207	213	16	-2	11	12	307	317	12	-3	9	13	54	24	-32	-1	8	14	200	188	19
-3	10	11	78	87	-34	-2	6	12	475	484	9	-1	11	12	297	275	18	-2	9	13	55	80	-32	0	8	14	279	273	16
-2	10	11	73	117	-36	-1	6	12	495	509	9	-7	12	12	260	265	14	-1	9	13	108	49	-32	-7	9	14	374	379	16
-1	10	11	80	62	-32	0	6	12	186	214	15	-6	12	12	94	116	-38	0	9	13	73	11	-28	-6	9	14	194	194	20
0	10	11	49	47	-25	-6	7	12	382	384	17	-5	12	12	293	306	17	-8	10	13	221	191	22	-5	9	14	325	312	14
-10	11	11	51	91	-30	-5	7	12	485	481	9	0	1	13	50	94	-25	-7	10	13	85	54	-32	-4	9	14	341	349	12
-9	11	11	122	113	-35	-4	7	12	445	443	13	-1	2	13	375	372	10	-6	10	13	116	74	-34	-3	9	14	180	192	24
-8	11	11	93	70	-40	-3	7	12	430	433	11	0	2	13	53	35	-27	-5	10	13	188	190	20	-2	9	14	295	298	14
-7	11	11	168	125	-32	-2	7	12	458	469	18	-2	3	13	55	40	-32	-4	10	13	56	39	-33	0	1	15	53	45	-27
-6	11	11	140	81	-30	-1	7	12	427	452	9	-1	3	13	60	26	-36	-3	10	13	77	82	-34	-1	2	15	266	295	17
-5	11	11	48	47	-28	0	7	12	350	362	12	0	3	13	53	30	-27	-2	10	13	177	172	24	0	2	15	67	34	-30
-4	11	11	167	121	21	-7	8	12	389	390	13	-3	4	13	156	117	-38	0	0	14	313	323	21	-2	3	15	94	67	-35
-3	11	11	84	96	-34	-6	8	12	409	420	11	-2	4	13	358	342	11	0	1	14	502	509	9	-1	3	15	121	59	-34
-2	11	11	78	55	-33	-5	8	12	413	430	12	-1	4	13	80	47	-32	-1	2	14	305	318	14	0	3	15	52	17	-26
-1	11	11	89	87	-36	-4	8	12	460	466	19	0	4	13	63	76	-32	0	2	14	459	454	9	-3	4	15	155	82	-27
0	11	11	109	83	-33	-3	8	12	435	438	10	-4	5	13	305	304	15	-2	3	14	435	440	10	-2	4	15	248	278	21
-10	12	11	95	24	-33	-2	8	12	408	410	15	-3	5	13	73	59	-32	-1	3	14	486	500	12	-1	4	15	63	44	-33
-9	12	11	82	8	-33	-1	8	12	422	428	10	-2	5	13	69	54	-32	0	3	14	266	269	14	0	4	15	125	77	-28
-8	12	11	69	79	-37	0	8	12	392	400	10	-1	5	13	312	304	27	-3	4	14	457	441	11	-4	5	15	271	264	16
-7	12	11	101	50	-49	-8	9	12	399	392	17	0	5	13	98	99	-32	-2	4	14	254	281	15	-3	5	15	74	53	-33
-6	12	11	56	8	-33	-7	9	12	387	375	20	-5	6	13	50	55	-29	-1	4	14	527	531	10	-2	5	15	94	11	-36
-5	12	11	155	140	23	-6	9	12	187	177	19	-4	6	13	75	22	-32	0	4	14	476	474	10	-1	5	15	275	270	17
-4	12	11	101	48	-31	-5	9	12	381	377	10	-3	6	13	79	18	-32	-4	5	14	271	251	17	0	5	15	69	60	-37
-3	12	11	63	7	-39	-4	9	12	388	398	16	-2	6	13	125	146	-31	-3	5	14	383	410	11	-5	6	15	68	47	-41
-2	12	11	102	117	-36	-3	9	12	165	178	22	-1	6	13	54	45	-32	-2	5	14	386	398	11	-4	6	15	80	41	-46
-8	13	11	58	77	-35	-2	9	12	359	364	14	0	6	13	67	9	-26	-1	5	14	246	274	16	-3	6	15	52	11	-30
-7	13	11	72	25	-31	-1	9	12	348	362	12	-6	7	13	74	111	-37	0	5	14	353	356	10	-2	6	15	103	60	-38
-6	13	11	105	78	-34	0	9	12	91	139	-30	-5	7	13	265	253	22	-5	6	14	389	378	19	-1	6	15	80	59	-33
-5	13	11	126	100	-29	-9	10	12	305	325	13	-4	7	13	50	36	-29	-4	6	14	476	468	15	0	6	15	109	18	-28
0	0	12	243	212	21	-8	10	12	303	307	15	-3	7	13	186	121	-33	-3	6	14	273	274	14	-6	7	15	87	92	-39
0	1	12	604	603	7	-7	10	12	300	312	13	-2	7	13	267	265	13	-2	6	14	369	383	22	-5	7	15	249	226	19
-1	2	12	648	664	8	-6	10	12	319	326	14	-1	7	13	65	25	-31	-1	6	14	404	409	17	-4	7	15	94	34	-36
0	2	12	578	590	11	-5	10	12	354	353	11	0	7	13	51	50	-26	0	6	14	230	230	14	-3	7	15	73	79	-33
-2	3	12	544	531	8	-4	10	12	318	311	21	-7	8	13	221	217	17	-6	7	14	353	363	15	-2	7	15	210	234	21
-1	3	12	596	600	10	-3	10	12	309	303	11	-6	8	13	63	80	-32	-5	7	14	198	195	19	-1	7	15	68	41	-34
0	3	12	228	235	13	-2	10	12	352	340	23	-5	8	13	98	70	-35	-4	7	14	441	437	10	0	0	16	287	281	24
-3	4	12	495	508	9	-1	10	12	298	296	14	-4	8	13	222	228	17	-3	7	14	396	384	16	0	1	16	370	383	10
-2	4	12	584	593	22	0	10	12	294	266	12	-3	8	13	124	103	-37	-2	7	14	212	198	18	-1	2	16	183	142	26
-1	4	12	556	565	9	-10	11	12	328	297	14	-2	8	13	50	42	-29	-1	7	14	436	434	11	0	2	16	403	393	10
0	4	12	499	501	11	-9	11	12	326	308	12	-1	8	13	227	222	17	0	7	14	403	399	12	-2	3	16	384	391	12
-4	5	12	583	575	10	-8	11	12	326	319	21	0	8	13	110	97	-29	-7	8	14	215	197	17	-1	3	16	393	396	11
-3	5	12	544	534	8	-7	11	12	327	334	12	-8	9	13	118	81	-34	-6	8	14	310	315	14	0	3	16	270	300	13
-2	5	12	531	518	8	-6	11	12	360	346	11	-7	9	13	62	6	-36	-5	8	14	318	308	22	-3	4	16	334	345	18
-1	5	12	529	530	9	-5	11	12	326	326	16	-6	9	13	51	15	-29	-4	8	14	198	205	25	-2	4	16	145	118	-36
0	5	12	477	489	10	-4	11	12	287	278	26	-5	9	13	64	55	-38	-3	8	14	312	308	19	-1	4	16	323	345	14
-5	6	12	490	501	14	-3	11	12	340	343	13	-4	9	13	50	38	-29	-2	8	14	335	311	21	0	4	16	314	329	16
-4	6	12	512	523	10																								

Observed and calculated structure factors for $SrBeSiO_4$

h	k	l	10Fo	10Fc	10s	h	k	l	10Fo	10Fc	10s	h	k	l	10Fo	10Fc	10s	h	k	l	10Fo	10Fc	10s	h	k	l	10Fo	10Fc	10s
0	1	0	10	15	-4	-5	8	1	78	88	15	-2	4	3	350	360	8	-6	9	4	658	701	29	-5	8	6	115	121	13
-1	2	0	1153	1171	13	-4	8	1	221	247	6	-1	4	3	122	128	5	-5	9	4	121	115	13	-4	8	6	630	629	7
0	2	0	17	21	-7	-3	8	1	56	61	-17	0	4	3	136	146	5	-4	9	4	76	64	18	-3	8	6	196	174	14
-2	3	0	137	132	3	-2	8	1	70	85	13	-4	5	3	372	345	4	-3	9	4	678	678	12	-2	8	6	196	163	9
-1	3	0	168	161	2	-1	8	1	185	177	6	-3	5	3	105	101	6	-2	9	4	122	119	10	-1	8	6	512	511	12
0	3	0	1976	2020	15	0	8	1	94	89	17	-2	5	3	88	120	10	-1	9	4	80	83	20	0	1	7	158	156	5
-3	4	0	166	161	3	-8	9	1	32	78	-23	-1	5	3	411	431	4	-6	10	4	152	123	12	-1	2	7	249	245	6
-2	4	0	1372	1377	24	-7	9	1	44	57	-17	0	5	3	76	77	9	-5	10	4	645	627	17	0	2	7	316	324	10
-1	4	0	152	152	4	-6	9	1	141	147	10	-5	6	3	100	82	7	-4	10	4	106	100	15	-2	3	7	184	184	9
0	4	0	17	21	-10	-5	9	1	30	51	-22	-4	6	3	114	119	7	0	1	5	226	229	3	-1	3	7	204	188	11
-4	5	0	920	975	7	-4	9	1	40	22	-29	-3	6	3	61	36	15	-1	2	5	640	589	18	0	3	7	109	127	18
-3	5	0	85	85	5	-3	9	1	162	157	7	-2	6	3	97	90	8	0	2	5	152	141	8	-3	4	7	187	190	9
-2	5	0	20	55	-15	-2	9	1	39	54	-21	-1	6	3	95	105	7	-2	3	5	198	199	5	-2	4	7	232	240	16
-1	5	0	980	983	3	-1	9	1	86	42	12	0	6	3	232	239	5	-1	3	5	190	187	7	-1	4	7	173	175	9
0	5	0	48	34	-12	0	9	1	27	16	-16	-6	7	3	99	111	10	0	3	5	261	266	5	0	4	7	182	180	15
-5	6	0	76	88	7	-8	10	1	269	257	5	-5	7	3	277	271	5	-3	4	5	151	161	5	-4	5	7	236	229	9
-4	6	0	155	150	4	-7	10	1	89	95	18	-4	7	3	128	116	8	-2	4	5	496	492	8	-3	5	7	156	170	8
-3	6	0	2084	2127	28	-6	10	1	51	75	-27	-3	7	3	120	103	9	-1	4	5	140	159	7	-2	5	7	150	144	12
-2	6	0	102	99	6	-5	10	1	190	175	6	-2	7	3	329	343	5	0	4	5	127	145	8	-1	5	7	228	228	10
-1	6	0	128	120	5	-4	10	1	90	89	17	-1	7	3	96	89	8	-4	5	5	411	413	5	0	5	7	198	178	8
0	6	0	1287	1304	8	-3	10	1	75	104	19	0	7	3	102	102	8	-3	5	5	244	252	7	-5	6	7	212	196	11
-6	7	0	69	69	10	-2	10	1	100	82	18	-7	8	3	303	279	6	-2	5	5	295	284	7	-4	6	7	159	158	11
-5	7	0	694	679	5	0	0	2	470	513	4	-6	8	3	100	81	9	-1	5	5	408	395	6	-3	6	7	46	18	-25
-4	7	0	25	39	-18	0	1	2	97	94	4	-5	8	3	24	47	-24	0	5	5	232	227	6	-2	6	7	167	139	13
-3	7	0	51	26	-22	-1	2	2	2009	1959	60	-4	8	3	296	276	6	-5	6	5	121	100	13	-1	6	7	188	195	9
-2	7	0	666	699	9	0	2	2	79	87	3	-3	8	3	90	61	15	-4	6	5	113	108	7	0	6	7	108	83	14
-1	7	0	109	110	6	-2	3	2	198	199	4	-2	8	3	84	108	12	-3	6	5	52	13	-33	-6	7	7	110	118	11
0	7	0	25	16	-15	-1	3	2	244	242	4	-1	8	3	238	247	5	-2	6	5	156	147	8	-5	7	7	172	192	7
-7	8	0	724	756	8	0	3	2	1607	1555	33	0	8	3	122	132	10	-1	6	5	113	130	9	-4	7	7	117	118	13
-6	8	0	109	107	9	-3	4	2	67	57	7	-8	9	3	96	104	13	0	6	5	144	157	9	-3	7	7	136	117	12
-5	8	0	27	15	-20	-2	4	2	1402	1448	29	-7	9	3	93	71	17	-6	7	5	107	123	10	-2	7	7	200	185	13
-4	8	0	568	589	3	-1	4	2	115	111	4	-6	9	3	133	130	14	-5	7	5	324	302	4	-1	7	7	135	128	10
-3	8	0	80	70	10	0	4	2	102	118	6	-5	9	3	84	87	20	-4	7	5	100	116	12	0	7	7	82	89	-22
-2	8	0	43	31	-20	-4	5	2	1367	1391	29	-4	9	3	48	81	-22	-3	7	5	122	129	14	-5	8	7	184	188	9
-1	8	0	726	712	6	-3	5	2	86	64	8	-3	9	3	136	135	17	-2	7	5	281	293	13	-4	8	7	188	179	9
0	8	0	46	34	-17	-2	5	2	22	26	-16	-2	9	3	59	67	-26	-1	7	5	107	124	9	-3	8	7	200	183	12
-8	9	0	34	57	-20	-1	5	2	1354	1360	14	-1	9	3	82	70	13	0	7	5	139	139	8	0	0	8	824	822	6
-7	9	0	141	135	8	0	5	2	187	186	5	0	9	3	31	14	-19	-7	8	5	233	249	6	0	1	8	307	321	3
-6	9	0	911	944	14	-5	6	2	70	57	15	-7	10	3	86	96	17	-6	8	5	118	133	9	-1	2	8	880	844	12
-5	9	0	68	46	15	-4	6	2	103	105	6	-6	10	3	66	68	-25	-5	8	5	58	79	-24	0	2	8	271	267	5
-4	9	0	138	125	12	-3	6	2	394	403	4	-5	10	3	192	208	8	-4	8	5	212	234	8	-2	3	8	222	239	6
-3	9	0	949	948	13	-2	6	2	51	25	-20	-4	10	3	94	87	14	-3	8	5	97	93	15	-1	3	8	221	228	6
-2	9	0	84	98	17	-1	6	2	124	126	5	-3	10	3	111	104	12	-2	8	5	152	139	11	0	3	8	602	587	5
-1	9	0	99	134	16	0	6	2	797	814	8	0	0	4	2613	2565	6	-1	8	5	238	233	6	-3	4	8	246	259	8
0	9	0	990	999	10	-6	7	2	69	68	11	0	1	4	296	292	13	0	8	5	170	168	7	-2	4	8	780	792	6
-8	10	0	429	427	5	-5	7	2	1196	1204	4	-1	2	4	1207	1134	32	-7	9	5	70	109	-25	-1	4	8	270	261	8
-7	10	0	27	43	-19	-4	7	2	101	127	12	0	2	4	276	264	5	-6	9	5	131	110	14	0	4	8	227	228	31
-6	10	0	76	62	16	-3	7	2	76	80	14	-2	3	4	87	85	7	-5	9	5	118	104	15	-4	5	8	770	724	40
-5	10	0	709	673	4	-2	7	2	1184	1208	18	-1	3	4	156	165	6	-4	9	5	111	111	26	-3	5	8	282	254	10
-4	10	0	65	95	-22	-1	7	2	101	89	7	0	3	4	1479	1385	45	-3	9	5	115	95	23	-2	5	8	267	273	9
-3	10	0	41	16	-22	0	7	2	33	68	-18	-3	4	4	232	227	6	-2	9	5	99	100	16	-1	5	8	767	701	17
-2	10	0	401	435	13	-7	8	2	764	790	6	-2	4	4	1160	1149	32	0	0	6	1163	1126	5	0	5	8	184	188	15
0	1	1	49	44	3	-6	8	2	117	129	9	-1	4	4	235	238	4	0	1	6	221	224	3	-5	6	8	236	206	19
-1	2	1	690	675	6	-5	8	2	92	48	11	0	4	4	168	169	5	-1	2	6	994	1008	5	-4	6	8	212	206	12
0	2	1	92	95	4	-4	8	2	1013	1056	9	-4	5	4	937	950	12	0	2	6	265	258	15	-3	6	8	624	584	27
-2	3	1	52	56	6	-3	8	2	85	69	10	-3	5	4	219	222	5	-2	3	6	306	276	13	-2	6	8	238	235	12
-1	3	1	51	46	6	-2	8	2	99	84	11	-2	5	4	275	271	5	-1	3	6	396	377	11	-1	6	8	185	170	13
0	3	1	757	737	4	-1	8	2	800	806	9	-1	5	4	953	925	5	0	3	6	1390	1263	34	0	6	8	462	438	19
-3	4	1	121	109	4	0	8	2	47	42	-17	0	5	4	99	97	8	-3	4	6	163	150	6	-4	7	8	198	211	10
-2	4	1	459	453	3	-8	9	2	69	82	17	-5	6	4	191	184	7	-2	4	6	929	878	34	-3	7	8	202	222	10
-1	4	1	106	101	5	-7	9	2	92	103	11	-4	6	4	150	162	5	-1	4	6	275	263	15	0	1	9	225	235	5
0	4	1	124	116	3	-6	9	2	554	586	39	-3	6	4	1448	1434	60	0	4	6	242	248	8	-1	2	9	194	199	7
-4	5	1	231	248	5	-5	9	2	68	58	-18	-2	6	4	227	221	10	-4	5	6	788	795	14	0	2	9	183	172	6
-3	5	1	100	122	6	-4	9	2	110	97	14	-1	6	4	116	128	9	-3	5	6	214	200	8	-2	3	9	212	215	11
-2	5	1	142	135	7	-3	9	2	562	575	4	0	6	4	927	938	6	-2	5	6	159	128	11	-1	3	9	214	214	5
-1	5	1	499	479	2	-2	9	2	88	101	12	-6	7	4	167	156	10	-1	5	6	873	813	24	0	3	9	70	59	-19
0	5	1	120	120	5	-1	9	2	98	83	15	-5	7	4	723	715	15	0	5	6	308	297	11	-3	4	9	176	169	13
-5	6	1	84	80	6	0	9	2	297	297	10	-4	7	4	101	122	12	-5	6	6	134	126	8	-2	4	9	178	181	18
-4	6	1	43	46	-19	-8	10	2	733	725	4	-3	7	4	154	152	7	-4	6	6	234	233	6	-1	4	9	158	174	9
-3	6	1	63	24	12	-7	10	2	27	49	-27	-2	7	4	732	736	5	-3	6	6	785	742	7	0	4	9	171	169	9
-2	6	1	70	74	9	-6	10	2	116	105	12	-1	7	4	93	104	9	-2	6	6	114	92	13	-4	5	9	168	164	11
-1	6	1	72	50	7	-5	10	2	618	628	5	0	7	4	176	169	6	-1	6	6	258	235	6	-3	5	9	196	223	10
0	6	1	289	303	3	-4	10	2	33	44	-24	-7	8	4	682	696	6	0	6	6	903	865	11	-2	5	9	221	219	8
-6	7	1	74	74	10	-3	10	2	68	84	-29	-6	8	4	54	71	-24	-6	7	6	130	115	12	-1	5	9	183	168	9
-5	7	1	185	170	8	-2	10	2	706	725	16	-5	8	4	144	139	17	-5	7	6	692	697	7	0	5	9	221	205	7
-4	7	1	92	84	9	0	1	3	165	157	4	-4	8	4	620	625	30	-4	7	6	185	197	8	0	0	10	785	803	7
-3	7	1	67	89	12	-1	2	3	302	320	5	-3	8	4	128	117	15	-3	7	6	129	144	14	0	1	10	221	249	4
-2	7	1	406	405	3	0	2	3	288	293	8	-2	8	4	94	72	13	-2	7	6	727	702	19	-1	2	10	456	444	4
-1	7	1	87	84	8	-2	3	3	129	122	4	-1	8	4	705	694	6	-1	7	6	232	218	8	0	2	10	249	283	6
0	7	1	72	84	14	-1	3	3	121	126	4	0	8	4	144	138	7	0	7	6	93	121	17	-2	3	10	243	238	10
-7	8	1	230	252	4	0	3	3	516	510	13	-8	9	4	158	151	9	-7	8	6	531	548	12	-1	3	10	298	315	4
-6	8	1	37	42	-18	-3	4	3	124	126	5	-7	9	4	92	95	13	-6	8	6	243	238	11	0	3	10	819	779	17

Observed and calculated structure factors for $Sr_{0.73}Ca_{0.27}BeSiO_4$

h	k	l	10Fo	10Fc	10s	h	k	l	10Fo	10Fc	10s	h	k	l	10Fo	10Fc	10s	h	k	l	10Fo	10Fc	10s	h	k	l	10Fo	10Fc	10s
0	1	0	62	66	2	0	13	0	33	14	-17	-8	10	1	84	71	10	-1	2	2	2028	1796	67	-13	14	2	306	307	5
-1	2	0	1009	994	6	-13	14	0	192	193	7	-7	10	1	24	18	-14	0	2	2	41	36	-9	-12	14	2	39	17	-23
0	2	0	13	32	-6	-12	14	0	31	38	-22	-6	10	1	56	52	-19	-2	3	2	220	220	8	-11	14	2	35	29	-20
-2	3	0	142	139	3	-11	14	0	33	11	-20	-5	10	1	155	151	6	-1	3	2	216	234	4	-10	14	2	305	319	5
-1	3	0	280	270	2	-10	14	0	285	298	5	-4	10	1	24	32	-14	0	3	2	1500	1339	44	-9	14	2	30	29	-17
0	3	0	1800	1792	15	-9	14	0	29	5	-17	-3	10	1	63	47	-14	-3	4	2	51	64	8	-8	14	2	54	43	-27
-3	4	0	128	131	3	-8	14	0	37	32	-22	-2	10	1	260	258	4	-2	4	2	1370	1314	12	-7	14	2	397	413	5
-2	4	0	1341	1279	8	-7	14	0	246	261	5	-1	10	1	33	33	-16	-1	4	2	39	38	-11	-6	14	2	33	20	-20
-1	4	0	267	255	2	-6	14	0	29	16	-17	0	10	1	28	38	-14	0	4	2	73	73	5	-5	14	2	82	66	-16
0	4	0	16	25	-8	-5	14	0	68	51	-20	-10	11	1	60	55	-17	-4	5	2	1307	1285	29	-4	14	2	311	307	5
-4	5	0	950	923	7	-4	14	0	320	323	7	-9	11	1	56	53	-21	-3	5	2	35	39	-35	-3	14	2	34	20	-20
-3	5	0	58	54	8	-3	14	0	30	9	-17	-8	11	1	102	103	10	-2	5	2	41	22	-12	-2	14	2	34	32	-20
-2	5	0	91	97	4	-2	14	0	34	3	-20	-7	11	1	171	175	5	-1	5	2	1298	1259	30	-1	14	2	331	312	5
-1	5	0	821	840	6	-1	14	0	195	186	7	-6	11	1	107	104	8	0	5	2	209	201	6	0	14	2	41	54	-21
0	5	0	29	38	-11	0	14	0	45	32	-24	-5	11	1	85	98	10	-5	6	2	111	123	5	-14	15	2	39	41	-23
-5	6	0	65	51	9	-14	15	0	37	25	-22	-4	11	1	62	58	-20	-4	6	2	37	53	-16	-13	15	2	54	52	-23
-4	6	0	256	230	2	-13	15	0	68	67	-28	-3	11	1	93	90	9	-3	6	2	250	238	3	-12	15	2	164	143	8
-3	6	0	1923	2018	16	-12	15	0	351	355	6	-2	11	1	33	36	-17	-2	6	2	73	78	7	-11	15	2	42	25	-25
-2	6	0	66	71	7	-11	15	0	31	12	-18	-1	11	1	169	176	6	-1	6	2	19	13	-13	-10	15	2	51	61	-22
-1	6	0	211	201	2	-10	15	0	100	95	13	0	11	1	56	70	-20	0	6	2	703	698	32	-9	15	2	252	226	7
0	6	0	1153	1204	5	-9	15	0	358	348	5	-11	12	1	32	46	-19	-6	7	2	83	86	8	-8	15	2	34	59	-21
-6	7	0	85	84	7	-8	15	0	57	49	-29	-10	12	1	34	29	-19	-5	7	2	1106	1119	6	-7	15	2	31	37	-18
-5	7	0	586	595	7	-7	15	0	52	56	-30	-9	12	1	111	89	11	-4	7	2	60	70	-12	-6	15	2	248	233	5
-4	7	0	102	99	5	-6	15	0	341	329	4	-8	12	1	46	26	-19	-3	7	2	88	95	9	-5	15	2	65	72	-29
-3	7	0	21	12	-13	-5	15	0	34	30	-20	-7	12	1	72	51	-16	-2	7	2	1177	1161	10	-4	15	2	35	30	-20
-2	7	0	649	635	4	-4	15	0	41	53	-25	-6	12	1	29	14	-17	-1	7	2	21	15	-12	-3	15	2	149	140	9
-1	7	0	129	128	4	-3	15	0	343	349	5	-5	12	1	26	8	-15	0	7	2	24	20	-12	-2	15	2	43	41	-26
0	7	0	23	4	-11	-2	15	0	62	33	-32	-4	12	1	58	38	-21	-7	8	2	777	774	5	-1	15	2	34	21	-19
-7	8	0	740	730	6	-1	15	0	49	35	-29	-3	12	1	86	88	11	-6	8	2	75	85	9	-13	16	2	34	22	-20
-6	8	0	44	58	-17	-13	16	0	33	10	-19	-2	12	1	30	38	-18	-5	8	2	65	60	10	-12	16	2	41	48	-30
-5	8	0	67	70	9	-12	16	0	36	39	-22	-1	12	1	37	41	-22	-4	8	2	1011	1015	9	-11	16	2	276	280	5
-4	8	0	520	533	3	-11	16	0	158	152	9	0	12	1	34	33	-18	-3	8	2	39	24	-15	-10	16	2	33	17	-19
-3	8	0	23	28	-14	-10	16	0	32	36	-19	-12	13	1	42	28	-24	-2	8	2	142	150	7	-9	16	2	35	43	-21
-2	8	0	91	87	6	-9	16	0	55	39	-22	-11	13	1	92	74	15	-1	8	2	698	724	8	-8	16	2	155	163	9
-1	8	0	689	717	6	-8	16	0	321	320	5	-10	13	1	29	28	-17	0	8	2	52	44	-17	-7	16	2	35	38	-21
0	8	0	24	19	-12	-7	16	0	40	57	-24	-9	13	1	31	38	-18	-8	9	2	84	74	10	-6	16	2	32	13	-19
-8	9	0	25	24	-14	-6	16	0	35	4	-20	-8	13	1	203	197	5	-7	9	2	77	86	12	-5	16	2	267	277	7
-7	9	0	187	192	5	-5	16	0	159	160	8	-7	13	1	27	18	-16	-6	9	2	522	525	3	-4	16	2	37	39	-22
-6	9	0	872	894	6	-4	16	0	53	52	-23	-6	13	1	65	59	-31	-5	9	2	153	141	5	-3	16	2	34	41	-19
-5	9	0	57	72	-13	-3	16	0	33	10	-24	-5	13	1	75	54	-15	-4	9	2	32	18	-17	-9	17	2	33	10	-19
-4	9	0	119	127	6	-10	17	0	162	162	9	-4	13	1	28	22	-16	-3	9	2	515	522	7	-8	17	2	36	28	-21
-3	9	0	845	875	5	-9	17	0	55	7	-23	-3	13	1	29	30	-20	-2	9	2	115	117	6	0	1	3	114	122	7
-2	9	0	68	59	-12	-8	17	0	33	4	-19	-2	13	1	57	61	-29	-1	9	2	27	26	-16	-1	2	3	383	325	15
-1	9	0	83	95	10	-7	17	0	149	151	10	-1	13	1	30	15	-17	0	9	2	261	235	8	0	2	3	357	395	8
0	9	0	958	982	5	0	1	1	48	56	6	0	13	1	43	24	-21	-9	10	2	73	82	-14	-2	3	3	173	155	9
-9	10	0	61	54	-17	-1	2	1	762	675	9	-13	14	1	80	93	-29	-8	10	2	672	697	7	-1	3	3	165	156	7
-8	10	0	383	394	5	0	2	1	141	164	4	-12	14	1	35	46	-21	-7	10	2	28	32	-17	0	3	3	520	475	10
-7	10	0	35	39	-18	-2	3	1	76	80	4	-11	14	1	87	84	-16	-6	10	2	98	75	8	-3	4	3	170	149	20
-6	10	0	61	50	-17	-1	3	1	81	83	4	-10	14	1	66	52	-23	-5	10	2	563	575	5	-2	4	3	407	370	9
-5	10	0	710	704	4	0	3	1	867	734	41	-9	14	1	47	52	-22	-4	10	2	84	77	10	-1	4	3	210	194	5
-4	10	0	104	110	8	-3	4	1	118	149	7	-8	14	1	61	46	-25	-3	10	2	59	27	-16	0	4	3	212	201	4
-3	10	0	24	5	-14	-2	4	1	452	425	2	-7	14	1	75	73	-17	-2	10	2	725	715	10	-4	5	3	434	416	5
-2	10	0	436	434	3	-1	4	1	47	24	-8	-6	14	1	42	52	-23	-1	10	2	76	72	-15	-3	5	3	74	88	7
-1	10	0	103	108	8	0	4	1	78	95	5	-5	14	1	81	68	-17	0	10	2	46	59	-19	-2	5	3	63	52	8
0	10	0	30	28	-14	-4	5	1	497	475	4	-4	14	1	40	65	-23	-10	11	2	560	573	4	-1	5	3	426	372	19
-10	11	0	337	332	12	-3	5	1	192	183	6	-3	14	1	98	87	13	-9	11	2	30	31	-18	0	5	3	81	82	7
-9	11	0	29	55	-17	-2	5	1	246	246	4	-2	14	1	39	41	-20	-8	11	2	113	106	8	-5	6	3	208	201	4
-8	11	0	43	50	-25	-1	5	1	178	191	4	-1	14	1	39	35	-23	-7	11	2	580	598	6	-4	6	3	62	67	9
-7	11	0	433	450	3	0	5	1	206	198	8	0	14	1	49	56	-23	-6	11	2	28	10	-16	-3	6	3	46	27	-15
-6	11	0	27	19	-16	-5	6	1	39	45	-13	-14	15	1	39	19	-23	-5	11	2	59	47	-18	-2	6	3	116	129	5
-5	11	0	33	30	-20	-4	6	1	88	97	5	-13	15	1	33	22	-19	-4	11	2	594	606	4	-1	6	3	115	120	6
-4	11	0	401	423	3	-3	6	1	54	30	-15	-12	15	1	32	24	-18	-3	11	2	99	90	10	0	6	3	243	243	12
-3	11	0	25	12	-15	-2	6	1	29	4	-17	-11	15	1	41	14	-24	-2	11	2	86	73	13	-6	7	3	149	157	5
-2	11	0	68	53	-19	-1	6	1	75	71	6	-10	15	1	39	13	-23	-1	11	2	559	564	11	-5	7	3	354	352	4
-1	11	0	298	308	4	0	6	1	308	310	10	-9	15	1	34	31	-20	0	11	2	72	41	-18	-4	7	3	136	143	5
0	11	0	28	2	-14	-6	7	1	38	54	-15	-8	15	1	31	21	-18	-11	12	2	79	79	-19	-3	7	3	137	148	5
-11	12	0	54	59	-29	-5	7	1	396	398	3	-7	15	1	39	28	-19	-10	12	2	49	49	-20	-2	7	3	301	281	5
-10	12	0	69	76	-17	-4	7	1	48	24	-13	-6	15	1	31	31	-18	-9	12	2	338	321	4	-1	7	3	127	123	7
-9	12	0	582	574	4	-3	7	1	59	74	9	-5	15	1	34	31	-20	-8	12	2	94	99	11	0	7	3	142	131	7
-8	12	0	50	30	-21	-2	7	1	158	149	3	-4	15	1	39	29	-20	-7	12	2	68	65	-16	-7	8	3	227	225	8
-7	12	0	103	99	9	-1	7	1	23	20	-14	-3	15	1	52	40	-30	-6	12	2	234	211	4	-6	8	3	70	64	11
-6	12	0	738	744	6	0	7	1	47	54	-16	-2	15	1	53	32	-31	-5	12	2	57	66	-20	-5	8	3	90	107	8
-5	12	0	50	38	-29	-7	8	1	158	159	5	-1	15	1	36	25	-21	-4	12	2	67	61	-17	-4	8	3	286	278	3
-4	12	0	96	110	10	-6	8	1	77	77	8	-13	16	1	34	18	-20	-3	12	2	308	307	4	-3	8	3	61	72	-12
-3	12	0	570	577	7	-5	8	1	102	101	6	-12	16	1	51	50	-27	-2	12	2	64	67	-21	-2	8	3	57	40	-14
-2	12	0	64	53	-19	-4	8	1	215	218	3	-11	16	1	87	56	-22	-1	12	2	37	17	-22	-1	8	3	305	284	11
-1	12	0	31	51	-18	-3	8	1	109	105	5	-10	16	1	32	17	-19	0	12	2	305	293	4	0	8	3	89	86	8
0	12	0	398	404	3	-2	8	1	106	115	8	-9	16	1	35	14	-20	-12	13	2	74	66	-20	-8	9	3	65	58	-17
-12	13	0	59	49	-34	-1	8	1	206	214	5	-8	16	1	51	44	-23	-11	13	2	252	273	7	-7	9	3	96	103	9
-11	13	0	401	404	4	0	8	1	150	152	7	-7	16	1	32	14	-18	-10	13	2	37	19	-19	-6	9	3	138	136	5
-10	13	0	29	31	-16	-8	9	1	61	60	-16	-6	16	1	32	27	-19	-9	13	2	32	42	-19	-5	9	3	82	82	9
-9	13	0	42	20	-20	-7	9	1	26	22	-15	-5	16	1	119	118	12	-8	13	2	472	489	5	-4	9	3	75	72	10
-8	13	0	252	262	4	-6	9	1	154	162	4	-4	16	1	33	12	-19	-7	13	2	28	36	-20	-3	9	3	141	135	5
-7	13	0	63	60	-20	-5	9	1	33	44	-19	-3	16	1	36	30	-21	-6	13	2	80	75	-14	-2	9	3	160	156	10
-6	13	0	30	16	-18	-4	9	1	61	60	-15	-10	17	1	47	36	-24	-5	13	2	482	494	5	-1	9	3	37	15	-18
-5	13	0	257	266	4	-3	9	1	168	166	4	-9	17	1	57	53	-23	-4	13	2	32	43	-19	0	9	3	42	30	-21
-4	13	0	31	61	-19	-2	9	1	49	45	-16	-8	17	1	37	46	-22	-3	13	2	44	30	-21	-9	10	3	157	156	12
-3	13	0	36	15	-22	-1	9	1	91	86	11	-7	17	1	41	17	-25	-2	13	2	270	289	5	-8	10	3	185	183	5
-2	13	0	389	395	5	0	9	1	51	32	-18	0	0	2	314	304	4	-1	13	2	80	67	-18	-7	10	3	164	168	6
-1	13	0	98	101	12	-9	10	1	25	52	-18	0	1	2	36	32	-12	0	13	2	33	5	-17	-6	10	3	122	116	7

Observed and calculated structure factors for $Sr_{0.73}Ca_{0.27}BeSiO_4$

h	k	l	10Fo	10Fc	10s	h	k	l	10Fo	10Fc	10s	h	k	l	10Fo	10Fc	10s	h	k	l	10Fo	10Fc	10s	h	k	l	10Fo	10Fc	10s
-5	10	3	206	204	4	-4	5	4	868	811	8	-4	14	4	297	284	9	-1	11	5	102	112	12	-4	8	6	551	542	14
-4	10	3	112	105	7	-3	5	4	235	224	17	-3	14	4	67	45	-20	0	11	5	71	76	-20	-3	8	6	106	100	9
-3	10	3	175	175	7	-2	5	4	141	158	5	-2	14	4	35	12	-21	-11	12	5	86	95	-17	-2	8	6	208	201	8
-2	10	3	229	232	5	-1	5	4	823	778	49	-1	14	4	188	179	11	-10	12	5	75	80	-19	-1	8	6	458	445	24
-1	10	3	53	79	-17	0	5	4	71	100	9	0	14	4	34	22	-17	-9	12	5	40	58	-23	0	8	6	77	66	-14
0	10	3	123	115	8	-5	6	4	56	28	-15	-13	15	4	77	82	-22	-8	12	5	32	40	-19	-8	9	6	91	92	12
-10	11	3	106	105	10	-4	6	4	257	233	18	-12	15	4	266	271	12	-7	12	5	83	72	-15	-7	9	6	61	64	-18
-9	11	3	67	28	-18	-3	6	4	1278	1266	19	-11	15	4	36	25	-21	-6	12	5	29	3	-17	-6	9	6	531	537	5
-8	11	3	70	42	-20	-2	6	4	91	76	8	-10	15	4	36	47	-21	-5	12	5	46	37	-21	-5	9	6	141	154	7
-7	11	3	187	191	5	-1	6	4	200	200	12	-9	15	4	254	251	8	-4	12	5	82	69	-15	-4	9	6	92	100	11
-6	11	3	77	71	13	0	6	4	823	836	8	-8	15	4	32	12	-23	-3	12	5	51	57	-22	-3	9	6	530	532	23
-5	11	3	79	48	11	-6	7	4	29	42	-16	-7	15	4	80	79	-25	-2	12	5	92	65	15	-2	9	6	149	142	13
-4	11	3	158	153	6	-5	7	4	629	611	4	-6	15	4	252	254	7	-1	12	5	90	82	-16	-1	9	6	40	36	-18
-3	11	3	88	54	14	-4	7	4	111	112	6	-5	15	4	41	36	-24	0	12	5	34	45	-20	0	9	6	342	342	5
-2	11	3	72	54	-15	-3	7	4	73	54	11	-4	15	4	92	66	-17	-12	13	5	46	41	-28	-9	10	6	107	111	12
-1	11	3	156	160	7	-2	7	4	689	636	29	-3	15	4	269	271	6	-11	13	5	107	86	14	-8	10	6	371	384	10
0	11	3	35	17	-18	-1	7	4	147	153	8	-2	15	4	37	7	-22	-10	13	5	76	70	-23	-7	10	6	56	44	-26
-11	12	3	34	13	-20	0	7	4	132	136	7	-12	16	4	38	16	-23	-9	13	5	40	42	-20	-6	10	6	101	95	11
-10	12	3	41	40	-25	-7	8	4	634	635	23	-11	16	4	146	146	12	-8	13	5	123	117	10	-5	10	6	394	372	9
-9	12	3	76	80	-15	-6	8	4	50	39	-20	-10	16	4	44	50	-27	-7	13	5	65	53	-25	-4	10	6	44	30	-21
-8	12	3	86	90	14	-5	8	4	71	66	-13	-9	16	4	33	19	-19	-6	13	5	57	34	-30	-3	10	6	72	80	-17
-7	12	3	54	64	-20	-4	8	4	541	539	9	-8	16	4	257	258	6	-5	13	5	99	104	12	-2	10	6	402	400	14
-6	12	3	30	6	-18	-3	8	4	97	116	8	-7	16	4	81	64	-21	-4	13	5	58	49	-26	-1	10	6	35	27	-21
-5	12	3	114	118	9	-2	8	4	57	61	-17	-6	16	4	65	32	-23	-3	13	5	83	73	-17	0	10	6	102	100	11
-4	12	3	70	58	-17	-1	8	4	611	604	28	-5	16	4	147	146	10	-2	13	5	69	84	-22	-10	11	6	332	333	16
-3	12	3	67	75	-20	0	8	4	103	95	8	-4	16	4	40	60	-22	-1	13	5	43	34	-26	-9	11	6	54	48	-31
-2	12	3	92	87	12	-8	9	4	74	52	-14	0	1	5	239	272	5	0	13	5	41	38	-28	-8	11	6	153	149	10
-1	12	3	58	32	-20	-7	9	4	130	136	8	-1	2	5	762	575	20	-13	14	5	63	79	-23	-7	11	6	333	349	10
0	12	3	42	41	-22	-6	9	4	617	632	5	0	2	5	126	152	7	-12	14	5	75	78	-26	-6	11	6	41	41	-18
-12	13	3	107	86	14	-5	9	4	28	8	-16	-2	3	5	225	195	21	-11	14	5	127	127	11	-5	11	6	96	79	12
-11	13	3	33	90	-20	-4	9	4	112	121	9	-1	3	5	244	208	26	-10	14	5	94	76	-17	-4	11	6	330	338	10
-10	13	3	38	56	-28	-3	9	4	632	634	12	0	3	5	225	237	6	-9	14	5	76	81	-20	-3	11	6	128	135	10
-9	13	3	119	120	10	-2	9	4	33	21	-16	-3	4	5	111	126	6	-8	14	5	75	70	-23	-2	11	6	96	103	15
-8	13	3	143	162	8	-1	9	4	145	144	8	-2	4	5	515	464	16	-7	14	5	86	69	-17	-1	11	6	322	321	7
-7	13	3	51	77	-20	0	9	4	684	691	25	-1	4	5	121	130	6	-6	14	5	39	62	-23	0	11	6	62	67	-19
-6	13	3	127	117	9	-9	10	4	28	18	-16	0	4	5	94	102	7	-5	14	5	67	90	-32	-11	12	6	95	96	-16
-5	13	3	100	110	11	-8	10	4	395	403	7	-4	5	5	391	384	7	-4	14	5	88	80	-17	-10	12	6	35	32	-20
-4	13	3	57	70	-24	-7	10	4	104	110	9	-3	5	5	381	342	5	-3	14	5	131	124	14	-9	12	6	354	338	7
-3	13	3	75	54	-17	-6	10	4	59	43	-19	-2	5	5	403	373	12	-2	14	5	90	73	-19	-8	12	6	105	109	13
-2	13	3	98	88	13	-5	10	4	575	570	4	-1	5	5	387	364	25	-1	14	5	77	67	-25	-7	12	6	30	20	-21
-1	13	3	60	54	-34	-4	10	4	126	134	7	0	5	5	305	287	9	0	14	5	105	95	15	-6	12	6	280	271	5
0	13	3	96	99	13	-3	10	4	81	72	12	-5	6	5	98	98	10	-13	15	5	34	19	-20	-5	12	6	81	85	-16
-13	14	3	96	95	-18	-2	10	4	455	428	7	-4	6	5	205	196	18	-12	15	5	34	6	-20	-4	12	6	64	39	-26
-12	14	3	36	5	-26	-1	10	4	139	132	7	-3	6	5	66	21	-20	-11	15	5	52	28	-22	-3	12	6	350	335	7
-11	14	3	64	47	-22	0	10	4	28	22	-14	-2	6	5	130	129	6	-10	15	5	51	32	-25	-2	12	6	91	88	-16
-10	14	3	38	60	-23	-10	11	4	305	314	16	-1	6	5	101	89	8	-9	15	5	41	31	-25	-1	12	6	51	45	-23
-9	14	3	33	19	-20	-9	11	4	83	91	-15	0	6	5	120	127	5	-8	15	5	66	68	-34	0	12	6	266	269	7
-8	14	3	33	15	-20	-8	11	4	39	48	-18	-6	7	5	92	89	10	-7	15	5	87	70	-22	-12	13	6	84	83	-20
-7	14	3	75	76	-19	-7	11	4	412	423	6	-5	7	5	255	274	4	-6	15	5	36	36	-21	-11	13	6	189	192	10
-6	14	3	30	13	-17	-6	11	4	87	93	11	-4	7	5	130	136	6	-5	15	5	33	23	-19	-10	13	6	31	10	-31
-5	14	3	67	12	-25	-5	11	4	60	48	-18	-3	7	5	103	97	8	-4	15	5	37	47	-22	-9	13	6	78	72	-20
-4	14	3	83	90	-17	-4	11	4	406	412	3	-2	7	5	307	285	14	-3	15	5	34	7	-20	-8	13	6	266	280	7
-3	14	3	32	50	-22	-3	11	4	45	31	-18	-1	7	5	115	107	8	-2	15	5	42	28	-25	-7	13	6	59	50	-22
-2	14	3	35	7	-20	-2	11	4	29	15	-20	0	7	5	135	133	7	-10	16	5	66	21	-30	-6	13	6	96	97	-18
-1	14	3	72	67	-21	-1	11	4	312	307	15	-7	8	5	225	229	6	-9	16	5	47	44	-24	-5	13	6	270	284	6
0	14	3	36	39	-18	0	11	4	44	34	-22	-6	8	5	138	153	7	-8	16	5	47	57	-26	-4	13	6	32	19	-18
-14	15	3	40	32	-30	-11	12	4	33	15	-20	-5	8	5	113	120	7	-7	16	5	34	34	-20	-3	13	6	57	34	-29
-13	15	3	39	48	-29	-10	12	4	107	112	14	-4	8	5	215	222	4	-6	16	5	44	36	-27	-2	13	6	194	192	8
-12	15	3	50	18	-21	-9	12	4	391	398	8	-3	8	5	89	96	10	0	0	6	943	927	8	-1	13	6	42	33	-25
-11	15	3	36	45	-22	-8	12	4	38	25	-23	-2	8	5	169	195	9	0	1	6	110	122	8	0	13	6	33	31	-19
-10	15	3	32	44	-18	-7	12	4	126	136	9	-1	8	5	200	214	10	-1	2	6	924	801	83	-13	14	6	174	185	12
-9	15	3	32	32	-18	-6	12	4	530	537	7	0	8	5	293	264	4	0	2	6	155	169	12	-12	14	6	34	23	-19
-8	15	3	34	23	-20	-5	12	4	52	33	-37	-8	9	5	106	129	10	-2	3	6	342	276	25	-11	14	6	39	37	-29
-7	15	3	35	25	-20	-4	12	4	90	87	14	-7	9	5	82	79	-14	-1	3	6	273	243	35	-10	14	6	174	191	12
-6	15	3	66	41	-25	-3	12	4	374	389	7	-6	9	5	99	98	10	0	3	6	1036	1029	57	-9	14	6	72	66	-22
-5	15	3	70	73	-29	-2	12	4	32	17	-19	-5	9	5	131	130	7	-3	4	6	157	175	8	-8	14	6	76	68	-21
-4	15	3	32	30	-19	-1	12	4	78	60	-18	-4	9	5	147	145	6	-2	4	6	835	694	25	-7	14	6	259	252	7
-3	15	3	39	26	-21	0	12	4	304	309	4	-3	9	5	129	111	8	-1	4	6	79	76	13	-6	14	6	46	48	-24
-2	15	3	98	88	16	-12	13	4	35	18	-20	-2	9	5	89	78	11	0	4	6	151	161	8	-5	14	6	109	94	14
-1	15	3	37	10	-21	-11	13	4	338	330	5	-1	9	5	166	153	11	-4	5	6	700	662	29	-4	14	6	188	195	8
-12	16	3	77	79	-25	-10	13	4	92	82	15	0	9	5	27	12	-15	-3	5	6	66	76	-17	-3	14	6	34	31	-19
-11	16	3	80	70	-23	-9	13	4	33	28	-20	-9	10	5	73	52	-16	-2	5	6	134	136	7	-2	14	6	39	52	-23
-10	16	3	62	70	-23	-8	13	4	264	265	7	-8	10	5	176	164	7	-1	5	6	660	647	23	-1	14	6	187	181	9
-9	16	3	39	54	-28	-7	13	4	29	51	-21	-7	10	5	68	57	-18	0	5	6	287	257	20	-12	15	6	163	146	11
-8	16	3	41	61	-24	-6	13	4	29	22	-17	-6	10	5	99	95	10	-5	6	6	147	154	7	-11	15	6	55	54	-22
-7	16	3	33	46	-19	-5	13	4	268	268	5	-5	10	5	194	183	5	-4	6	6	82	94	12	-10	15	6	58	36	-34
-6	16	3	102	91	16	-4	13	4	95	95	13	-4	10	5	105	89	9	-3	6	6	637	587	25	-9	15	6	232	220	8
-5	16	3	116	103	13	-3	13	4	35	55	-20	-3	10	5	90	70	11	-2	6	6	145	145	6	-8	15	6	70	65	-30
-4	16	3	34	40	-24	-2	13	4	331	334	10	-2	10	5	179	180	7	-1	6	6	81	78	12	-7	15	6	33	22	-19
0	0	4	1955	2229	9	-1	13	4	71	66	-25	-1	10	5	88	64	13	0	6	6	681	708	23	-6	15	6	229	216	7
0	1	4	215	202	23	0	13	4	48	54	-25	0	10	5	71	49	-18	-6	7	6	144	161	6	-5	15	6	94	86	-17
-1	2	4	1133	928	47	-13	14	4	183	187	12	-10	11	5	112	113	10	-5	7	6	595	579	5	-4	15	6	34	17	-20
0	2	4	221	213	17	-12	14	4	61	44	-38	-9	11	5	87	73	-15	-4	7	6	103	102	9	-3	15	6	149	143	10
-2	3	4	72	107	9	-11	14	4	33	31	-23	-8	11	5	144	158	8	-3	7	6	142	143	7	-8	16	6	113	123	17
-1	3	4	51	71	-14	-10	14	4	269	279	6	-7	11	5	170	163	6	-2	7	6	623	590	33	0	1	7	105	122	7
0	3	4	1306	1234	38	-9	14	4	31	22	-18	-6	11	5	150	179	8	-1	7	6	82	90	13	-1	2	7	252	223	5
-3	4	4	131	141	6	-8	14	4	31	17	-18	-5	11	5	152	178	7	0	7	6	75	71	11	0	2	7	290	317	6
-2	4	4	1042	966	31	-7	14	4	230	231	6	-4	11	5	133	140	8	-7	8	6	457	454	16	-2	3	7	192	193	19
-1	4	4	262	236	13	-6	14	4	40	44	-24	-3	11	5	146	149	11	-6	8	6	141	159	8	-1	3	7	244	202	-54
0	4	4	92	108	6	-5	14	4	31	22	-18	-2	11	5	75	73	-17	-5	8	6	141	144	7	0	3	7	97	100	9

Observed and calculated structure factors for $Sr_{0.73}Ca_{0.27}BeSiO_4$

h	k	l	10Fo	10Fc	10s	h	k	l	10Fo	10Fc	10s	h	k	l	10Fo	10Fc	10s	h	k	l	10Fo	10Fc	10s	h	k	l	10Fo	10Fc	10s
-3	4	7	159	163	12	-7	14	7	68	46	-30	-2	12	8	67	57	-30	-2	11	9	36	47	-22	-8	11	10	106	97	16
-2	4	7	288	223	22	-6	14	7	89	79	-22	-1	12	8	97	78	-18	-1	11	9	58	45	-24	-7	11	10	137	141	12
-1	4	7	230	205	29	-5	14	7	90	51	-23	0	12	8	119	135	11	0	11	9	49	40	-19	-6	11	10	62	68	-26
0	4	7	174	186	10	-4	14	7	41	53	-24	-12	13	8	34	31	-20	-11	12	9	62	68	-24	-5	11	10	90	81	-27
-4	5	7	259	218	15	-3	14	7	48	35	-27	-11	13	8	191	206	11	-10	12	9	54	68	-25	-4	11	10	148	139	13
-3	5	7	94	89	11	-2	14	7	39	37	-23	-10	13	8	94	79	-22	-9	12	9	34	17	-20	-3	11	10	85	91	-22
-2	5	7	135	135	8	-11	15	7	46	52	-30	-9	13	8	54	62	-38	-8	12	9	87	56	-22	-2	11	10	101	87	17
-1	5	7	231	208	11	-10	15	7	48	59	-26	-8	13	8	198	198	10	-7	12	9	75	79	-33	-1	11	10	127	134	12
0	5	7	188	189	10	-9	15	7	43	29	-25	-7	13	8	34	76	-24	-6	12	9	34	3	-20	0	11	10	63	70	-31
-5	6	7	195	215	10	-8	15	7	41	37	-22	-6	13	8	37	34	-22	-5	12	9	111	83	14	-11	12	10	80	76	-24
-4	6	7	127	124	8	-7	15	7	44	36	-27	-5	13	8	206	202	12	-4	12	9	84	57	-23	-10	12	10	89	72	-23
-3	6	7	28	15	-16	-6	15	7	38	26	-22	-4	13	8	100	98	-21	-3	12	9	34	24	-24	-9	12	10	213	209	9
-2	6	7	135	128	8	-5	15	7	78	67	-25	-3	13	8	44	60	-26	-2	12	9	111	91	16	-8	12	10	80	74	-32
-1	6	7	197	189	7	-4	15	7	49	50	-28	-2	13	8	188	209	10	-1	12	9	74	67	-29	-7	12	10	57	67	-31
0	6	7	109	92	7	0	0	8	640	617	6	-1	13	8	105	98	17	0	12	9	35	20	-17	-6	12	10	196	195	11
-6	7	7	135	140	8	0	1	8	170	201	5	0	13	8	46	54	-24	-11	13	9	59	34	-34	-5	12	10	78	75	-30
-5	7	7	231	194	6	-1	2	8	614	626	21	-11	14	8	70	57	-26	-10	13	9	93	87	-22	-4	12	10	85	70	-28
-4	7	7	156	147	7	0	2	8	166	194	9	-10	14	8	188	190	10	-9	13	9	100	74	-19	-3	12	10	196	205	9
-3	7	7	126	126	9	-2	3	8	131	119	20	-9	14	8	60	49	-24	-8	13	9	83	41	-27	-2	12	10	73	82	-35
-2	7	7	162	164	9	-1	3	8	138	132	12	-8	14	8	63	49	-24	-7	13	9	92	74	-21	-1	12	10	87	65	-22
-1	7	7	148	149	8	0	3	8	453	442	56	-7	14	8	170	178	9	-6	13	9	101	72	-22	-10	13	10	94	47	-23
0	7	7	133	131	9	-3	4	8	166	165	14	-6	14	8	35	61	-20	-5	13	9	35	53	-20	-9	13	10	86	74	-29
-7	8	7	162	154	7	-2	4	8	644	603	36	-5	14	8	39	17	-23	-4	13	9	77	61	-32	-8	13	10	126	123	14
-6	8	7	117	117	11	-1	4	8	176	176	27	-4	14	8	191	190	9	-3	13	9	107	92	-19	-7	13	10	63	68	-45
-5	8	7	199	191	7	0	4	8	156	149	13	-3	14	8	72	58	-30	-2	13	9	62	41	-33	-6	13	10	60	65	-27
-4	8	7	187	163	6	-4	5	8	584	552	33	-8	15	8	39	36	-23	-10	14	9	35	39	-20	-5	13	10	108	122	17
-3	8	7	177	175	7	-3	5	8	198	197	7	-7	15	8	81	83	-28	-9	14	9	43	55	-32	-4	13	10	60	59	-31
-2	8	7	130	118	9	-2	5	8	187	172	10	0	1	9	160	193	6	-8	14	9	46	29	-27	-3	13	10	46	54	-23
-1	8	7	179	163	11	-1	5	8	532	540	26	-1	2	9	190	180	6	-7	14	9	36	29	-21	0	1	11	111	103	8
0	8	7	67	55	-20	0	5	8	125	107	11	0	2	9	150	157	9	-6	14	9	42	31	-24	-1	2	11	198	200	7
-8	9	7	86	86	14	-5	6	8	123	111	14	-2	3	9	157	168	8	-5	14	9	41	58	-24	0	2	11	152	181	9
-7	9	7	119	133	10	-4	6	8	175	173	13	-1	3	9	149	161	8	-4	14	9	40	26	-24	-2	3	11	126	127	9
-6	9	7	49	59	-24	-3	6	8	542	463	30	0	3	9	101	66	13	0	0	10	567	590	6	-1	3	11	133	142	11
-5	9	7	113	107	10	-2	6	8	150	131	9	-3	4	9	129	121	18	0	1	10	147	152	6	0	3	11	70	34	-18
-4	9	7	115	114	10	-1	6	8	160	164	11	-2	4	9	179	167	8	-1	2	10	288	284	4	-3	4	11	75	82	-20
-3	9	7	31	50	-19	0	6	8	345	348	16	-1	4	9	151	142	14	0	2	10	175	177	7	-2	4	11	167	168	8
-2	9	7	158	144	7	-6	7	8	98	91	13	0	4	9	150	136	10	-2	3	10	180	192	6	-1	4	11	110	114	11
-1	9	7	83	69	-19	-5	7	8	479	450	13	-4	5	9	198	152	19	-1	3	10	141	162	8	0	4	11	96	80	12
0	9	7	41	10	-20	-4	7	8	168	161	9	-3	5	9	185	180	23	0	3	10	557	592	11	-4	5	11	128	133	12
-9	10	7	127	126	10	-3	7	8	142	121	10	-2	5	9	204	212	11	-3	4	10	173	173	8	-3	5	11	132	129	11
-8	10	7	101	114	12	-2	7	8	485	462	24	-1	5	9	168	161	19	-2	4	10	221	232	8	-2	5	11	146	143	13
-7	10	7	154	155	12	-1	7	8	145	151	10	0	5	9	171	166	11	-1	4	10	118	125	17	-1	5	11	146	146	15
-6	10	7	111	108	12	0	7	8	137	137	8	-5	6	9	121	116	15	0	4	10	149	163	12	0	5	11	176	168	18
-5	10	7	131	129	13	-7	8	8	415	421	18	-4	6	9	166	158	12	-4	5	10	251	235	17	-5	6	11	115	130	18
-4	10	7	118	109	10	-6	8	8	117	117	11	-3	6	9	48	12	-34	-3	5	10	137	130	16	-4	6	11	99	97	-17
-3	10	7	149	145	8	-5	8	8	106	115	12	-2	6	9	158	153	13	-2	5	10	162	146	14	-3	6	11	32	9	-19
-2	10	7	133	119	10	-4	8	8	433	413	9	-1	6	9	97	93	15	-1	5	10	256	242	17	-2	6	11	84	71	-18
-1	10	7	98	92	15	-3	8	8	131	128	10	0	6	9	39	28	-16	0	5	10	152	168	13	-1	6	11	134	129	14
0	10	7	106	102	11	-2	8	8	73	48	-28	-6	7	9	121	121	12	-5	6	10	149	138	9	0	6	11	73	39	-28
-10	11	7	74	73	-23	-1	8	8	376	408	11	-5	7	9	163	118	9	-4	6	10	114	120	18	-6	7	11	57	50	-25
-9	11	7	87	100	-16	0	8	8	124	117	10	-4	7	9	171	156	8	-3	6	10	424	422	11	-5	7	11	69	95	-38
-8	11	7	106	88	15	-8	9	8	99	99	13	-3	7	9	153	133	14	-2	6	10	148	135	18	-4	7	11	99	77	-18
-7	11	7	96	101	14	-7	9	8	158	153	11	-2	7	9	113	117	12	-1	6	10	128	122	-29	-3	7	11	61	47	-39
-6	11	7	41	42	-25	-6	9	8	268	266	5	-1	7	9	122	119	15	0	6	10	426	433	20	-2	7	11	128	127	11
-5	11	7	88	46	-17	-5	9	8	79	61	-26	0	7	9	149	147	9	-6	7	10	157	143	12	-1	7	11	104	89	-19
-4	11	7	113	112	12	-4	9	8	145	138	9	-7	8	9	101	96	13	-5	7	10	243	221	15	0	7	11	94	62	-16
-3	11	7	108	94	12	-3	9	8	266	267	9	-6	8	9	105	100	12	-4	7	10	134	124	12	-7	8	11	101	98	16
-2	11	7	107	105	13	-2	9	8	73	78	-23	-5	8	9	98	90	-18	-3	7	10	142	127	11	-6	8	11	106	106	16
-1	11	7	78	85	-21	-1	9	8	153	146	12	-4	8	9	123	106	-21	-2	7	10	226	214	19	-5	8	11	145	152	16
0	11	7	126	103	10	0	9	8	282	272	9	-3	8	9	70	74	-30	-1	7	10	129	127	15	-4	8	11	88	89	-26
-11	12	7	51	45	-29	-9	10	8	65	67	-21	-2	8	9	130	129	10	0	7	10	124	112	11	-3	8	11	127	139	15
-10	12	7	36	57	-21	-8	10	8	299	300	6	-1	8	9	102	97	12	-7	8	10	164	169	11	-2	8	11	130	116	16
-9	12	7	40	40	-24	-7	10	8	109	110	15	0	8	9	125	129	9	-6	8	10	119	131	13	-1	8	11	41	79	-25
-8	12	7	102	100	14	-6	10	8	86	76	-19	-8	9	9	106	115	13	-5	8	10	153	136	12	0	8	11	116	103	12
-7	12	7	91	85	-16	-5	10	8	357	365	13	-7	9	9	92	88	-17	-4	8	10	229	209	13	-8	9	11	85	72	-22
-6	12	7	49	5	-22	-4	10	8	152	146	9	-6	9	9	44	36	-27	-3	8	10	132	119	15	-7	9	11	93	85	-23
-5	12	7	96	101	15	-3	10	8	80	82	-19	-5	9	9	133	121	13	-2	8	10	152	135	11	-6	9	11	37	19	-22
-4	12	7	108	101	13	-2	10	8	331	315	12	-4	9	9	121	108	13	-1	8	10	141	166	10	-5	9	11	68	70	-30
-3	12	7	32	39	-19	-1	10	8	132	128	11	-3	9	9	51	42	-26	0	8	10	97	85	15	-4	9	11	125	91	13
-2	12	7	101	81	-17	0	10	8	85	72	-16	-2	9	9	115	111	12	-8	9	10	90	85	-21	-3	9	11	40	5	-30
-1	12	7	75	67	-29	-10	11	8	234	243	11	-1	9	9	109	101	14	-7	9	10	95	97	-16	-2	9	11	80	63	-33
0	12	7	59	34	-21	-9	11	8	81	89	-19	0	9	9	39	18	-19	-6	9	10	340	331	11	-1	9	11	89	75	-22
-12	13	7	61	73	-38	-8	11	8	33	25	-23	-9	10	9	112	99	17	-5	9	10	122	115	13	0	9	11	35	5	-17
-11	13	7	66	62	-29	-7	11	8	296	300	7	-8	10	9	88	79	-22	-4	9	10	113	121	-23	-9	10	11	77	39	-33
-10	13	7	45	53	-26	-6	11	8	111	113	13	-7	10	9	107	98	14	-3	9	10	338	335	7	-8	10	11	97	85	-25
-9	13	7	105	99	15	-5	11	8	111	95	13	-6	10	9	140	122	11	-2	9	10	107	110	15	-7	10	11	90	65	-22
-8	13	7	76	77	-23	-4	11	8	282	293	8	-5	10	9	107	78	17	-1	9	10	101	81	-17	-6	10	11	38	42	-23
-7	13	7	70	83	-28	-3	11	8	37	43	-22	-4	10	9	106	108	16	0	9	10	238	246	9	-5	10	11	85	77	-32
-6	13	7	107	95	13	-2	11	8	38	64	-28	-3	10	9	125	92	16	-9	10	10	108	90	-19	-4	10	11	76	64	-38
-5	13	7	60	70	-32	-1	11	8	226	230	9	-2	10	9	109	69	15	-8	10	10	165	161	9	-3	10	11	35	44	-25
-4	13	7	80	81	-20	0	11	8	77	69	-19	-1	10	9	101	88	15	-7	10	10	110	90	15	-2	10	11	43	62	-25
-3	13	7	79	58	-24	-11	12	8	47	32	-26	0	10	9	105	90	15	-6	10	10	107	95	15	-1	10	11	44	52	-22
-2	13	7	44	62	-27	-10	12	8	100	110	-17	-10	11	9	51	48	-23	-5	10	10	142	137	18	0	10	11	61	43	-23
-1	13	7	72	61	-32	-9	12	8	173	173	12	-9	11	9	62	43	-30	-4	10	10	99	84	-20	-10	11	11	60	64	-25
0	13	7	90	93	-18	-8	12	8	49	50	-27	-8	11	9	98	86	-21	-3	10	10	107	94	17	-9	11	11	92	86	-20
-12	14	7	34	31	-20	-7	12	8	130	125	11	-7	11	9	37	54	-22	-2	10	10	166	162	10	-8	11	11	108	97	17
-11	14	7	39	38	-23	-6	12	8	229	219	9	-6	11	9	82	89	-28	-1	10	10	87	84	-23	-7	11	11	95	61	-27
-10	14	7	59	61	-24	-5	12	8	91	76	-17	-5	11	9	84	99	-22	0	10	10	80	81	-22	-6	11	11	68	71	-25
-9	14	7	37	69	-22	-4	12	8	114	99	13	-4	11	9	93	73	-25	-10	11	10	122	132	13	-5	11	11	63	77	-45
-8	14	7	89	73	-19	-3	12	8	166	180	10	-3	11	9	82	79	-26	-9	11	10	58	76	-33	-4	11	11	55	68	-39

Observed and calculated structure factors for $Sr_{0.73}Ce_{0.27}BeSiO_4$

h	k	l	10Fo	10Fc	10s	h	k	l	10Fo	10Fc	10s	h	k	l	10Fo	10Fc	10s	h	k	l	10Fo	10Fc	10s	h	k	l	10Fo	10Fc	10s
-3	11	11	100	97	-20	0	7	12	99	102	-24	0	3	13	57	22	-18	-7	10	13	104	76	-20	-1	8	14	51	54	-29
-2	11	11	61	89	-25	-7	8	12	185	184	11	-3	4	13	87	83	-17	-6	10	13	75	79	-36	-6	9	14	126	128	13
-1	11	11	39	43	-23	-6	8	12	95	97	-22	-2	4	13	103	124	13	-5	10	13	84	76	-24	-5	9	14	53	52	-27
0	11	11	106	99	15	-5	8	12	108	110	17	-1	4	13	99	87	14	-4	10	13	65	70	-25	-4	9	14	82	92	-27
-10	12	11	46	46	-28	-4	8	12	164	183	17	0	4	13	99	89	13	-3	10	13	85	76	-26	-3	9	14	135	131	12
-9	12	11	39	12	-23	-3	8	12	98	102	-26	-4	5	13	87	114	-21	-2	10	13	40	59	-24	0	1	15	57	50	-26
-8	12	11	59	62	-26	-2	8	12	111	93	15	-3	5	13	68	73	-24	0	0	14	135	185	16	-1	2	15	100	105	15
-7	12	11	37	56	-21	-1	8	12	194	187	16	-2	5	13	95	91	-16	0	1	14	104	109	12	0	2	15	86	77	-19
-6	12	11	37	1	-22	0	8	12	105	100	-21	-1	5	13	125	131	11	-1	2	14	35	84	-21	-2	3	15	61	59	-23
-5	12	11	87	41	-41	-8	9	12	100	90	-20	0	5	13	78	64	-23	0	2	14	122	114	9	-1	3	15	92	65	-22
-4	12	11	79	75	-31	-7	9	12	87	78	-31	-5	6	13	99	73	-18	-2	3	14	124	110	11	0	3	15	35	10	-18
-3	12	11	36	18	-21	-6	9	12	64	62	-64	-4	6	13	89	80	-18	-1	3	14	116	107	12	-3	4	15	37	34	-22
-2	12	11	52	33	-23	-5	9	12	89	80	-22	-3	6	13	42	7	-25	0	3	14	202	205	6	-2	4	15	84	92	-20
0	0	12	147	138	12	-4	9	12	97	82	-18	-2	6	13	99	89	-17	-3	4	14	121	106	12	-1	4	15	37	49	-22
0	1	12	147	149	7	-3	9	12	40	65	-23	-1	6	13	52	53	-25	-2	4	14	38	70	-21	0	4	15	43	33	-18
-1	2	12	237	267	5	-2	9	12	104	91	-28	0	6	13	34	10	-17	-1	4	14	113	102	15	-4	5	15	48	78	-24
0	2	12	137	149	8	-1	9	12	81	87	-36	-6	7	13	94	82	-19	0	4	14	120	110	10	-3	5	15	58	67	-23
-2	3	12	138	141	9	0	9	12	104	74	17	-5	7	13	96	100	-21	-4	5	14	37	70	-22	-2	5	15	90	72	-18
-1	3	12	107	109	12	-9	10	12	102	81	-23	-4	7	13	99	93	-17	-3	5	14	99	98	15	-1	5	15	61	84	-28
0	3	12	48	89	-20	-8	10	12	120	135	15	-3	7	13	85	86	-22	-2	5	14	111	89	13	0	5	15	91	80	-16
-3	4	12	141	143	9	-7	10	12	83	76	-31	-2	7	13	114	111	15	-1	5	14	42	76	-25	-5	6	15	54	58	-25
-2	4	12	253	254	10	-6	10	12	79	78	-31	-1	7	13	84	78	-22	0	5	14	128	101	14	-4	6	15	43	47	-26
-1	4	12	120	108	14	-5	10	12	187	166	12	0	7	13	96	90	-17	-5	6	14	94	75	-17	-3	6	15	37	5	-22
0	4	12	118	125	10	-4	10	12	112	82	18	-7	8	13	95	90	-22	-4	6	14	83	93	-20	-2	6	15	42	32	-22
-4	5	12	220	233	6	-3	10	12	59	71	-26	-6	8	13	40	38	-29	-3	6	14	132	158	12	-1	6	15	90	59	-19
-3	5	12	133	136	10	-2	10	12	130	139	16	-5	8	13	65	41	-30	-2	6	14	97	75	16	0	6	15	39	13	-19
-2	5	12	139	148	11	-1	10	12	94	72	-25	-4	8	13	34	100	-34	-1	6	14	93	98	-17	-5	7	15	51	58	-22
-1	5	12	209	233	7	0	10	12	64	63	-37	-3	8	13	39	27	-28	0	6	14	161	165	10	-4	7	15	34	36	-24
0	5	12	126	124	11	-9	11	12	86	64	-22	-2	8	13	52	58	-28	-6	7	14	41	77	-31	-3	7	15	34	18	-20
-5	6	12	121	112	12	-8	11	12	64	64	-28	-1	8	13	92	94	-23	-5	7	14	53	68	-25	-2	7	15	42	69	-22
-4	6	12	108	96	-20	-7	11	12	131	138	16	0	8	13	44	36	-32	-4	7	14	113	100	14	0	0	16	82	98	-35
-3	6	12	144	124	14	-6	11	12	106	84	-22	-8	9	13	34	58	-34	-3	7	14	83	86	-21	0	1	16	106	83	14
-2	6	12	129	128	13	-5	11	12	105	88	-26	-7	9	13	58	57	-42	-2	7	14	48	65	-27	-1	2	16	94	98	-17
-1	6	12	122	101	14	-4	11	12	128	130	14	-6	9	13	35	14	-25	-1	7	14	98	99	-17	0	2	16	104	87	13
0	6	12	60	81	-22	-3	11	12	84	63	-42	-5	9	13	60	72	-29	0	7	14	82	86	-24	-2	3	16	92	92	-21
-6	7	12	119	104	19	-2	11	12	97	74	-30	-4	9	13	43	55	-30	-7	8	14	35	58	-20	-1	3	16	50	58	-24
-5	7	12	165	192	11	0	1	13	107	99	12	-3	9	13	42	17	-31	-6	8	14	95	91	-21	0	3	16	39	87	-20
-4	7	12	127	107	20	-1	2	13	98	126	13	-2	9	13	89	74	-41	-5	8	14	87	75	-29	-3	4	16	101	89	16
-3	7	12	130	114	13	0	2	13	113	85	9	-1	9	13	35	43	-25	-4	8	14	46	68	-28	-2	4	16	71	89	-29
-2	7	12	155	191	13	-2	3	13	89	92	-15	0	9	13	34	10	-34	-3	8	14	87	83	-22	-1	4	16	72	54	-28
-1	7	12	96	89	-20	-1	3	13	96	83	14	-8	10	13	61	84	-61	-2	8	14	77	67	-32						